TECHNISCHE UNIVERSITÄT MÜNCHEN

Ingenieurfakultät Bau Geo Umwelt
Professur für Siedlungsstruktur und Verkehrsplanung

Handling Non-Motorized Trips in Macroscopic Travel Demand Models

Calculating Intrazonal Impedances and Identifying an Appropriate Level of Spatial Resolution

Matthew Bediako Okrah

Vollständiger Abdruck der von der Ingenieurfakultät Bau Geo Umwelt der Technischen Universität München zur Erlangung des akademischen Grades eines

Doktor-Ingenieurs (Dr.-Ing.)

genehmigten Dissertation.

Vorsitzender: Univ.-Prof. Dr.-Ing. Constantinos Antoniou

Prüfer der Dissertation:

1. Univ.-Prof. Dr.-Ing. Gebhard Wulfhorst
2. Univ.-Prof. Dr.-Ing. Markus Friedrich, Universität Stuttgart
3. Univ.-Prof. Dr.-Ing. Rolf Moeckel

Die Dissertation wurde am 27.10.2016 bei der Technischen Universität München eingereicht und durch die Ingenieurfakultät Bau Geo Umwelt am 18.01.2017 angenommen.

Acknowledgement

I would like to express my sincere gratitude to God for His guidance and protection throughout my doctoral study.

This doctoral research was funded by the Hans-Boeckler-Foundation and established within the mobil.LAB doctoral research group working on sustainable mobility in the metropolitan region of Munich.

I wish to acknowledge the invaluable support of my supervisors Prof. Dr.-Ing. Gebhard Wulfhorst, Prof. Dr.-Ing Markus Friedrich, and Prof. Dr.-Ing. Rolf Moeckel. Throughout the development of this dissertation, Prof. Wulfhorst has been inspirational and supportive in creating a good working environment for the success of this work. Thank your Prof. Wulfhorst for your time, comments and advice. Many thanks to Prof. Friedrich for his constructive criticisms which kept me on my toes. Special thanks to Prof. Moeckel for his guidance, encouragement and feedback.

I extend my sincere thanks and appreciation to Stadt Dachau and Gevas Humberg & Partner GmbH for providing me with data for the research. Mr. Andreas Meyer and Ms. Julia Brummer, thanks for your emails and the further clarifications on the data. I am also indebted to PTV for providing me with a version of the Visum software for this research. Map data copyrighted OpenStreetMap contributors and available from http://www.planet.openstreetmap.org.

I would like to thank my colleagues at the mobil.LAB and the Professorship of Urban Structure and Transport Planning. In particular, I would like to thank Dr. Stefan Klug and Ms. Ursula Uhse for their assistance with respect to my administrative needs. Thanks to Louis Ackah for proofreading my work.

Finally, I would like to thank my parents Seth and Hannah Okrah, my siblings, Ben and Esther, and my girlfriend, Lena for being there for me.

Abstract

Non-motorized trips are generally short trips, and in macroscopic models, many of them end up in the same transport analysis zones from which they originate. Since the spatial aggregation nature of these models makes it difficult to model intrazonal trips, the treatment of non-motorized trips in such models is limited. Non-motorized trips can however not be neglected in urban transport analyses considering the high share of walking and cycling in urban areas, and their importance for sustainable mobility. Recognizing the mitigation of the intrazonal problem as key to improving non-motorized trip modeling in macroscopic models, the research seeks to enhance the macroscopic modeling of non-motorized trips by finding a suitable method for calculating intrazonal impedances, and identifying an appropriate level of spatial resolution for analysis zones.

To find a suitable method for calculating intrazonal impedances, the study compares both calculated intrazonal impedances and modeled intrazonal trips. The study considers existing methods for calculating intrazonal impedances and a new method that calculates intrazonal impedance by finding the average impedance between node pairs within a zone. The results show that whereas the proposed method provides better estimates of intrazonal impedances, better intrazonal impedance estimates do not guarantee better intrazonal trip estimates. Consequently, non-motorized trips cannot be adequately handled in macroscopic models by improving the calculation of intrazonal impedances. Efforts aimed at improving the calculation of intrazonal impedances should therefore be geared towards reducing the need to deal with intrazonal trips.

In identifying an appropriate level of spatial resolution, the study seeks to minimize a cost function with respect to the number of zones and the deviations in traffic assignment results. The objective is to keep the number of zones to the minimum possible while ensuring low deviations in assignment results. Using network length per zone to define spatial resolution, the study applies the gradual rasterization process with the quadtree concept to create 24 different raster cell systems for different levels of spatial resolution. The study identifies 1,000 m network length per raster cell as an appropriate level of spatial resolution for the study area and indicates

the possibility of adjusting input variables to define context-specific appropriate levels of spatial resolution. The results show that there is a limit beyond which the benefits derived by further increases in spatial resolution is not worth the costs associated with the extremely high increase in the resultant number of zones.

The application of the research findings in the travel demand model of Dachau confirms that mitigating the intrazonal problem improves the modeling of non-motorized trips. The research outcome should facilitate the integration of bicycle and pedestrian travel in the models of planning agencies to enable impact assessment of actions taken to encourage non-motorized travel. This will ensure the successful development and implementation of sustainable mobility concepts.

Contents

List of Tables **v**

List of Figures **vii**

List of Appendices **xi**

List of Abbreviations **xiii**

1 Introduction **1**

1.1 Problem Definition 1

1.2 Research Objectives and Hypotheses 3

1.3 Overview of Methodology 4

1.4 Structure of Dissertation 6

2 State of the Art **8**

2.1 Non-Motorized Trips in Macroscopic Travel Demand Models 8

2.1.1 Factors Influencing Non-Motorized Travel Behavior 8

2.1.2 Structural Choices for Integrating Non-Motorized Travel 11

2.1.3 Intrazonal Trips and Non-Motorized Travel 14

2.2 Intrazonal Impedances of Macroscopic Models 14

2.2.1 Background 14

2.2.2 Existing Methods 15

2.3 Spatial Resolution of Macroscopic Models 18

2.3.1 Constraints to TAZ Definition 18

2.3.2 TAZ Design Approaches 20

2.3.3 Analysis Zones for Non-Motorized Trips 21

2.4 Chapter Summary and Conclusion 22

3 Input Data Preparation 24

3.1 Study Area 24

3.2 Data Assembly and Processing 25

3.2.1 Household Survey Data 25

3.2.2 Zone Systems and Socio-economic Data 34

3.2.3 Transport Network Data 36

3.3 Development of Initial Trip Tables 38

3.3.1 Disaggregation of TAZ level Data to Building Blocks 39

3.3.2 Trip Generation 42

3.3.3 Trip Distribution 45

3.4 Chapter Summary and Conclusion 54

4 Calculating Intrazonal Travel Impedances 56

4.1 Introduction 56

4.2 Proposed Method for Calculating Intrazonal Travel Impedances 57

4.2.1 Measures of Node Centrality 57

4.2.2 The Proposed Method 60

4.3 Comparison of Intrazonal Travel Impedances 62

4.3.1 Aggregation of TAZ 62

4.3.2 Reference Intrazonal Times 62

4.3.3 Calculated Intrazonal Times 63

4.3.4 Comparing Intrazonal Walking Times 65

4.3.5 Comparing Intrazonal Cycling Times 70

4.3.6 Comparing Intrazonal Driving Times 75

4.3.7 Discussion of the Intrazonal Travel Impedance Comparison 80

4.4 Comparison of Model Results 82

4.4.1 Development of Scenarios 83

4.4.2 Trip Length Checks 84
4.4.3 Comparing Intrazonal Trips 86
4.5 Chapter Summary and Conclusion 88

5 Identifying an Appropriate Level of Spatial Resolution 91
5.1 Introduction 91
5.2 Test Area and Reference Raster Cell System 92
5.2.1 Rasterization of Test Area 92
5.2.2 Disaggregation of Initial Trip Tables to Reference Raster Cells 94
5.2.3 Reference Trip Length Frequency Distributions 95
5.2.4 Assignment of Reference Trip Table 95
5.3 Gradual Rasterization and Different Raster Cell Systems 96
5.3.1 Gradual Rasterization Process 97
5.3.2 Aggregation of Reference Trip Table 102
5.3.3 Trip Length Frequency Distributions 102
5.3.4 Traffic Assignment 102
5.4 Comparison of Trip Length Distributions 103
5.5 Comparison of Number of Intrazonal Trips 105
5.6 Comparison of Network Volumes 106
5.7 Comparison of Number of Raster Cells 107
5.8 An Appropriate Resolution 108
5.9 Chapter Summary and Conclusion 111

6 Application in Dachau's Travel Demand Model 113
6.1 Introduction 113
6.2 TAZ Redefinition 113
6.3 Modeling Travel Demand with the Refined Zone System 116

6.4 Comparison to the Classical Travel Demand Model 123
6.4.1 The Classical Travel Demand Model 123
6.4.2 Comparison of Zone Characteristics 123
6.4.3 Comparison of Trip Generation Results 126
6.4.4 Comparison of Trip Distribution Results 128
6.4.5 Comparison of Mode Choice Results 129
6.4.6 Comparison of Assignment Results 131
6.5 Chapter Summary and Conclusion 131

7 Conclusions and Outlook 133
7.1 Summary of Findings 133
7.2 Significance of Research 134
7.3 Limitations of the Study 135
7.4 Further Research Needs 136

References 139

Appendices 145

List of Tables

Table 3.1: Summary of the processed household survey data 29
Table 3.2: Number of trips by age and gender 31
Table 3.3: Number of trips by purpose and car ownership 33
Table 3.4: Summary of network objects 37
Table 3.5: Total connector times per O-D pair 38
Table 3.6: Disaggregating socio-economic data 41
Table 3.7: Disaggregating travel survey data 42
Table 3.8: Trip production rates 43
Table 3.9: Trip attraction variables, estimated rates and model fit 44
Table 3.10: Impedance function parameters 47
Table 3.11: Trip distribution results summary 54
Table 4.1: Intrazonal impedance calculation methods 64
Table 4.2: Impedance function parameters 83
Table 4.3: Intrazonal trips and shares 87

List of Figures

Figure 1.1: Methodological and conceptual framework 5
Figure 2.1: Non-motorized trips in four-step models (Source: Singleton and Clifton, 2013) 12
Figure 3.1: Dachau in District of Dachau (Inset: Municipalities in Bavaria; Source: Hagar66, 2010) 25
Figure 3.2: Modal split of all trips (expanded) 28
Figure 3.3: Modal split of internal trips (expanded) 28
Figure 3.4: Modal split of final sample (expanded) 30
Figure 3.5: Number of trips by mode and distance (expanded) 30
Figure 3.6: Modal split by age and gender (expanded) 32
Figure 3.7: Modal split by purpose and car ownership (expanded) 33
Figure 3.8: TAZ in Dachau (Source: Civil Engineering Department, Stadt Dachau) 34
Figure 3.9: Building blocks (Source: Civil Engineering Department, Stadt Dachau) 35
Figure 3.10: Hypothetical study area 39
Figure 3.11: TLFD for HBW trips by car owners 48
Figure 3.12: TLFD for HBW trips by non-owners 49
Figure 3.13: TLFD for HBS trips by car owners 49
Figure 3.14: TLFD for HBS trips by non-owners 50
Figure 3.15: TLFD for HBE trips 50
Figure 3.16: TLFD for HBR trips by car owners 51
Figure 3.17: TLFD for HBR trips by non-owners 51
Figure 3.18: TLFD for HBO trips by car owners 52
Figure 3.19: TLFD for HBO trips by non-owners 52
Figure 3.20: TLFD for NHB trips by car owners 53
Figure 3.21: TLFD for NHB trips by non-owners 53
Figure 4.1: A star network (Source: Freeman, 1978) 58
Figure 4.2: Proposed intrazonal impedance calculation method 61
Figure 4.3: Distribution of reference and calculated intrazonal walking times 66
Figure 4.4: Deviations from reference 1 intrazonal walking times 67
Figure 4.5: Deviations from reference 2 intrazonal walking times 68

Figure 4.6: Deviations from reference 1 walking times by zone system 69
Figure 4.7: Deviations from reference 2 walking times by zone system 69
Figure 4.8: Distribution of reference and calculated intrazonal cycling times 71
Figure 4.9: Deviations from reference 1 intrazonal cycling times 72
Figure 4.10: Deviations from reference 2 intrazonal cycling times 73
Figure 4.11: Deviations from reference 1 cycling times by zone system 74
Figure 4.12: Deviations from reference 2 cycling times by zone system 74
Figure 4.13: Distribution of reference and calculated intrazonal driving times 76
Figure 4.14: Deviations from reference 1 intrazonal driving times 77
Figure 4.15: Deviations from reference 2 intrazonal driving times 78
Figure 4.16: Deviations from reference 1 driving times by zone system 79
Figure 4.17: Deviations from reference 2 driving times by zone system 79
Figure 4.18: Summary of deviations from reference intrazonal times 80
Figure 4.19: Deviations from observed average trip lengths 84
Figure 4.20: Coincidence ratios between modeled and observed TLFD 85
Figure 4.21: Deviations from observed intrazonal trips 86
Figure 4.22: Deviations from observed intrazonal trip shares 88
Figure 5.1: Dachau and the test area 92
Figure 5.2: Reference raster cells (Background image: OpenStreetMap contributors, 2016) 94
Figure 5.3: Gradual rasterization process 98
Figure 5.4: Gradual rasterization output 1 (Background image: OpenStreetMap contributors, 2016) 99
Figure 5.5: Gradual rasterization output 2 (Background image: OpenStreetMap contributors, 2016) 99
Figure 5.6: Gradual rasterization output 3 (Background image: OpenStreetMap contributors, 2016) 100
Figure 5.7: Gradual rasterization output 4 (Background image: OpenStreetMap contributors, 2016) 100
Figure 5.8: Gradual rasterization output 5 (Background image: OpenStreetMap contributors, 2016) 101
Figure 5.9: Gradual rasterization output 6 (Background image: OpenStreetMap contributors, 2016) 101
Figure 5.10: Deviations from reference average trip lengths 103

Figure 5.11: Coincidence ratio between reference and computed TLFD 104
Figure 5.12: Intrazonal trips as a share of total trips 105
Figure 5.13: Deviations from reference network volumes 107
Figure 5.14: Number of raster cells 108
Figure 5.15: Cost function input variables 110
Figure 5.16: Cost function curves 110
Figure 6.1: Initial single raster cell (Background image: OpenStreetMap contributors, 2016) 114
Figure 6.2: Final output (Background image: OpenStreetMap contributors, 2016) 115
Figure 6.3: Refined zone system 116
Figure 6.4: Mode shares for HBWa 117
Figure 6.5: Mode shares for HBWb 118
Figure 6.6: Mode shares for HBSa 118
Figure 6.7: Mode shares for HBSb 119
Figure 6.8: Mode shares for HBE 119
Figure 6.9: Mode shares for HBRa 120
Figure 6.10: Mode shares for HBRb 120
Figure 6.11: Mode shares for HBOa 121
Figure 6.12: Mode shares for HBOb 121
Figure 6.13: Mode shares for NHBa 122
Figure 6.14: Mode shares for NHBb 122
Figure 6.15: Refined zones in Dachau (Background image: OpenStreetMap contributors, 2016) 124
Figure 6.16: Original TAZ in Dachau (Background image: OpenStreetMap contributors, 2016) 125
Figure 6.17: Variability in trip productions 127
Figure 6.18: Variability in trip attractions 127
Figure 6.19: Intrazonal trips as a share of total trips 129
Figure 6.20: Difference in mode shares between refined and original TAZ systems 130

List of Appendices

Appendix 1: Python Script for Calculating Intrazonal Impedances 146
Appendix 2: Python Script for Gradual Rasterization..... 151

List of Abbreviations

ft.	Feet
h	Hour
HBE	Home-based education
HBO	Home-based other
HBOa	Home-based other trips by car owners
HBOb	Home-based other trips by non-owners
HBR	Home-based recreation
HBRa	Home-based recreation trips by car owners
HBRb	Home-based recreation trips by non-owners
HBS	Home-based shopping
HBSa	Home-based shopping trips by car owners
HBSb	Home-based shopping trips by non-owners
HBW	Home-based work
HBWa	Home-based work trips by car owners
HBWb	Home-based work trips by non-owners
km	Kilometer
m	Meter
NHB	Non-home-based
NHBa	Non-home-based trips by car owners
NHBb	Non-home-based trips by non-owners
O-D	Origin-Destination

TAZ Transport Analysis Zone

TLFD Trip Length Frequency Distribution

1 Introduction

1.1 Problem Definition

In the quest for sustainable mobility solutions, non-motorized modes of transport have received increased attention due to the potential environmental, social, and health benefits associated with pedestrian and bicycle travel. By serving as a cheaper alternative to automobile travel, walking and cycling can alleviate stress on fuel resources, reduce congestion, and improve environmental quality. Likewise, walking and cycling can contribute to the improved health of a society, serve as an avenue for recreation, and promote livable communities by providing increased opportunities for interaction among individuals. Consequently, the desire to promote non-motorized transport has increased, and the subject of non-motorized transport has been studied not only in the field of transport, but also in the field of public health (Bhat et al., 2005; Sallis et al., 2004). Whereas transport agencies see walking and cycling as means to alleviate traffic congestion and reduce vehicular emissions, health agencies consider these modes as means to boost the levels of physical activity among individuals (Bhat et al., 2005; Guo et al., 2007).

Improved conditions for bicyclists and pedestrians have been considered means to increase walking and cycling, and as stated by Litman et al. (2015), virtually all communities that have increased non-motorized transport have achieved this by improving their walking and cycling environments. However, Porter et al. (1999) caution against adopting the attitude of “if you build it, they will come”, and emphasize the need for reasonable estimates of usage and corresponding benefits. Evaluation of usage and benefits arising from improvements to non-motorized transport as against alternative transport projects is required for efficient allocation of the finite resources available for transport improvements.

Furthermore, the built environment is considered to influence non-motorized travel (Cervero et al., 2009; Cervero and Duncan, 2003; Guo et al., 2007; Rodríguez and Joo, 2004), and a number of urban-planning philosophies such as new urbanism, transit-oriented development, and traditional town planning have sought to reduce motorized trips while increasing non-motorized trips (Cervero and Kockelman, 1997).

However, Guo et al. (2007) emphasize that not all strategies aimed at increasing non-motorized travel result in decreased motorized travel. According to Guo et al. (2007), a complementary effect can emerge where levels of motorized travel stay the same; a synergistic effect can also appear where motorized travel increases along with an increase in non-motorized travel. As important as it is to identify actions that can encourage the use of non-motorized transport modes, the ability to assess the impacts of these actions is even more crucial. Assessing the impacts of potential actions, according to Forschungsgesellschaft für Straßen- und Verkehrswesen (2014), will ensure the successful development and implementation of sustainable mobility concepts. Such assessments require a good understanding of non-motorized travel behavior, and the development of methods capable of estimating non-motorized travel demand along with motorized travel in a single framework.

Non-motorized modes are already very important modes for urban travel, and although most travel surveys under-record non-motorized trips (Litman et al., 2015), they constitute a high share of trips in urban areas. In Munich, 42% of all trips are made by non-motorized travel modes, and the non-motorized share is even higher in Amsterdam and Paris making up 50% of all trips (Van Audenhove et al., 2014). In addition, they are important access and egress modes that make up a decent share of trips that are not accounted for. Non-motorized trips can therefore not be ignored in urban transport analyses.

The need to consider non-motorized modes in mainstream travel demand modeling has been recognized and many planning agencies have attempted or desired to incorporate non-motorized travels in their models. However, conventional models, which forecast travel demand in four steps, have traditionally focused on motorized transport, and although these could incorporate non-motorized transport in several ways, the coarse nature of such models poses difficulty in the representation of non-motorized travel. Non-motorized trips are generally short trips, and in such macroscopic models, many of them end up in the same transport analysis zone (*TAZ*) from which they originate. Since the spatial aggregation nature of these models makes it difficult to model intrazonal trips, the treatment of non-motorized trips in such models is limited.

Two possible ways to mitigate the intrazonal problem of macroscopic models for non-motorized trip modeling include: (1) improving the modeling of intrazonal trips; and (2) reducing the need to model intrazonal trips. According to the Center for Urban Transportation Studies (1999), the number of intrazonal trips within the gravity model for trip distribution is controlled entirely by the size of the intrazonal impedance. Accordingly, improving the modeling of intrazonal trips requires good estimates of intrazonal impedances. However, because each TAZ is represented by a single centroid, the centroid-to-centroid approach of measuring travel impedances would amount to zero impedance for intrazonal trips. Whereas a number of methods exist for approximating intrazonal impedances, they are, according to Kordi et al. (2012), not applicable under all circumstances because of the assumptions they are based on. The calculation of intrazonal impedance is thus an ongoing challenge in macroscopic models.

The second approach to mitigating the intrazonal problem, which seeks to reduce the need to model intrazonal trips, requires a reduction in sizes of TAZ to limit the frequency of intrazonal trips. Although the use of more refined TAZ systems will ensure that models are compatible with the scale of short trips, Viegas et al. (2009) point out the loss of statistical precision associated with more detailed TAZ. Moeckel and Donnelly (2015) also allude to the conceptual and computational issues associated with the use of highly disaggregate models which include the instability of destination choice models and the slowing down of traffic assignment due to the resultant large number of zones. Ortúzar and Willumsen (2011) also draw attention to the difficulty in forecasting at the same level of detail, changes at the individual household level affecting demand. As indicated by Wegener (2011), the future of urban transport and land use modeling is not refinement and detail but the identification of the appropriate level of conceptual, spatial and temporal resolution.

1.2 Research Objectives and Hypotheses

The research seeks to enhance the capability of macroscopic travel demand models in modeling non-motorized travel demand by finding a suitable method for calculating intrazonal impedances, and identifying an appropriate level of spatial resolution for TAZ. The study is motivated by the recognition of the role of non-motorized travel in

sustainable mobility, the usefulness of models in forecasting travel demand, and the limited representation of non-motorized trips in macroscopic travel demand models.

To find a suitable method for calculating intrazonal impedances, and to identify an appropriate level of spatial resolution for modeling non-motorized trips, the research works with the following hypotheses:

1. The average impedance between network node pairs within a zone is a better measure of the zone's intrazonal impedance than values calculated with existing methods;
2. Better estimates of intrazonal impedances guarantee better estimates of intrazonal trips; and
3. If zone resolution is made finer, while network detail among other things is held constant, a point will be reached beyond which further increases in zone resolution will lead to decreases in overall model benefit.

While the first hypothesis seeks to devise a method to improve the calculation of intrazonal impedances, the second hypothesis assesses the extent of influence of intrazonal impedance on the number of intrazonal trips. The third hypothesis determines the extent to which TAZ should be refined.

1.3 Overview of Methodology

To achieve the objectives of the research, the study was broken down into a number of tasks, which are summarized in Figure 1.1 along with the conceptual framework that guided the research.

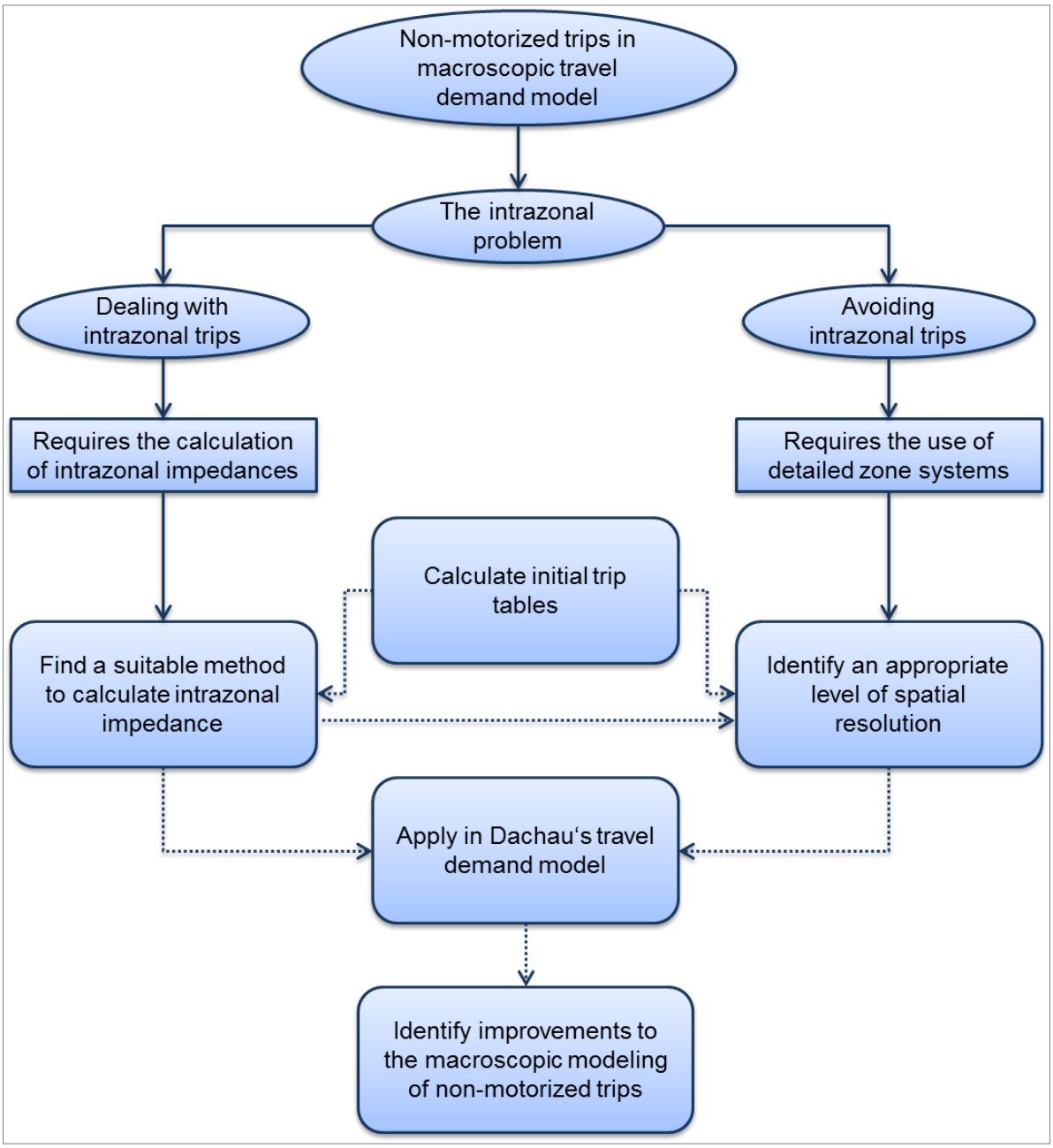

Figure 1.1: Methodological and conceptual framework

The main goal of the research was to enhance the capability of macroscopic travel demand models in modeling non-motorized travel demand. Recognizing the mitigation of the intrazonal problem as key to improving non-motorized trip modeling in macroscopic models, the study started with the first mitigation approach which sought to find a suitable method for calculating intrazonal impedances to improve the modeling of intrazonal trips. To accomplish this task, the study developed initial trip tables that were used to compute reference values against which calculated intrazonal impedances would be compared. The search for a suitable intrazonal

impedance calculation method involved comparisons of intrazonal impedances as well as intrazonal trips.

Since the outcome of the first approach indicated that intrazonal trips could not be dealt with adequately in a macroscopic model, the research explored the second approach which sought to reduce the need to deal with intrazonal trips by identifying an appropriate level of spatial resolution for TAZ. To accomplish this task, the initial trip tables that had been developed for the first approach were used to create a reference scenario against which comparisons would be made. Different zone systems were generated at different levels of spatial resolution and their results were compared to model results from the reference scenario.

While an appropriate level of spatial resolution seeks to reduce the influence of intrazonal trips on model results, dealing with surplus intrazonal trips requires the calculation of intrazonal impedances. The outcomes of the two-part study were applied to model travel Demand in Dachau. Subsequently, model results were compared to results from a classical travel demand model of Dachau to enable an assessment of the enhancement to macroscopic modeling of non-motorized trips that the research sought to achieve.

1.4 Structure of Dissertation

This dissertation is organized into seven chapters. Following this introductory chapter that presents the research objectives and the methodological framework of the research, chapter 2 presents the state of the art on macroscopic modeling of non-motorized trips, intrazonal impedance calculation as well as the definition of TAZ. This is followed by a description of the study area and the data assembly process in chapter 3. Chapter 3 also includes a description of the process involved in developing initial trip tables used as input to the approaches explored in this research.

Chapters 4 and 5 describe the two main foci of this research. While chapter 4 focuses on finding a suitable method for calculating intrazonal impedances, chapter 5 focuses on identifying an appropriate level of spatial resolution for modeling non-motorized trips in macroscopic travel demand models. The application of the research

outcomes to the travel demand model of Dachau is described in chapter 6, along with an assessment of the enhancement to macroscopic modeling of non-motorized trips offered by the study.

Finally, chapter 7 summarizes the contributions of this research and provides an overview of follow-up studies that could be done to build on the research findings.

2 State of the Art

2.1 Non-Motorized Trips in Macroscopic Travel Demand Models

After a comprehensive review of the state of practice for forecasting non-motorized travel, Schwartz et al. (1999) identified a number of areas where additional research and methodological development could be particularly useful. They made three major recommendations which included: (1) the need for a manual covering bicycle and pedestrian sketch-planning in the short term; (2) further research on factors influencing non-motorized travel behavior; and (3) integration of bicyclists and pedestrian considerations into mainstream transport models and planning.

In emphasizing the need to focus on improving macroscopic travel demand models to include bicycle and pedestrian travel, Porter et al. (1999) argued that such models had the unique advantage of offering an integrated framework for predicting travel decisions. They also maintained that the inclusion of non-motorized modes in travel demand models would improve capabilities for forecasting both motorized and non-motorized travel and would place non-motorized modes on a level playing field with motorized modes in transport planning. Eash (1999) described the modeling of non-motorized travel as part of total travel a necessity if agencies were to evaluate how development scenarios affected growth in vehicle travel.

According to Kuzmyak et al. (2014), if choices are captured correctly, the macroscopic travel demand model allows for multiple forces to interact in producing the final outcome while providing multiple places for testing planning interventions or other assumptions.

2.1.1 Factors Influencing Non-Motorized Travel Behavior

As described by Bhat et al. (2005), assessments of the usage and benefits of non-motorized transport options against other alternative transport projects require a good understanding of non-motorized travel behavior to ascertain the impact of policy actions aimed at encouraging bicycle and pedestrian travel.

Travel behavior encompasses a wide range of decisions that people make with respect to trip making. These include among others the decision to make a trip, the choice of destination, the choice of travel mode, the choice of time of day to make a trip as well as the choice of route. The decision to make a trip to a particular destination at a particular time with a non-motorized mode of transport is influenced by a number of factors beyond those used to predict demand for motorized travel. According to Schwartz et al. (1999), standard travel demand modeling procedures generally predict total trip-making and mode choice based on a limited number of variables, such as household characteristics and the time and cost of competing modes which only partially explain the decision to bicycle or walk.

A broad range of factors influence the level of non-motorized travel, and according to Bhat et al. (2005) these can be categorized into: (1) demographic and socio-economic characteristics; (2) trip characteristics; (3) environment factors; and (4) attitude and perception. Whereas strong evidence exists to support the influence of traveler demographics and trip conditions on the choice of non-motorized travel, the influence of the built environment is inconclusive. Cervero and Kockelman (1997) identified three dimensions of the built environment that affect travel behavior, namely density, diversity, and design which they termed the 3Ds. Destination accessibility and distance to transit are often added as the fourth and fifth Ds respectively (Boarnet, 2012).

Using household activity data from San Francisco region, Cervero and Duncan (2003) studied the links between urban environments and non-motorized travel. After controlling for various demographic, environmental and design factors, their results suggested that built environment factors had relatively little effect while demographic factors and trip conditions had a stronger effect on non-motorized mode choice. Rodríguez and Joo (2004) on the other hand found attributes of the local physical environment to contribute to explaining mode choice. They examined the relationship between travel mode choice and attributes of the local physical environment while accounting for typical modal characteristics such as travel time and cost. Their results revealed that local topography and sidewalk availability were significantly associated with the attractiveness of non-motorized modes.

A number of urban design philosophies that aim at shaping travel demand assert that high density, mixed land use and pedestrian friendly neighborhoods increase non-motorized travel (Cervero and Kockelman, 1997; Guo et al., 2007). Cervero et al. (2009) examined the association of built environment characteristics to non-motorized travel in Bogota, Colombia, which is well known for its sustainable urban transport systems including an extensive network of bike lanes. Their results suggested that non-motorized choices were affected by facility design characteristics such as connectivity and density of streets rather than other built environment factors such as density, land-use mix and destination accessibility. They concluded that it was facility design, and not generic land-use attributes that swayed non-motorized travel.

With regards to the route choice of pedestrians, a study by Seneviratne and Morrall (1985) using O-D survey conducted in Calgary, Alberta found that most pedestrians chose the shortest route and factors such as level of congestion, safety and visual attractions were only secondary. Their results suggested that distance was a major determinant to pedestrians' route choice.

Using survey data to examine the factors that influence the route choice of pedestrians who walked to railway stations in Portland and San Francisco Bay Area, Agrawal et al. (2008) found that pedestrians perceived time and distance minimization to be their primary consideration in selecting routes while safety, route attractiveness, sidewalk quality and the absence of long waits at traffic lights were secondary factors pedestrians considered.

On the route choice of cyclists, a study by Stinson and Bhat (2003) estimated binary logit models to evaluate the importance of factors affecting commuter bicyclits' route choices using data from a stated preference survey they conducted across the United States. Their results suggested that travel time was the most important factor commuter bicyclists considered in choosing a route. They also found the presence of a bicycle facitlity, the level of automobile traffic, pavement or riding surface quality, and presence of a bicycle facility on a bridge as very important determinants of commuter bicyclists' route choices.

In a similar study by Sener et al. (2009), they estimated mixed multinomial logit models using data from a web-based stated preference survey of Texas bicyclists. Their results emphasized the importance of a comprehensive evaluation of both route-related attributes and bicyclists' demographics in route choice decisions. Their results also confirmed the study by Stinson and Bhat (2003) that travel time was the most important factor that influenced the route choice of commuter bicyclists. They also found traffic volume, speed limit, on-street parking characteristics, bicycle route continuity, number of stop signs, red lights, cross streets and roadway terrain to have impact on bicyclists' route choice.

While there are many factors that can potentially influence non-motorized travel behavior, Porter et al. (1999) emphasize the need to focus on factors that can be modeled, are significant and can be created with relative ease from existing data sources or future survey efforts.

2.1.2 Structural Choices for Integrating Non-Motorized Travel

In reviewing the current practice of incorporating non-motorized travel in macroscopic models, Liu et al. (2012) observed that some progress with the representation of non-motorized travel in macroscopic models had been made. They identified several ways in the four-step modeling framework in which the non-motorized travel component could be structured, and underscored the need to consider these structural choices in the quest to improve non-motorized travel modeling.

According to Singleton and Clifton (2013), non-motorized trips can be generated on their own, separated from motorized trips before or after trip distribution, distinguished from trips of other modes during mode choice, or further segmented into walk and bicycle trips. Liu et al. (2012) categorized these structural choices into pre-distribution, pre-mode choice, and mode choice structures. They also pointed out the possibility of carrying the treatment of non-motorized travel through a route choice-trip assignment stage. The different structural options are summarized in Figure 2.1.

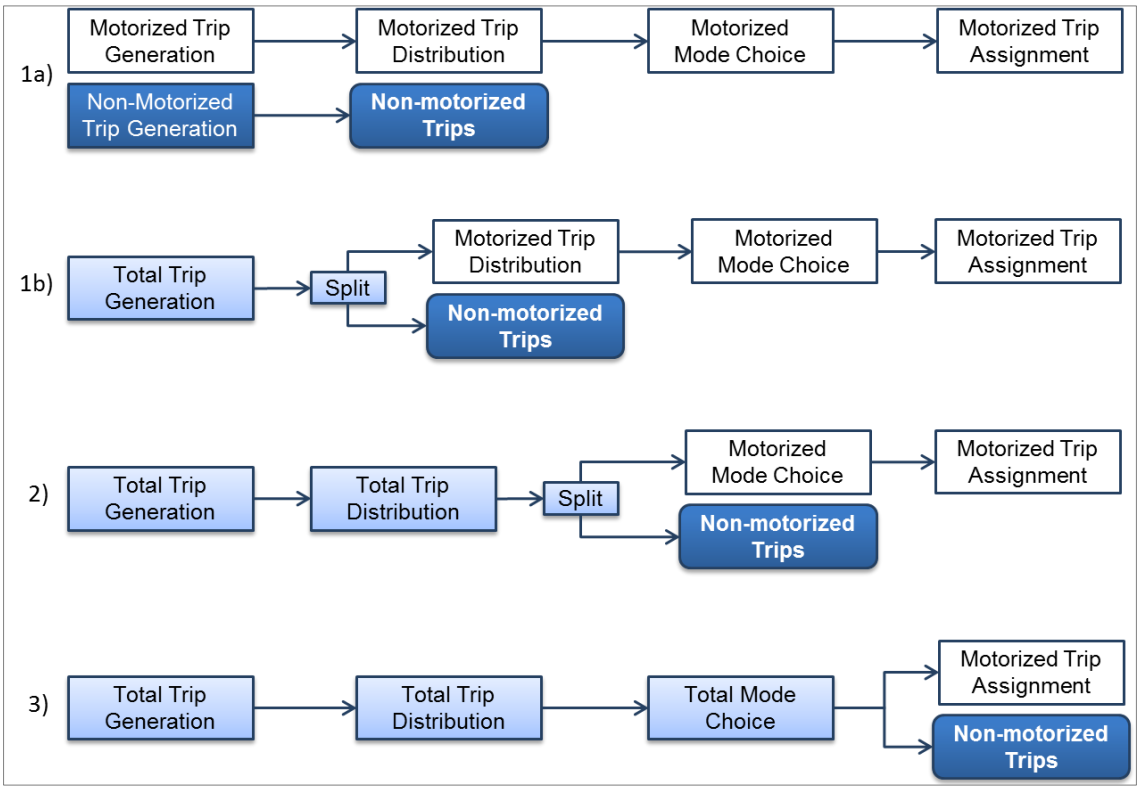

Figure 2.1: Non-motorized trips in four-step models (Source: Singleton and Clifton, 2013)

Options 1a and 1b are both pre-trip distribution structures. Whereas option 1a involves separately generating motorized and non-motorized trips, option 1b generates these trips together but then separates non-motorized trips from motorized trips before trip distribution. Option 2, the pre-mode choice structure, generates and distributes trips together but separates non-motorized trips from motorized trips before mode choice. According to Singleton and Clifton (2013), option 2 is appropriate for agencies with insufficient pedestrian and bicycle records who wish to avoid the complication of estimating a full mode choice model. Here, binary logit models are used to split total trips into motorized and non-motorized trips and the motorized trips are split further at the mode choice step. Option 3, on the other hand, considers non-motorized trips as modal options in a full mode choice model. Here, pedestrian and bicycle can be represented as individual modes and placed in equal competition with other modes or lumped together into a single non-motorized mode. They can also be placed in a non-motorized nest for a stronger intra-non-motorized mode substitution effect.

The advantages of options 1a and 1b lie in the ease with which they can be integrated in existing models (Liu et al., 2012; Singleton and Clifton, 2013) as well as their potential to incorporate a variety of policy-related variables (Liu et al., 2012). However, because measures that require knowledge of both origins and destinations such as distance and travel time cannot be directly incorporated, these options, according to Liu et al. (2012) are limited in their capacity to evaluate non-motorized travel O-D patterns.

Whereas Option 2, can incorporate variables at the O-D level, thereby increasing its potential for planning applications, Liu et al. (2012) point out its inability to evaluate trade-offs among different modes since the split occurs before the mode choice step. According to Liu et al. (2012), option 3 handles this limitation and permits the incorporation of trade-offs into the model, enabling a more accurate representation of travel behavior in a systematic way.

Despite the advantages that option 3 offers, Liu et al. (2012) observed a limitation in the lack of policy sensitivities to potential trade-offs in current practices. They indicated that aggregation errors might explain why some policy related variables became insignificant during model estimation. Macroscopic models use TAZ as their geospatial structure and according to Kuzmyak et al. (2014), their level of aggregation is incompatible with the scales of non-motorized travel since they lack the fine granularity necessary to capture the essence of non-motorized travel choice factors. To enhance the capability of macroscopic models in modeling non-motorized travel, several authors (Eash, 1999; Liu et al., 2012; Porter et al., 1999; Singleton and Clifton, 2013) have recommended the use of more refined zone systems as well as the revision of the variables considered.

Beyond the challenges posed by the sizes of TAZ, Singleton and Clifton (2013) have identified a number of other barriers to representing non-motorized travel. These include: (1) insufficient non-motorized travel survey records; (2) limited data collection and model development resources; as well as (3) lack of decision-maker interest.

2.1.3 Intrazonal Trips and Non-Motorized Travel

The coarse nature of analysis zones has been identified as one of the main challenges in handling non-motorized trips in macroscopic travel demand models. Besides the lack of fine granularity necessary to capture the essence of non-motorized travel choice factors (Kuzmyak et al., 2014), it causes a majority of non-motorized trips to terminate in the same zones in which they originate. In summarizing criticisms of the four-step model, Schiller et al. (2010) cited its inability to predict non-motorized travel behavior as a limitation, and attributed this difficulty to the short intrazonal nature of non-motorized trips.

The close relationship between non-motorized trips and intrazonal travel has been described by many researchers in different ways. Eash (1999) observed that most walking and cycling trips took place inside the large analysis zones of travel demand models. Bhatta & Larsen (2011) also concluded that intrazonal trips were more likely to be made by non-motorized modes compared with motorized modes. Since walking and cycling trips tend to be relatively short compared with motorized trips, Liu et al. (2012) pointed out that non-motorized trips frequently fell into the rather uninformative intrazonal trip category.

Non-motorized trips can not be treated without recourse to intrazonal travel. With the spatial aggregation nature of macroscopic models making it difficult to model intrazonal trips, the treatment of non-motorized trips in such models is limited. However, considering the high share and increasing importance of non-motorized modes for urban travel (Litman et al., 2015; Van Audenhove et al., 2014), it is unacceptable to disregard these trips in urban transport analyses. There is therefore the need to mitigate the intrazonal problem of macroscopic models to enhance the modeling of non-motorized trips.

2.2 Intrazonal Impedances of Macroscopic Models

2.2.1 Background

Intrazonal trips have their origins and destinations in the same TAZ, and since all trip ends within a zone are represented by a single centroid, these trips are not

represented on the network in aggregate transport modeling analysis. Due to the lack of representation on the transport network, volume-delay-functions do not respond to intrazonal traffic and vehicle miles travelled cannot be correctly estimated. Modeling intrazonal trips requires the calculation of intrazonal impedances but the absence of paths over which these impedances can be measured makes it difficult to model intrazonal trips.

A common approach to avoid the intrazonal impedance problem is to simply exclude intrazonal trips from the analysis (Kordi et al., 2012). However, excluding intrazonal trips in model estimation results in biased sample which produces biased parameter estimates (Bhatta and Larsen, 2011) and also leads to inefficient allocation of trips to other zones (Greenwald, 2006). At the same time, the issue of intrazonal travel has become more important due to the increased representation of non-motorized modes in travel demand models. Non-motorized trips are generally short trips, so in macroscopic models, many of them end up in the same TAZ.

Although recent modeling practices tend to use more refined zone systems to reduce the need to deal with intrazonal trips, for many areas, structural data needed for modeling are mostly available at relatively coarser levels of spatial resolution. If zone sizes cannot be refined to reduce the frequency of intrazonal trips, there is the need for estimates of the number of trips that stay within each zone in order to ensure efficient allocation of trips to other zones.

2.2.2 Existing Methods

Travel impedances, which measure the cost of traveling between an origin and a destination, play a significant role in travel demand modeling. They are important for trip distribution, mode choice, route choice, and in cases where accessibility is considered, trip generation. In macroscopic models, travel impedances are measured along the paths joining the centroids of zone pairs. However, because intrazonal trips begin and end on the same centroid, there are no paths along which their impedances can be measured. As a result, various methods have been used over the years to calculate intrazonal impedances. These methods have been

described by Kordi et al. (2012) as highly approximate, and applicable only in certain circumstances.

2.2.2.1 Nearest Neighbor Technique

One of the earliest attempts to determine intrazonal driving time halves the average of the driving times to adjacent zones (United States Bureau of Public Roads, 1965). This approach, called the nearest neighbor technique, forms the basis of most of the methods used to calculate intrazonal travel times (Bhatta and Larsen, 2011). Recognizing the importance of intrazonal trips in the analysis of air quality, Venigalla et al. (1999) used the technique to calculate intrazonal trip length and duration as half the distance and travel time respectively to the centroid of the nearest zone.

2.2.2.2 Area-Based Methods

Other methods compute the average length of an intrazonal trip as a function of the area of the zone (Bhatta and Larsen, 2011), relying mostly on various assumptions regarding zone shape and population distribution (Kordi et al., 2012).

Batty 1976

One of the simplest forms of this approach suggested by (Batty, 1976) works on the assumption that zones are roughly circular in shape and population is spread evenly at constant density within a zone. With these two assumptions, he approximated the intrazonal travel cost c_{ii} as:

$$c_{ii} = \frac{r_i}{\sqrt{2}}$$

where r_i is the radius of the zone in terms of travel cost. Assuming that population density was not constant but varied in a regular way, he made a modification to the approximation but maintained that both methods were probably more of analytical than practical interest.

Martin and McGuckin 1998

Another form of the area-based methods described in Martin & McGuckin (1998) calculates intrazonal travel time as:

$$Intrazonal\ Time = 0.5 \times \sqrt{(Zonal\ Area)} \times 60 + Intrazonal\ Speed(Area\ Type)$$

where the intrazonal time is expressed in minutes, the zonal area is expressed in square miles, and the intrazonal speed in miles per hour, varying by the area type of the zone.

2.2.2.3 Average Trip Length Methods

Dowling 2005

A method used to calculate intrazonal travel time for the Dallas-Fort-Worth Area (Dowling, 2005) first divides each zone into 13 concentric squares, and determines the mean intrazonal distance by averaging the distances from the zone centroid to the perimeter of each of the squares. Afterwards, a table of speeds by area type and time of day is used to compute the intrazonal travel time from the intrazonal distance.

Batty 1976

After suggesting a number of these approximate methods, Batty (1976) asserted that the most consistent way of defining intrazonal trip distance was to disaggregate trip and distance data within individual zones and calculate the average trip distance. This he viewed as a problem of finding the average length of trips within a zone. If a zone *i* is divided into *x* origin subzones and *y* destination subzones, then the intrazonal distance d_{ii} can be expressed as:

$$d_{ii} = \frac{\sum_x \sum_y T_{xy} \times d_{xy}}{\sum_x \sum_y T_{xy}}; \quad x, y \in i$$

where T_{xy} is the number of trips from subzone *x* to *y* and d_{xy} is the travel distance between subzones *x* and *y*. The lack of data for this process however makes the method practically difficult to use (Batty, 1976; Kordi et al., 2012).

Kordi et al. 2012

Recognizing the lack of data for the consistent process described by Batty (1976), Kordi et al. (2012) developed a method where origins and destinations of intrazonal trips are scattered within their zones and their average trip length is computed. Two approaches they suggested to create multiple origins and destinations within zones include: (1) randomly scattering trip ends; and (2) using available density surfaces to

scatter trip ends. While the random nature of the scattering makes the first approach unstable, the second approach requires density surfaces which are not always available at the desired high resolutions. In addition, the method considers Euclidean distances between trip ends which do not reflect actual travel distances.

2.3 Spatial Resolution of Macroscopic Models

2.3.1 Constraints to TAZ Definition

According to Ortúzar and Willumsen (2011), one of the most important early choices facing the transport modeler is that of the level of detail to be adopted in a study and this entails the zoning system as well as network definition. Although the zone system has substantial influence on model results (Ding, 1998; Khatib et al., 2001; Moeckel and Donnelly, 2015; Openshaw, 1977; Viegas et al., 2009), the resolution and design of zones is rarely analyzed systematically and is often considered more art than science (Moeckel and Donnelly, 2015).

Nevertheless, decades of practice and research have led to the establishments of some guidelines and constraints to the definition of TAZ. Martínez et al. (2009) summarized these guidelines and consraints as follows:

1. Trip generation / attraction homogeneity;
2. Contiguity and convexity of zones;
3. Compactness of TAZ shapes;
4. Exclusiveness (no doughnuts or islands) of zones;
5. Equity in terms of trip generation (small standard deviation across zones);
6. Adjustment of TAZ boundaries to political, administrative, or statistical boundaries;
7. Respect of physical separators;
8. Consideration of decision makers' preferences in determining the number of TAZ;
9. Avoidance of main roads as zone boundaries;
10. Selection of zone size to minimize aggregation errors caused by the assumption that all activities are concentrated at the centroid (geographical precision);

11. Minimization of intrazonal trips; and
12. Maximization of the statistical precision of the estimation of the O-D matrix cells.

Ortúzar and Willumsen (2011) added that zones did not have to be of equal size, and if anything, they could be of similar dimensions in travel time units, therefore generating smaller zones in congested than in uncongested areas. Wulfhorst (2013) also highlighted the need for smaller zones in the core of the planning area, with size increasing as zones get farther away from the core.

According to Ding (1998), homogeneity contributes to the improvement of trip generation estimates and the reduction of intrazonal trips for various trip purposes, while contiguity ensures that the TAZ system is exclusive, complete and unique. The convexity and compactness of TAZ shapes allows an easy determination of their centroid connectors (Ortúzar and Willumsen, 2011), and improves the estimates of O-D matrices (Ding, 1998). The equity of trip generation, according to Ding (1998), ensures diverse trip assignments so that every network has a chance of getting loaded.

The adjustment of TAZ boundaries to political, administrative, or statistical boundaries is important from the point of view of data collection (Ding, 1998). According to Ortúzar and Willumsen (2011), this is probably the fundamental criterion and therefore other criteria should only be followed if they do not lead to inconsistencies with it. The respect of physical separators ensures that there is no travel barrier imposed within a zone (Ding, 1998). Nevertheless, the use of main roads as boundaries, according to Ortúzar and Willumsen (2011) should be avoided since it increases the difficulty of assigning trips to zones when they start or end at the boundary between two or more zones.

It is difficult to give equal consideration to and implement all criteria in a single process because some criteria contradict others (Ding, 1998; Martínez et al., 2009). To account for these conflicts, a zone design algorithm developed by Ding (1998) considered three key principles which include: (1) taking as many criteria as possible

into account; (2) ranking criteria and putting them in a non-conflicting order; and (3) introducing decision makers' preferences.

Despite the existence of guidelines and constraints for defining TAZ, a very important criterion that is mostly overlooked in the definition of TAZ is the consideration of the represented transport network. Travel demand modeling involves interaction between travel demand represented by the TAZ, and transport supply whose key component is the transport network. Whereas intuition supports the relevance of the represented network in the definition of TAZ, hardly is there any empirical evidence to support this. According to Moeckel and Donnelly (2015), the right balance between zones and network has hardly been studied systematically. With network given as a fixed model component, any balance between zone and network requires the modification of zone sizes to match network.

2.3.2 TAZ Design Approaches

Like spatial analysis, travel demand modeling requires spatial data aggregation in TAZ, which according to Martínez et al. (2009) is one source of inaccuracy of transport analysis derived from the arbitrary delineation of TAZ boundaries. However, unlike spatial analysis that has less concern about zone shape (Moeckel and Donnelly, 2015), travel demand modeling needs to avoid oddly shaped zones (Ding, 1998; Martínez et al., 2009; Moeckel and Donnelly, 2015; Ortúzar and Willumsen, 2011).

According to Moeckel and Donnelly (2015), most existing approaches that automatically generate zones allow the creation of irregular shapes which are to be avoided in modeling. Nevertheless, a number of systematic approaches have been developed particularly for TAZ design.

Ding (1998) developed a GIS-based human-interactive TAZ design algorithm that took as many zone design criteria as possible into account, ranking them in a non-conflicting order and introducing decision makers' preferences. Their algorithm searched for seed units into which all other units would merge, considering the highest population density units and ensuring spatial separation between seeds.

Martínez et al. (2009) developed a comprehensive approach to the definition of TAZ based on a smoothed density surface of geocoded travel demand data. Their algorithm aimed to minimize the loss of information when moving from a continuous representation of the origin and destination of each trip to their discrete representation through zones. They focused on the trade-off between the statistical precision, geographical error, and the percentage of intrazonal trips of the resulting O-D matrix.

Moeckel and Donnelly (2015) developed a methodology to automatically create a new zone system based on the quadtree algorithm. Using disaggregated population and employment data, they generated gradual raster cells where smaller raster cells dominated in urban areas and larger raster cells dominated in low density rural areas.

2.3.3 Analysis Zones for Non-Motorized Trips

According to Kuzmyak et al. (2014), many planning authorities have updated their models using finer-grained systems of TAZ to provide more resolution and also open up opportunity for including non-motorized travel.

A number of approaches exist for the redefinition of zone systems to achieve levels of spatial resolution suitable for non-motorized travel. To model destination and mode choice for nonmotorized travel, Eash (1999) defined non-motorized subzones for northeastern Illinois by dividing vehicle zones that followed a regular grid pattern into quarter sections. Each zone contained four non-motorized subzones, and for the central area, where vehicle zones were relatively smaller, the non-motorized zones matched the vehicle zones. For zones that did not follow a regular grid pattern, non-motorized zones were formed from census tracts.

Clifton et al. (2013) considered three approaches in their selection of a geographical unit for pedestrian trips. These included: (1) using a 264 ft × 264 ft (80 m × 80 m) raster grid system across the entire study area; (2) segmenting existing TAZ into smaller subareas suitable for walking trips; and (3) operating at the parcel level. They found option 3 to be the most spatially accurate method since it did not require spatial data aggregation to a hypothetical centroid point. Nevertheless, they did not select

option 3 because socio-demographic data at the parcel level were incomplete for the entire area. They also eliminated option 2 since it required the development of a procedure to split TAZ. They settled on option 1 because it had already been developed for their study area. The grid cells were also hypothesized to be small enough to capture fine-grained attributes of household and the physical environment, as well as variation within the attributes, in order to accurately represent walking. However, Moeckel and Donnelly (2015) argue that the use of uniform grid cells result in many zones with little traffic where spatial data is irrelevant.

Regarding the use of parcels, Kuzmyak et al. (2014) asserts that the finer scale at which analysis is performed allows for a much sharper characterization of the travel environment as well as the factors affecting non-motorized travel. Despite admitting the elimination of aggregation issues by the use of parcel-level zone systems, Moeckel and Donnelly (2015) maintain that computational and conceptual limits remain to reducing zone sizes to parcel level, mainly due to the large number of zones that results. These include the instability of logit models for destination choice decisions if the number of alternatives is too high, as well as the exponential increase in the size of matrices, which slows down traffic assignment. Detailed information is also not available for most areas, either for privacy reasons or because of infrequency of full censuses (Wegener, 2011). Ortúzar and Willumsen (2011) also draw attention to the difficulty in forecasting at the same level of detail, changes at the individual household level affecting demand.

Wegener (2011) contends that disaggregation has a price, and the principle that, “the more micro the better” may be misleading. A balanced level of spatial resolution is therefore recommended for modeling (Moeckel and Donnelly, 2015). According to Wegener (2011), the future of urban transport and land use modeling is not refinement and detail but the identification of the appropriate level of conceptual, spatial and temporal resolution.

2.4 Chapter Summary and Conclusion

This chapter presented the state of the art on macroscopic modeling of non-motorized trips, intrazonal impedance calculation as well as the definition of TAZ.

A number of options exist for integrating non-motorized trips in macroscopic models but the coarse sizes of analysis zones presents a challenge. Considering the close relationship between non-motorized travel and intrazonal trips, there is the need to mitigate the intrazonal problem of macroscopic models to enhance the modeling of non-motorized trips.

Dealing with intrazonal trips require the calculation of intrazonal impedances and a number of methods exist for approximating intrazonal impedances since intrazonal impedances cannot be measured via the centroid-to-centroid approach. However, these methods are not applicable in all circumstances. Although the most consistent approach to define intrazonal impedance is to find the average impedance of trips within a zone, the lack of data for this approach limits its practicability. There is therefore the need for a method that is not only consistent, but also practicable.

To make zone sizes compatible with the scale of non-motorized trips, a number of approaches exist for the redefinition of zone systems to achieve finer levels of spatial resolution. While refining zone systems will improve the representation of short trips in macroscopic models, the literature reveals that finer resolution is not always better. There are conceptual and computational issues associated with the use of very fine zones, and therefore a balanced level of resolution is required.

3 Input Data Preparation

3.1 Study Area

To explore the various approaches, Dachau was selected for the study. Dachau is a town in the Bavarian state of Germany located northwest of Munich. Dachau, as used in the dissertation needs to be distinguished from the District of Dachau to which the town belongs. Figure 3.1 shows Dachau in red together with the neighboring towns that make up the District of Dachau. Dachau covers an area of 34.96 km^2 and as at December 2015, had a total population of 46,705 (Bayerisches Landesamt für Statistik, 2016). Dachau is popularly known for its concentration camp, and it is a popular residential area for people working in Munich.

Dachau is connected to the S-Bahn network of Munich and is served by six bus lines that can be used to travel within the town and beyond. Dachau lies on the regional train connection Munich-Ingolstadt-Treuchtlingen-Nuremberg. The Munich Central Station which provides connection to the national and international long distance travel can be reached with the S-Bahn within 20 minutes from Dachau. In a short time, all important highways in the region can be reached from Dachau. These include the A8 linking Munich to Stuttgart, the A9 linking Munich to Nuremberg as well as the Munich beltway A99.

The choice of Dachau for the study was influenced by its high share of non-motorized trips as well as the planning committee's recognition of the need to integrate non-motorized travel in their model. A household travel survey conducted in 2009 indicated that 29% of trips made within Dachau were by bicycle and 19% were made on foot (Gevas Humberg & Partner GmbH, 2010). Together, non-motorized trips made up 48% of all trips made within Dachau. Dachau intends to make pedestrian travel the basis of urban mobility (Stadt Dachau, 2012). To model out priorities for improvement to non-motorized facilities, the planning committee desires to have pedestrian and bicycle travel integrated in their models (Stadt Dachau, 2011).

Figure 3.1: Dachau in District of Dachau (Inset: Municipalities in Bavaria; Source: Hagar66, 2010)

3.2 Data Assembly and Processing

Since much of the required input data were available as secondary data, the data assembly process involved the collection of data from secondary sources and the processing of these data into forms useful for the study. The data collected included household survey, TAZ level socio-economic, as well as transport network data.

3.2.1 Household Survey Data

The main data for the study was acquired from the 2009 Household Travel Survey conducted by Gevas Humberg & Partner GmbH for Stadt Dachau. The survey collected information on all trips undertaken by 2,186 individuals from 1,078 Dachau households on 23rd July, 2009. The 2,186 individuals represented a 5.3% sample of Dachau inhabitants aged 6 and above. The information included trip purpose, travel mode(s) used, the start and end times of travel, the approximate distance travelled,

and the destination address. In addition, data on individual and household socio-demographics, individual employment-related characteristics, household car ownership as well as individual car availability were also collected. The returned questionnaires were obtained from the Civil Engineering Department of Stadt Dachau, while a more organized form of the survey data was received from Gevas Humberg & Partner GmbH.

The data received from Gevas Humberg & Partner GmbH had been organized into three tables: (1) a household table with 1,078 records; (2) a person table with 2,186 records; and (3) a trip table with 7,486 records. Each record had been assigned an expansion factor to make the data representative of the total population. For the household records, expansion factors had been defined for each Stadtbezirk as the ratio between the total number of households in the Stadtbezirk and the number obtained in the sample. For the person records, expansion factors had been defined for the different combinations of Stadtbezirk, gender and age group. Trip records had been expanded by the person expansion factors and multiplied by 1.10995, a factor applied by Gevas Humberg & Partner GmbH using the returned questionnaires to compensate for trips made by respondents who indicated that they had travelled but failed to provide information on their trips.

The three organized tables were checked for inaccuracies and inconsistencies using the returned questionnaires. First, six trips with duplicate trip IDs and inconsistent trip numbers were removed from the trip tables to bring the trip records from 7,486 to 7,479. Afterwards, 259 trip records with no defined origin and/or destination were removed from the trip table to bring the trip records to 7,220. While some respondents reported access, main and egress legs of a trip as separate trips, others reported them as combined single trips, making it difficult to capture the access and egress legs of such trips, which are generally made by non-motorized modes. To make the trip information consistent across all respondents, trip legs were combined into single trips and their individual trip legs removed from the trip table. For example, a trip with the following legs: (1) Home - Bus Stop; (2) Bus Stop - Train Station; (3) Train Station - Train Station; and (4) Train Station – Work, which had previously been represented as four different trip records were combined into a single Home - Work trip. The correction to the trip legs brought the number of trip records to 7,106.

Since the household and person tables contained some missing and inconsistent information, the returned questionnaires were used to complete and correct this information. Specifically, information on age and car availability was completed and corrected for the person records while information on car ownership and household size were corrected for households. Using household car ownership and person car availability information, car ownership information was developed for the person records. To categorize a person as a car owner, the person must have regular car availability, and be from a household whose number of persons with regular car availability does not exceed the number of cars in the household.

Although expansion factors had been provided by Gevas Humberg & Partner, GmbH, the corrections to the survey data necessitated a recalculation of the expansion factors. Specifically, the person expansion factors had to be recalculated to reflect the corrections in the age information. These were recalculated as the ratio of the total number of persons in each combination of Stadtbezirk, gender and age group, to the corresponding number obtained in the corrected sample, resulting in factors ranging between 3.8 and 39.6. The household records did not require new expansion factors since there had not been any corrections to the Stadtbezirk information used for the household record expansion. The 7,106 trip records were expanded by the new person expansion factors and multiplied by the 1.10995 factor used to compensate for trips made by respondents who indicated that they had travelled but failed to provide information on their trips.

To prepare the trip records for trip-based modeling, trips with home as destinations were removed from the data since these are deemed to be a reflection of trips with home as origins. In effect, the trip records were reduced to 4,308 records expanded to 93,742 trips. Furthermore, for the approaches explored in this research, only trips internal to Dachau were of interest, therefore trips that had at least one end outside Dachau were removed from the data, bringing the records to 2,739 expanded to 58,980 trips. To enable a comparison between the internal trips and all trips made by residents of Dachau, Figure 3.2 shows the modal split of all trips made by Dachau residents while Figure 3.3 shows the modal split of internal trips made by Dachau residents.

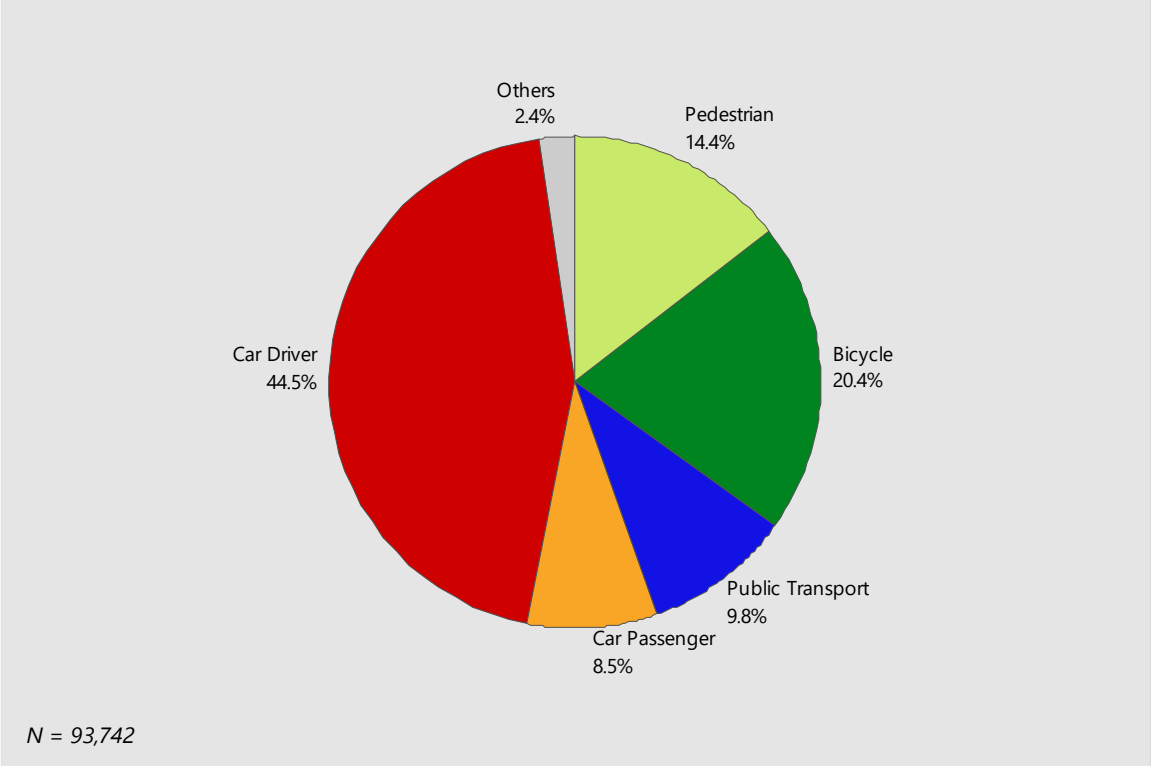

Figure 3.2: Modal split of all trips (expanded)

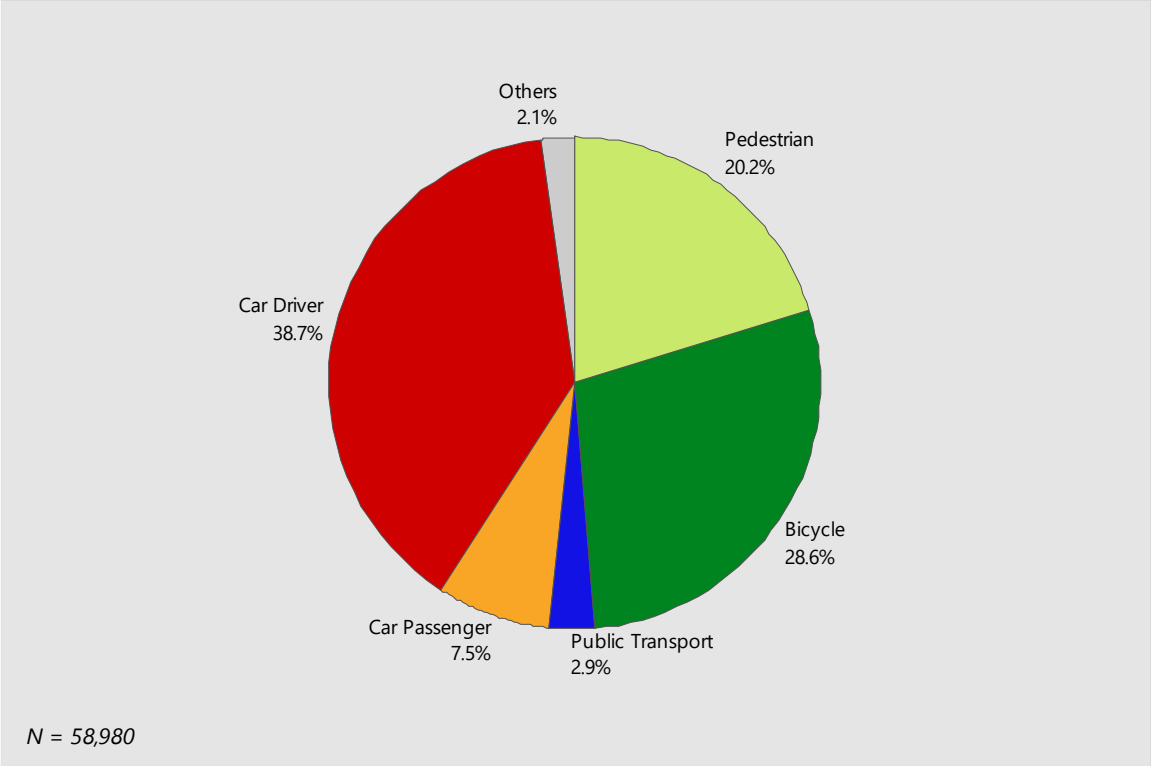

Figure 3.3: Modal split of internal trips (expanded)

As can be seen from Figures 3.2 and 3.3, the shares of non-motorized trips get higher while the shares of motorized trips drop when only internal trips are considered. An important observation is the high share of non-motorized trips among the internal trips despite the fact that access and egress trips are not considered. Considering access and egress trips will further increase the share of non-motorized trips beyond 49%, and this justifies the need to pay particular attention to non-motorized modes in urban transport modeling.

In the case of public transport, whereas the share is almost 10% for all trips, it is approximately 3% for internal trips. This indicates that majority of the public transport trips have at least one end outside Dachau. Since public transport loses its significance when only internal trips are considered, public transport trips were removed from the trip table. In addition, trips that had undefined travel modes were removed to get the final trip table for the study.

Table 3.1 presents a summary of the processed household survey data. The processed data consists of trip and person records along with their expansion factors organized into person and trip tables. Table 3.1 therefore shows the records in the sample as well as their corresponding expanded values.

Table 3.1: Summary of the processed household survey data

Database Summary	Sample	Expanded Sample
Trips	2,606	56,018
Persons	2,186	41,230
Male	1,046	20,002
Female	1,140	21,228
Car Owners	1,331	24,992
Non-Owners	855	16,238

As seen from Table 3.1, there are more females than males, and more car owners than non-owners. Figure 3.4 shows the modal split of the final sample while Figure 3.5 shows the number of trips by mode and distance. Since reported distances did not provide complete and reliable information, the distances were skimmed from the respective modal networks using the corresponding origins and destinations in the survey data.

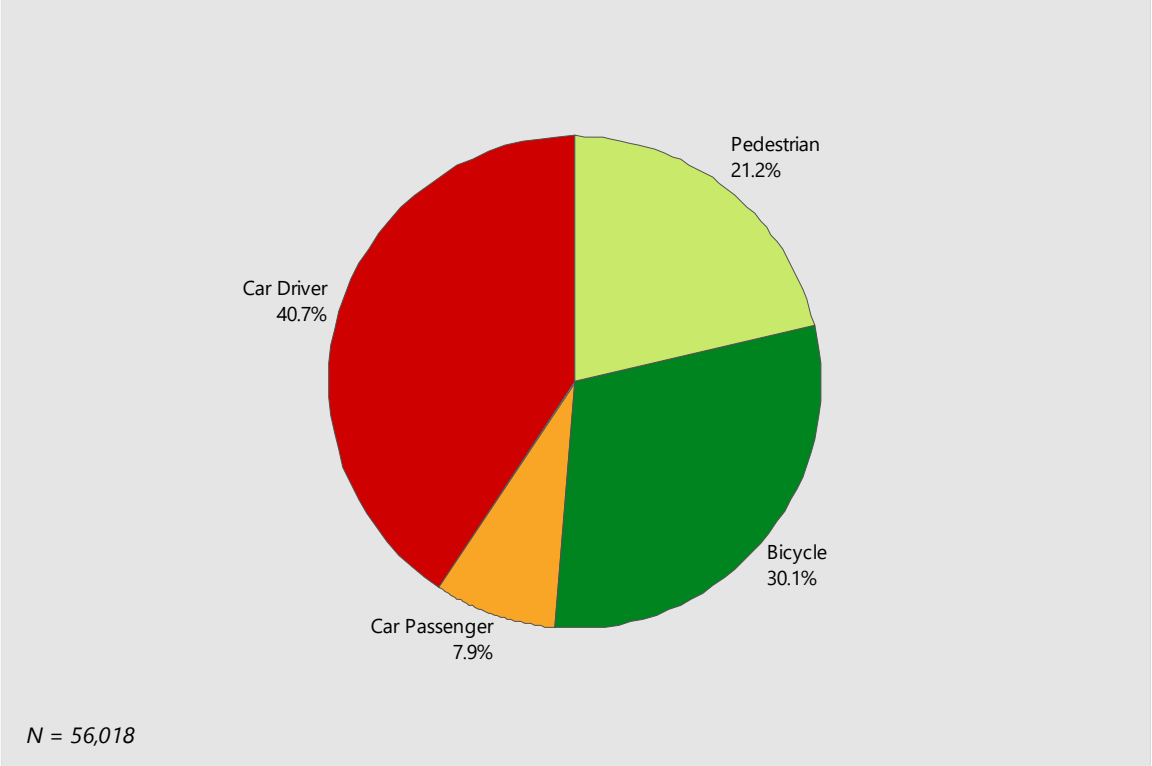

Figure 3.4: Modal split of final sample (expanded)

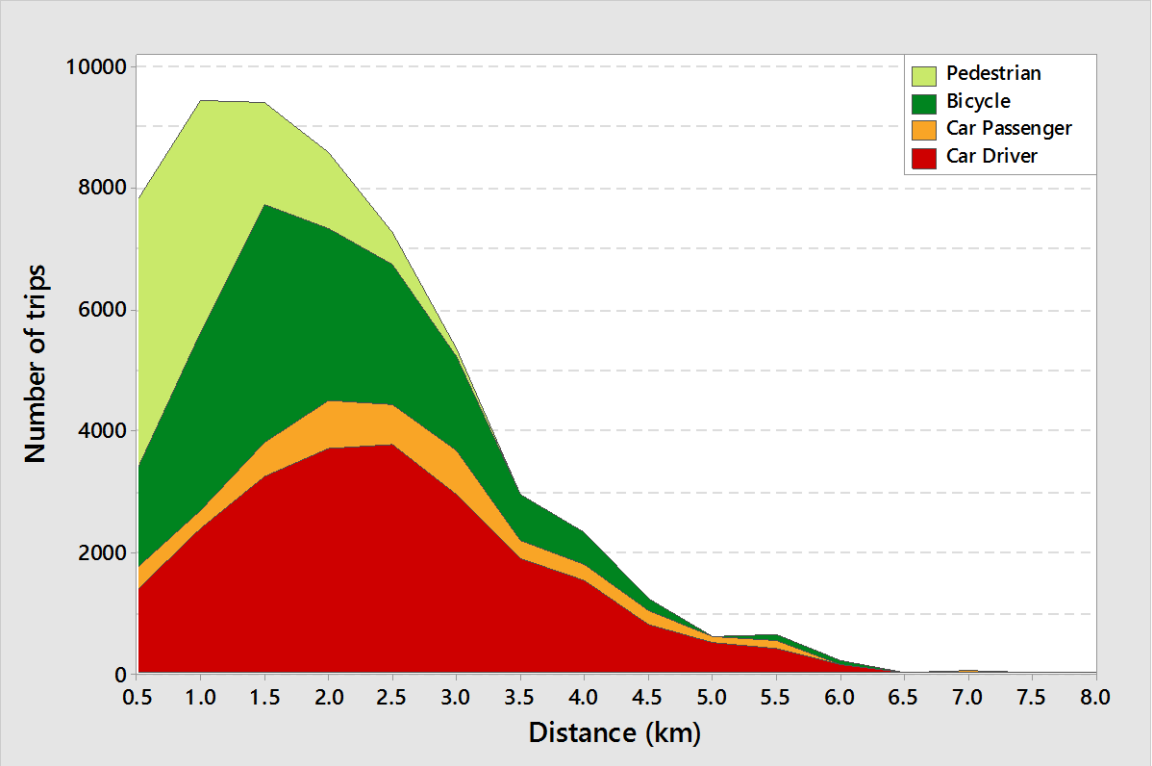

Figure 3.5: Number of trips by mode and distance (expanded)

As can be seen from Figure 3.4, a high share of internal trips made by Dachau residents are made by non-motorized modes, with cycling being the most common form of non-motorized travel. Together, these non-motorized modes account for 51.3%, highlighting the important role of non-motorized modes for travel within Dachau.

Figure 3.5 shows that the majority of trips that take place within Dachau do not exceed 6.5 km. With bicycle speed of 15.5 km/h, 6.5 km can be covered in 25 minutes, making bicycle a competitive mode for trips within Dachau. A pedestrian with a speed of 5 km/h on the other hand requires approximately 78 minutes for that same distance. This explains why pedestrian trips tend not to exceed 3.5 km where it requires 42 minutes with a walking speed of 5 km/h. Whereas walking is the most popular mode for trips of up to 1 km, bicycles dominate trips between 1 km until 1.5 km, and beyond 1.5 km, it is the car driver mode that has the highest share.

Table 3.2 presents the number of trips grouped by age and gender along with their expanded values in brackets while Figure 3.6 shows the corresponding modal split.

Table 3.2: Number of trips by age and gender

Age	Gender	
	Male	Female
6 – 17	209 (4,665)	180 (3,393)
18 – 25	60 (1,325)	36 (718)
26 – 40	102 (2,683)	302 (6,877)
41 – 64	395 (9,630)	582 (13,379)
65 +	374 (6,162)	330 (6,458)

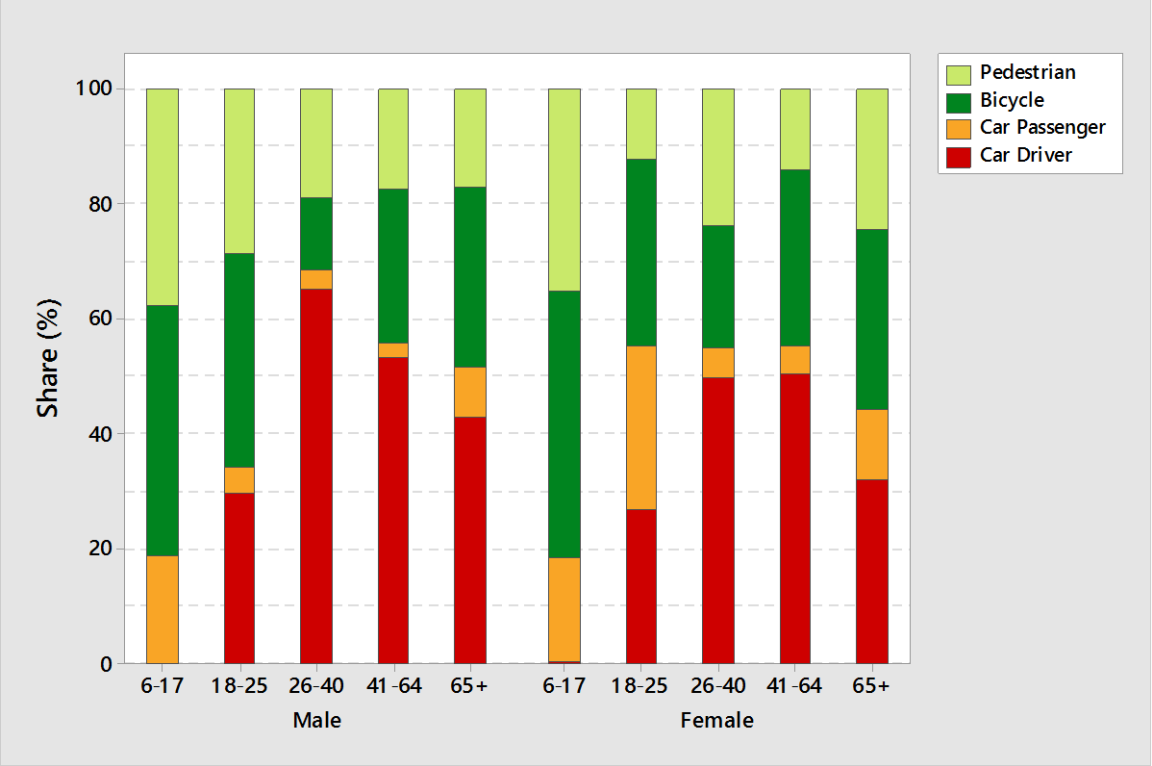

Figure 3.6: Modal split by age and gender (expanded)

Regarding the modal split by age and gender in Figure 3.6, the share of bicycle use is lowest between the ages of 26 and 40 irrespective of gender. Non-motorized mode use is highest for persons under the age of 18 who have limited modal options because they generally do not have permits to drive. It can also be observed that, females between the ages of 18 and 26 were more likely to travel as car passengers than their male counterparts.

Table 3.3 presents the number of trips grouped by purpose and car ownership along with their expanded values in brackets while Figure 3.7 shows the corresponding modal split.

Table 3.3: Number of trips by purpose and car ownership

Trip Purpose	Car Ownership	
	Car Owners	Non-Owners
Home-based work (HBW)	154 (3,424)	60 (1,454)
Home-based shopping (HBS)	388 (8,614)	158 (3,348)
Home-based education (HBE)	18 (398)	200 (4,123)
Home-based recreation (HBR)	194 (4,062)	153 (3,105)
Home-based other (HBO)	387 (8,113)	130 (2,779)
Non-home-based (NHB)	504 (11,013)	260 (5,585)

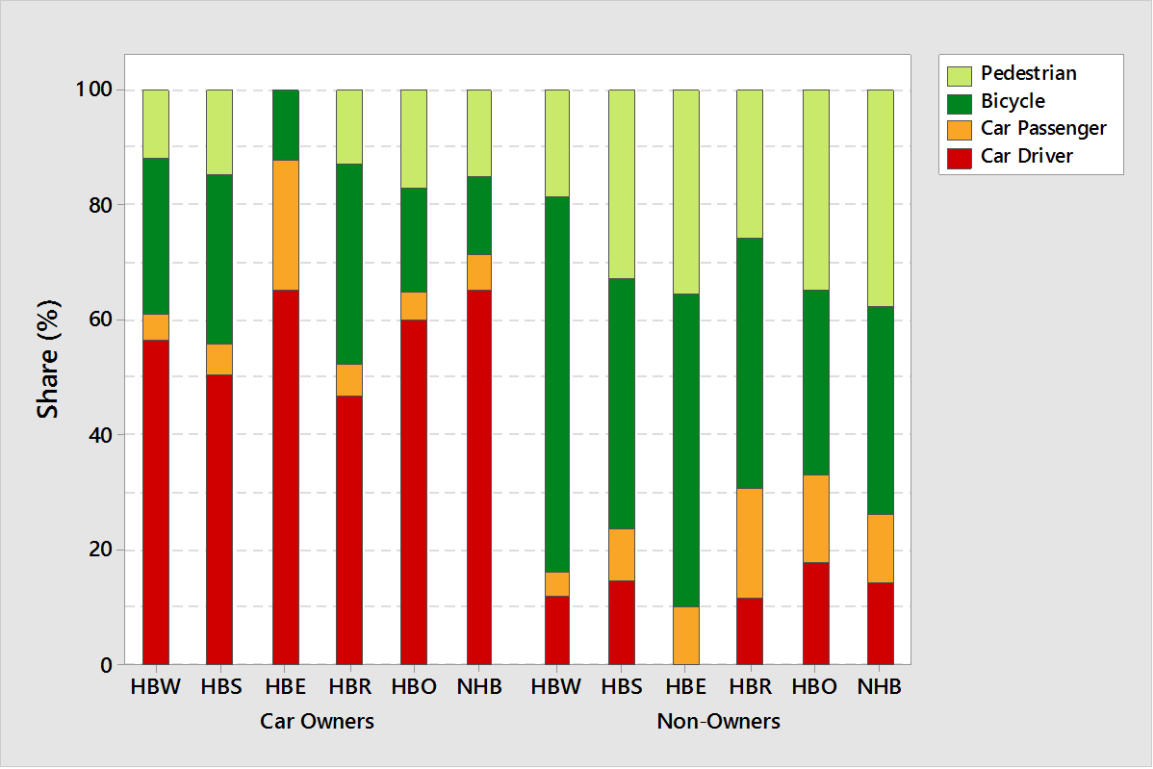

Figure 3.7: Modal split by purpose and car ownership (expanded)

From Figure 3.7, it can be seen that car ownership influences non-motorized travel as walking and cycling are more popular among non-owners. Whereas a high share of non-owners made HBE trips on foot, none of the car owners made an HBE trip on foot. On the other hand, a high share of car owners made HBE trips as car drivers whereas none of the non-owners made an HBE trip as a car driver. Non-Owners making HBE trips are generally school children who do not have permits to drive cars.

3.2.2 Zone Systems and Socio-economic Data

Besides the TAZ defined by Stadt Dachau for the purpose of transport analysis, the building blocks in Dachau were used as an additional geographic unit in this study. Dachau is divided into 102 TAZ and contains 717 building blocks as shown in Figures 3.8 and 3.9 respectively.

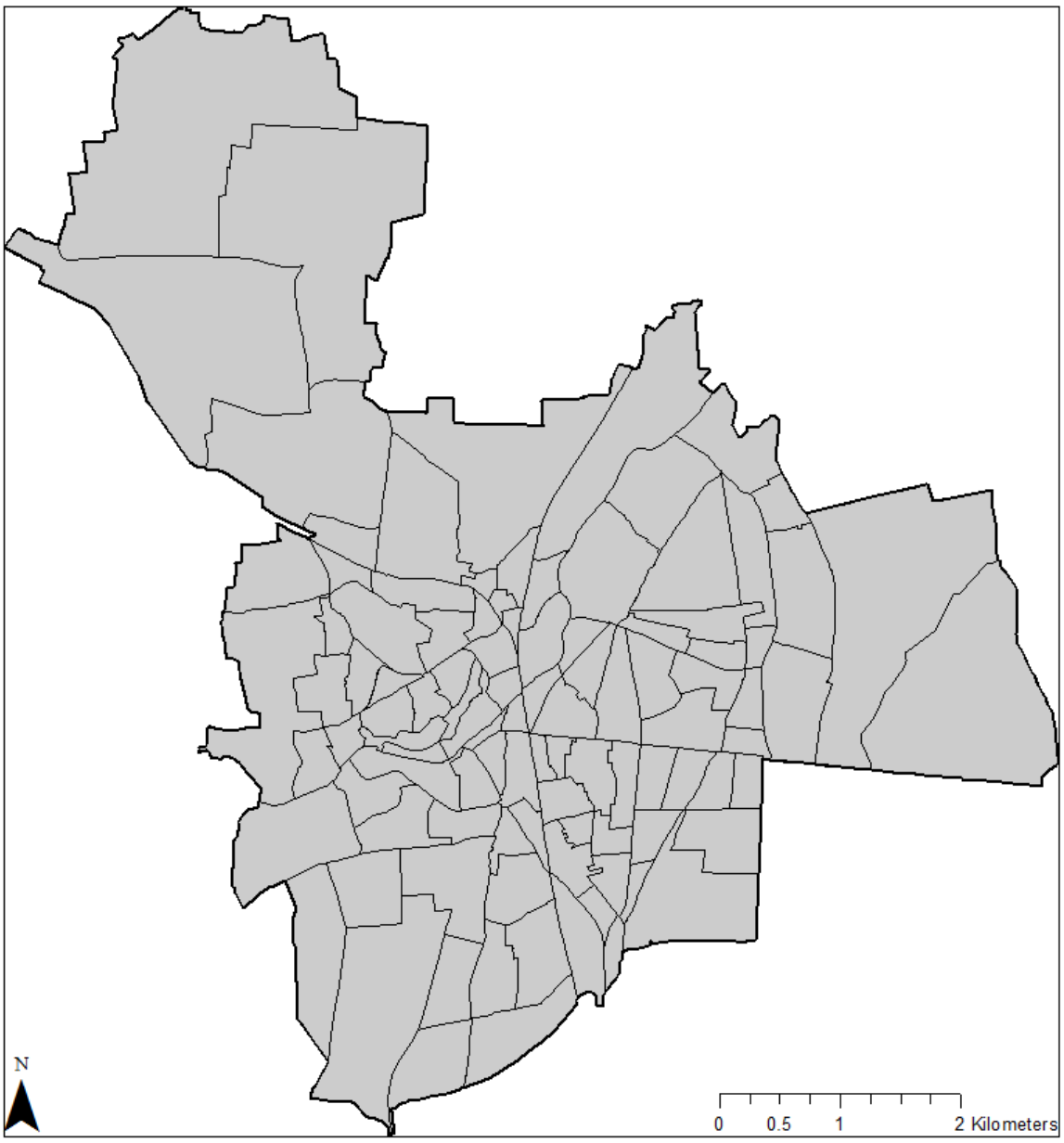

Figure 3.8: TAZ in Dachau (Source: Civil Engineering Department, Stadt Dachau)

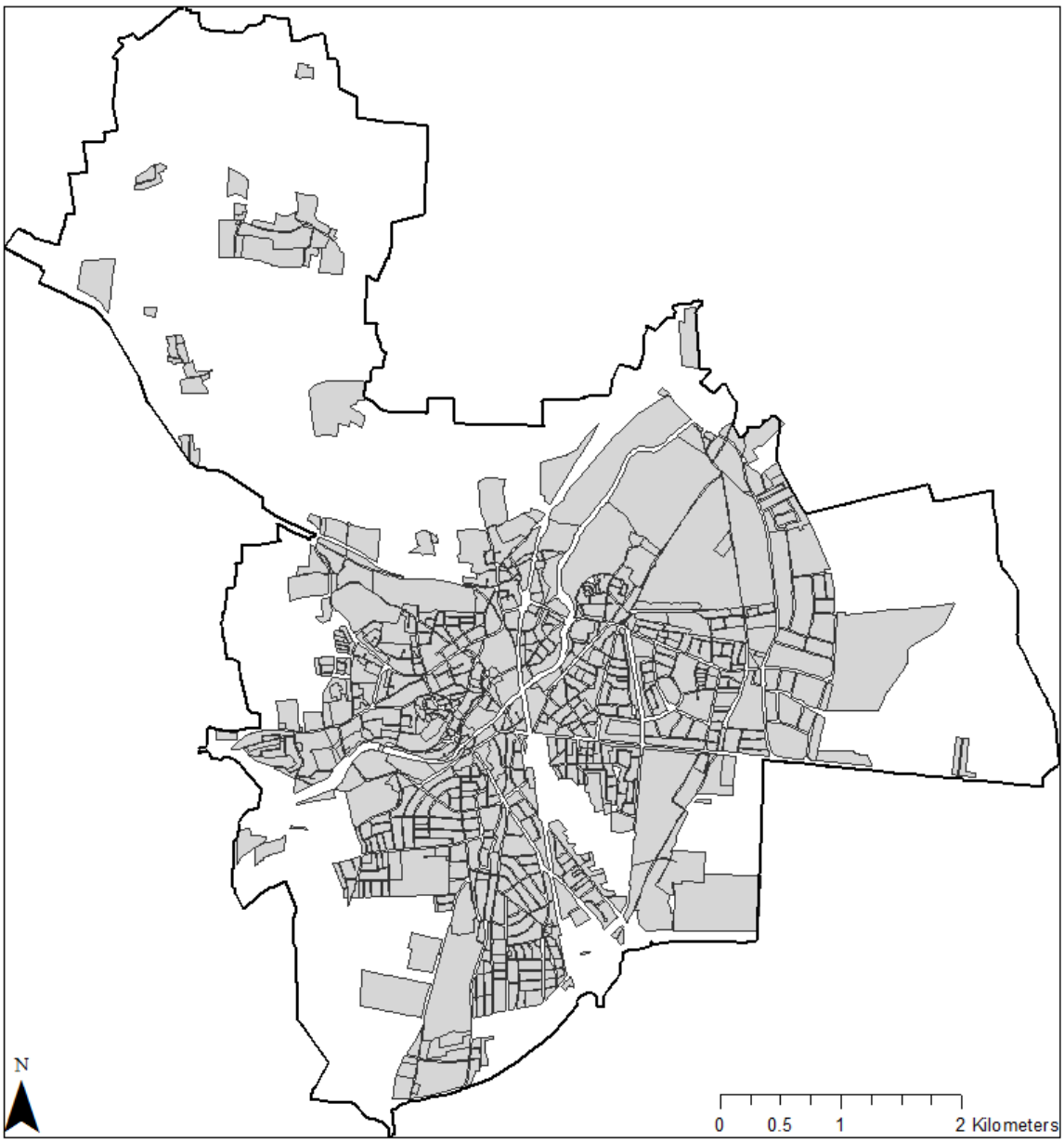

Figure 3.9: Building blocks (Source: Civil Engineering Department, Stadt Dachau)

Gevas Humberg & Partner GmbH provided TAZ level socioeconomic data on the following variables: (1) number of inhabitants aged 6 and above; (2) number of workplaces; (3) number of school and vocational training places; (4) total area of shopping spaces; (5) number of recreation places; and (6) number of kindergarten places.

Building block level data was provided by the Civil Engineering Department of Stadt Dachau. However, this only included the number of inhabitants so a further categorization of the building block inhabitants by age group was collected from the

Town Planning Department of Stadt Dachau. The Town Planning Department also provided a land use plan.

There were discrepancies between the available building block level data and the TAZ level data. As a result, the information from both levels could not be used together. Despite the fact that building blocks offer a finer level of resolution than TAZ, the TAZ level data was preferred for a number of reasons. First, the household survey data had been provided at the TAZ level. Secondly, the TAZ level data did not only include information on inhabitants but also information on other socio-economic variables, and coming from the same source, provided a compatible set of variables to work with. In addition, the TAZ level data corresponded to the period of the household survey, and therefore provided information compatible with other model inputs in terms of time.

3.2.3 Transport Network Data

Transport network data obtained from Gevas Humberg & Partner GmbH did not include paths for bicycles and pedestrians, so a more detailed network was obtained from OpenStreetMap contributors (2014) to make the network model relevant for non-motorized trips. The Civil Engineering Department of Stadt Dachau also provided an overview map of the speed zones in Dachau, as well as elevation maps used to determine link slopes for the calculation of cycling speeds.

Although the network data from OpenStreetMap contributors (2014) was more detailed with respect to spatial representation, the attributes of the links needed to be checked and corrected. While parallel walking, cycling and driving links in the same direction had been represented as separate links for some network segments, these links had been combined into single links open to pedestrians, bicycles and cars for other network segments. To ensure consistency in the network representation, parallel links in the same direction that had previously been represented as separate links were combined into single links and opened to the respective modes.

In addition, the turning movements at nodes were checked for consistency with regards to the permitted transport systems on connected links. Redundant nodes were also removed from the network. Furthermore, the map of speed zones was used to correct car speeds and the elevation maps were used to calculate bicycle speeds of individual links. Using the speed-gradient relationship derived by Gölz (2007), the bicycle speed *y* of a link in km/h was calculated as:

$$y = f(x) = \begin{cases} 29 & ,x \leq -8 \\ 19 - \frac{25}{20}x & ,-8 < x < 12 \\ 4 & ,12 \leq x \end{cases}$$

where *x* is the link gradient expressed as a percentage. Table 3.4 presents a summary of the network objects used for modeling.

Table 3.4: Summary of network objects

Network Object	Quantity
Zones (TAZ)	102
Zones (Building Blocks)	717
Nodes	2,076
Links (Directional)	5,188

In the development of the network model, it was desirable to consider possible differences in connector times for different area types. Using the land use plan and map of Dachau, and considering the concentration of activities in different locations, three area types were defined for Dachau, namely high, moderate and low activity areas.

The areas in the center of Dachau described by the land use plan as special residential areas were defined as high activity areas. These included areas directly north and west of the town hall, as well as areas to the west of the Dachau train station. Whereas the less inhabited areas described in the land use plan as agricultural land were defined as low activity areas, all other areas were defined as moderate activity areas. The TAZ were subsequently categorized into these area types.

Since the transport network was fully represented, connector times would involve access, egress and parking search times, but not times travelled on secondary

network. Whereas the same pedestrian and bicycle connector times were used for all origin-destination (*O-D*) pairs, car connector times were set to vary by the destination area type since the level of activity at the destination influences parking pressure and, in effect parking search times. Table 3.5 shows the total connector times for the different types of connectors as well as the assumed connector time components.

Table 3.5: Total connector times per O-D pair

Connector Type	Access Time	Parking Search Time	Egress Time	Total Time (minutes)
Car (High Activity Areas)	1	1.5	1	3.5
Car (Moderate Activity Areas)	1	0.75	1	2.75
Car (Low Activity Areas)	1	0	1	2
Bicycle	0.25	0	0.35	1
Pedestrian	0.1	0	0.15	0.25

3.3 Development of Initial Trip Tables

This section describes the process involved in developing the initial trip tables used as input to the approaches explored in this research. To identify the most suitable method for calculating intrazonal impedances, trip tables were needed for the calculation of reference values against which comparisons would be made. Similarly, finding the appropriate level of spatial resolution required trip tables that would be assigned to the network to provide reference network volumes against which comparisons would be made.

The development of the initial trip tables required modeling at the finest possible level of spatial resolution. Since building blocks in Dachau offered a finer level of resolution than TAZ, the trip tables were developed at the building block level. Ideally, trip tables at parcel level would have been more suitable. However, the lack of parcel level data necessitated the use of building blocks.

3.3.1 Disaggregation of TAZ level Data to Building Blocks

To develop trip tables at the building block level, the socio-economic data as well as the household survey data were disaggregated from the TAZ level to the building block level. The relationship between building blocks and TAZ was generally many-to-one, such that each building block could be linked to a single TAZ, and not the other way round. However, there were instances where building blocks were related to more than one TAZ. To relate the different sections of such blocks to separate TAZ, the Intersect tool in ArcGIS was used to split building blocks at the TAZ borders. The intersection resulted in building block sections with each unit belonging to a single TAZ. Working on the assumption that areas outside building blocks are not activity locations, the building block areas within each TAZ were summed up to get the useful area for the TAZ.

To illustrate the disaggregation process, Figure 3.10 shows a hypothetical study area with three TAZ (1, 2, 3), and three building blocks (A, B, C).

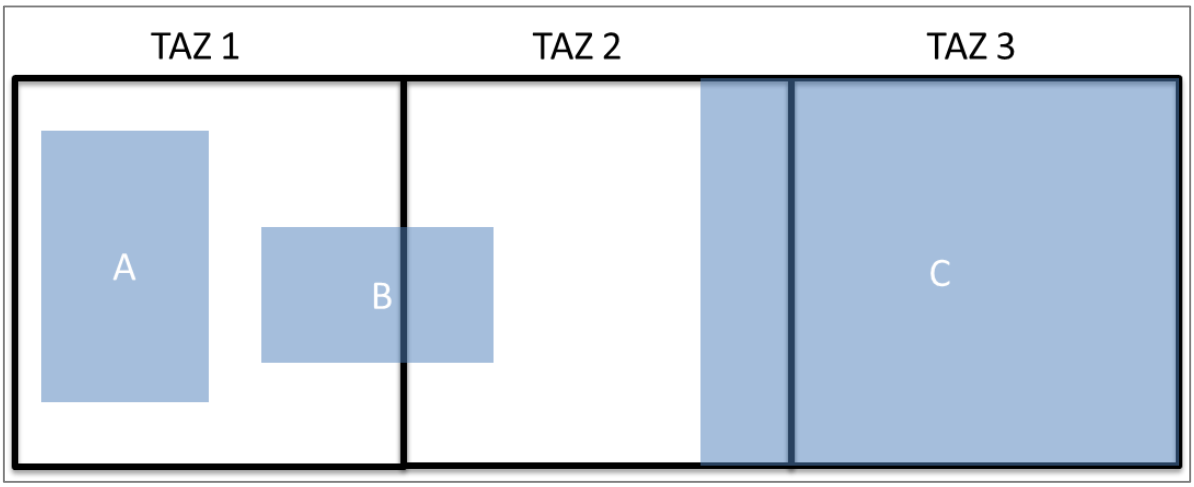

Figure 3.10: Hypothetical study area

As seen in Figure 3.10, besides Block A that lies completely in TAZ 1, the other blocks have relationships with more than one TAZ. Whereas Block B has a section in TAZ 1 and another section in TAZ 2, Block C occupies the whole of TAZ 3 and extends further into TAZ 2. Splitting the building blocks at the TAZ boundaries results in five different block sections, and each section is denoted by its respective TAZ and

building block identifier such that 1B represents the section of Block B in TAZ 1. The resultant block sections are thus 1A, 1B, 2B, 2C, and 3C.

To get the useful area of each TAZ, their corresponding block section areas are summed up. The useful area of TAZ 1 is the sum of the areas of 1A and 1B. Similarly, the useful area of TAZ 2 is the sum of the areas of 2B and 2C. Since TAZ 3 is wholly occupied by 3C, its whole area is deemed useful, and as such the useful area of TAZ 3 is the same as the total area of TAZ 3.

3.3.1.1 Disaggregation of Socio-economic Data

With the assumption that TAZ data are equally distributed over the useful areas within each TAZ, the ratio of the area of a block section to the useful area of the TAZ represented the relative participation of the block section within the TAZ. Correspondingly, these ratios were used to disaggregate TAZ level data to block sections, and the data for block sections belonging to the same building blocks were subsequently summed up to get the data at the building block level.

Although the study assumes an even distribution of TAZ data among building blocks, it is worth noting that trip generation levels of building blocks differ depending on the function of each block as well as the number of floors of each block. Nevertheless, since the disaggregation is controlled by TAZ, the errors involved will be limited.

To explain the disaggregation of the socio-economic data, the hypothetical study area in Figure 3.10 is used along with the following assumptions: (1) the number of inhabitants in TAZ 1, 2 and 3 are 70, 50, and 30 respectively; and (2) the areas of Sections 1A, 1B, 2B, 2C, and 3C in square kilometers are 4, 3, 2, 3, and 12 respectively. With these additional assumptions, the number of inhabitants in each block section is computed as shown in Table 3.6.

Table 3.6: Disaggregating socio-economic data

Block Section	Block Section Area (km^2)	TAZ Inhabitants	TAZ Useful Area (km^2)	Block Section Inhabitants
1A	4	70	4+3 = 7	(4/7)×70 = 40
1B	3	70	4+3 = 7	(3/7)×70 = 30
2B	2	50	3+2 = 5	(2/5)×50 = 20
2C	3	50	3+2 = 5	(3/5)×50 = 30
3C	12	30	12	(12/12)×30 = 30

The number of inhabitants for each building block is calculated by summing up the number of inhabitants in the respective block sections. For Block A, the number of inhabitants is 40, the same as the number of inhabitants in Section 1A since Block A has only one section. The number of inhabitants in Block B is the sum of the number of inhabitants in Section 1B and 2B, which equals 50. Similarly, the number of inhabitants in Block C is the sum of the number of inhabitants in Section 2C and 3C, which equals 60.

3.3.1.2 Disaggregation of Travel Survey Data

Each trip record in the final sample was replicated multiple times using the block sections of their respective origins and destinations. The number of replicas for each trip record was a product of the number of block sections in the origin TAZ and the number of block sections in the destination TAZ. The trip expansion factor for the original record was then distributed among the replicas based on the relative participation of the block section pair in their respective origin and destination TAZ.

Using the hypothetical data, and assuming a trip from TAZ 1 to TAZ 2 with an expansion factor of 15, the disaggregation of the travel survey data is explained and shown in Table 3.7. The disaggregation requires that the trip be quadruplicated since the origin and destination TAZ had 2 block sections each. To determine the weight of each replica, the relative participation of the origin block section in its TAZ is multiplied by the relative participation of the destination block section in its TAZ. The sum of the replica weights for a single original trip record should equal 1 since the replication is exhaustive. An expansion factor for each new record is then computed by multiplying the replica weight by the expansion factor of the original record.

Table 3.7: Disaggregating travel survey data

Origin	Destination	Origin Weight	Destination Weight	Path Weight	Expansion Factor
1A	2B	4/7	2/5	(4/7)×(2/5) = 0.23	0.23×15 = 3.45
1A	2C	4/7	3/5	(4/7)×(3/5) = 0.34	0.34×15 = 5.10
1B	2B	3/7	2/5	(3/7)×(2/5) = 0.17	0.17×15 = 2.55
1B	2C	3/7	3/5	(3/7)×(3/5) = 0.26	0.26×15 = 3.90

3.3.2 Trip Generation

To calculate the number of trips produced by and attracted to each building block, trip generation rates were computed for the six different trip purposes introduced in Table 3.3 which include:

1. Home-based work (HBW);
2. Home-based shopping (HBS);
3. Home-based education (HBE);
4. Home-based recreation (HBR);
5. Home-based other (HBO); and
6. Non-home-based (NHB).

3.3.2.1 Trip Production

The trip production models used the person category approach of the cross-classification method. The persons were segmented by car ownership for all but the HBE trips, resulting in 11 demand groups for which trip production rates had to be computed. The HBE trips were not segmented because of the low number of HBE trips made by car owners as shown in Table 3.3. Using the expanded survey data, trip production rates were computed for each demand group as the ratio of the expanded number of trips for the group to the expanded number of persons in the corresponding person group. Since the computation involved aggregate values, the rates were independent of the level of aggregation used. Table 3.8 shows the summary of the computed trip production rates.

Table 3.8: Trip production rates

Trip Purpose	Person Group	
	Car Owners	Non-Owners
HBW	0.137	0.090
HBS	0.345	0.206
HBE		0.11
HBR	0.163	0.191
HBO	0.325	0.171
NHB	0.441	0.344

As can be seen from Table 3.8, the trip production rates are lower than usual. This is due to the fact that the rates were determined only for trips having their origins and destinations in Dachau. Besides, public transport trips and trips with undefined modes had also been excluded. The rates involve trips taking place within Dachau on foot, by bicycle, by car as a driver or by car as a passenger.

From Table 3.8, it can also be observed that, for all but the HBR trips, car owners have higher trip rates than non-owners. This supports the logic that car owners make more trips with the exception of HBR trips which are mostly made for physical activities, and as such involve the use of non-motorized modes.

3.3.2.2 Trip Attraction

The trip attraction models consisted of regression-type equations with independent variables drawn from TAZ level socio-economic data. Whereas trip production rates are independent of the level of aggregation used, trip attraction rates are responsive to spatial aggregation levels. This is mainly because of the residuals involved in linear regressions and the differences in their distributions for different levels of spatial aggregation. Since the input variables had been provided at the TAZ level, the trip attraction rates were estimated at the TAZ level. Table 3.9 shows the variables and rates used for the different demand groups in the trip attraction model, as well as the R-squared statistic providing information on the fit of the attraction models.

Table 3.9: Trip attraction variables, estimated rates and model fit

Variables	Trip Purpose					
	HBW	HBS	HBE	HBR	HBO	NHB
Total Workplaces	0.2085					
Total School places			0.435			
Shopping Area (m^2)		0.06643				0.02342
Recreation Places				24.76	20.42	36.01
Inhabitants (Aged 6+)					0.0651	0.0949
Kindergarten Places					1.222	
R-squared statistic (%)	79.86	83.84	33.50	51.79	62.71	80.52

It can be seen from Table 3.9 that the trip attraction models for the HBW, HBS and NHB trips produce very good fits. On the other hand, the trip attraction model for HBE trips produces a poor fit. An inspection of the household survey data and the TAZ level data showed that, there were HBE trips that took place in TAZ with no school places, and instances of TAZ with school places that attracted no HBE trips. Whereas the latter could be attributed to the limited number of sampled trips, the former implies primary data error which is beyond the scope of this research.

3.3.2.3 Trip Balancing

The trip production and attraction rates estimated at the TAZ level were applied at the building block level to calculate the number of trips produced by and attracted to each building block using the socio-economic data disaggregated from TAZ to building blocks. Since the available socio-economic data did not contain information on car ownership, the share of car owners was computed as an aggregate value from the expanded person table. The share was then multiplied by the number of inhabitants aged 6 and above in each building block to get the number of car owners in each building block.

Total productions and attractions for each demand group were subsequently balanced by scaling the attractions to the production total. For the NHB trips however, the productions were replaced with the scaled attractions after scaling the attractions to match total productions. In this way, the inhabitants determine the total number of NHB trips while the trips take place at non-home locations.

3.3.3 Trip Distribution

To determine the number of trips that travel between pairs of building blocks, trip distribution models were developed for each demand group using travel distance by car as a measure of spatial separation and a gamma impedance function F_{ij} given by the formula:

$$F_{ij} = a \times t_{ij}^{b} \times e^{(c \times t_{ij})}$$

where t_{ij} is the measure of spatial separation and *a, b,* and *c* are the impedance function parameters to be estimated during model calibration.

Travel distance by car has traditionally been used to measure spatial separation between trip ends, and although the use of distance limits the responsiveness of trip distribution to congestion effects, travel distance by car was suitable for a number of reasons. First, the purpose of the trip distribution was to produce a trip table that would serve as input to the approaches explored in the research which required no consideration of congestion effects. Secondly, the car network offered a complete and more connected graph compared to the bicycle and pedestrian network, such that reasonable paths existed between each O-D pair. Moreover, many of the network links used in the study were multimodal such that they were open to cars, bicycles, and pedestrians. Therefore, the shortest paths used to measure distances by cars were mostly the same paths along which distances by bicycle and pedestrians would be measured.

3.3.3.1 Calculation of Impedance Matrix

The driving distance between a building block pair was calculated as the length of the shortest car path joining the building block pair. To enable the skimming of the network, the building blocks were connected to the network by centroid connectors, using three two-way connectors for each building block. The centroid connectors for each building block were connected to the closest nodes on multimodal links that provided access to pedestrians, bicycles and cars.

A connector distance of 20 m was considered to take care of the distance taken to access or egress the network at each end of a trip. Since the network was represented in detail, the connector didn’t consider travel on secondary networks as

a component. Besides taking care of the access and egress distances, the connector distance ensured that building blocks with connectors joining the same node will not have a zero distance between them. Correspondingly, for each building block pair, a total connector distance of 40 m was added to the driving distance to get the travel distance by car.

With the assumption that population is evenly distributed within a building block and calculating the building block radius (r_i) from the building block area, intra-block driving distance (d_{ii}) was computed as:

$$d_{ii} = \frac{r_i}{\sqrt{2}}$$

Subsequently, the previously described total connector distance of 40 m was added to the computed intra-block driving distance to get the intra-block travel distance by car.

3.3.3.2 Model Calibration

Using trip records from the disaggregated household travel survey data, as well as the modeled productions and attractions resulting from the trip generation step, the KALIBRI function in the PTV Visum software was applied to estimate the impedance function parameters for the different demand groups. HBE and HBW trips were modeled doubly constrained while all other trip purposes were modeled singly constrained at the production end.

In addition to the type of impedance function and the measure of spatial separation, the KALIBRI function requires the observed trip length distribution as input. Since reported trip lengths in surveys do not provide true reflections of actual trip lengths, observed trip lengths were computed by applying the skimmed travel distances to the respective origins and destinations in the survey data. The trip length distributions were done in intervals of 0.5 km.

Table 3.10 shows the estimated impedance function parameters for the different demand groups. To simplify the representation of the 11 demand groups, ‘a’ and ‘b’ has been used as suffices in place of car owners and non-owners respectively. For

instance, HBOa represents HBO trips by car owners, whereas HBOb represents HBO trips by non-owners.

Table 3.10: Impedance function parameters

Demand Strata	a	b	c
HBWa	0.23	-0.12	-0.44
HBWb	0.15	-0.63	-0.18
HBSa	0.14	-1.07	-0.15
HBSb	0.17	-1.06	-0.45
HBE	0.03	-1.70	0.66
HBRa	0.23	0.21	-0.46
HBRb	0.19	-0.28	-0.32
HBOa	0.11	-0.79	-0.02
HBOb	0.22	-0.63	-0.44
NHBa	0.16	-0.61	-0.22
NHBb	0.24	-0.47	-0.47

While the parameter a is a scaling factor that does not change the shape of the function, parameters b and c, which should generally be negative are negative for all but two demand groups. The parameter b is negative for all but the HBRa demand group, implying that the function curve of the HBRa trips rises for very short distances before it monotonically drops. The parameter c is also negative for all but the HBE demand group, implying that the function curve for HBE trips monotonically decreases until it reaches an inflexion point at a large value of impedance. However, in the case of the HBE trips, the inflexion point occurs at a smaller than expected value of impedance.

3.3.3.3 Trip Distribution Model Calculation and Checks

Using the estimated impedance function parameters, the building block productions and attractions, as well as the travel distance by car matrix, a trip distribution model was developed for each demand group. The model development followed the same constraints as the KALIBRI estimation with the HBE and HBW trips being doubly constrained while the other trip purposes were singly constrained at the production end.

In order to check the trip distribution model results, trip lengths and intrazonal trips between the observed and modeled trips were compared. The trip length check involved a comparison of average trip lengths as well trip length frequency distributions (*TLFD*). The intrazonal trip check involved a comparison of intrazonal trip shares. Figures 3.11 to 3.21 show the observed and modeled TLFD for each demand group while Table 3.11 gives a summary of the trip distribution check results. For each demand group, a coincidence ratio *CR* between the observed and modeled TLFD was calculated as follows:

$$CR = \frac{\sum_D [min(PM_D, PO_D)]}{\sum_D [max(PM_D, PO_D)]}$$

where PM_D is the proportion of modeled distribution in distance interval *D* and PO_D is the proportion of observed distribution in distance interval *D.*

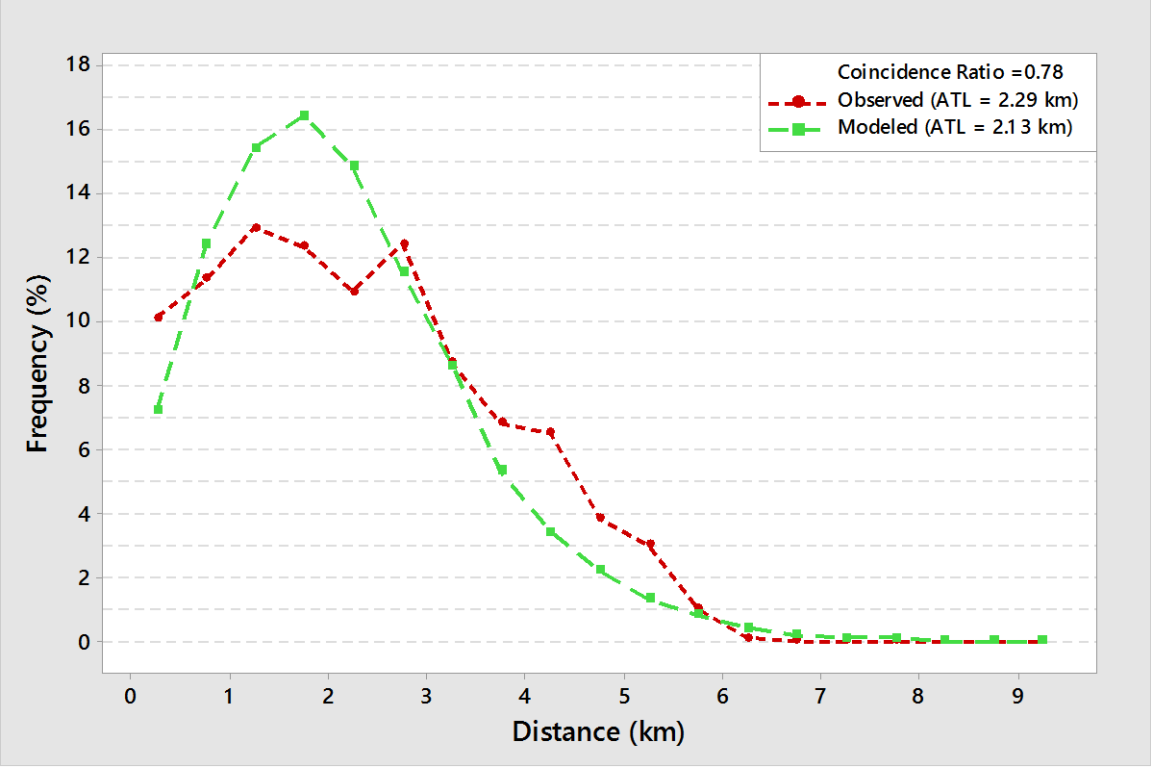

Figure 3.11: TLFD for HBW trips by car owners

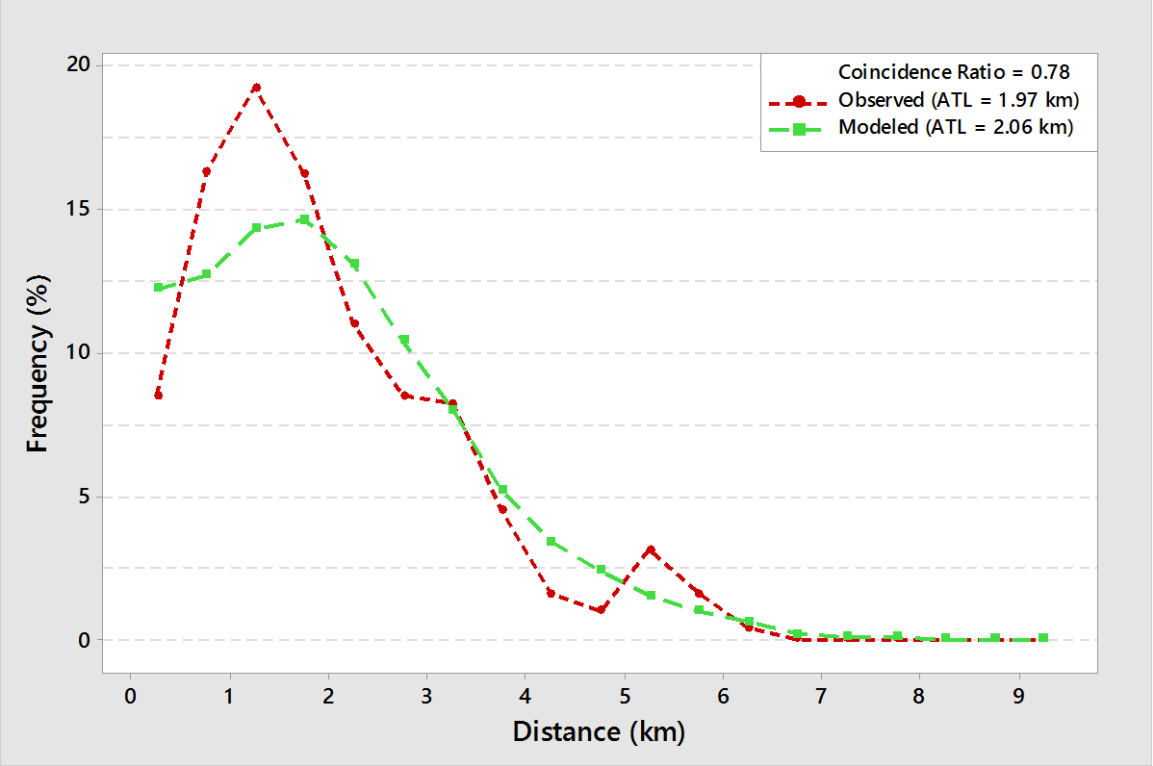

Figure 3.12: TLFD for HBW trips by non-owners

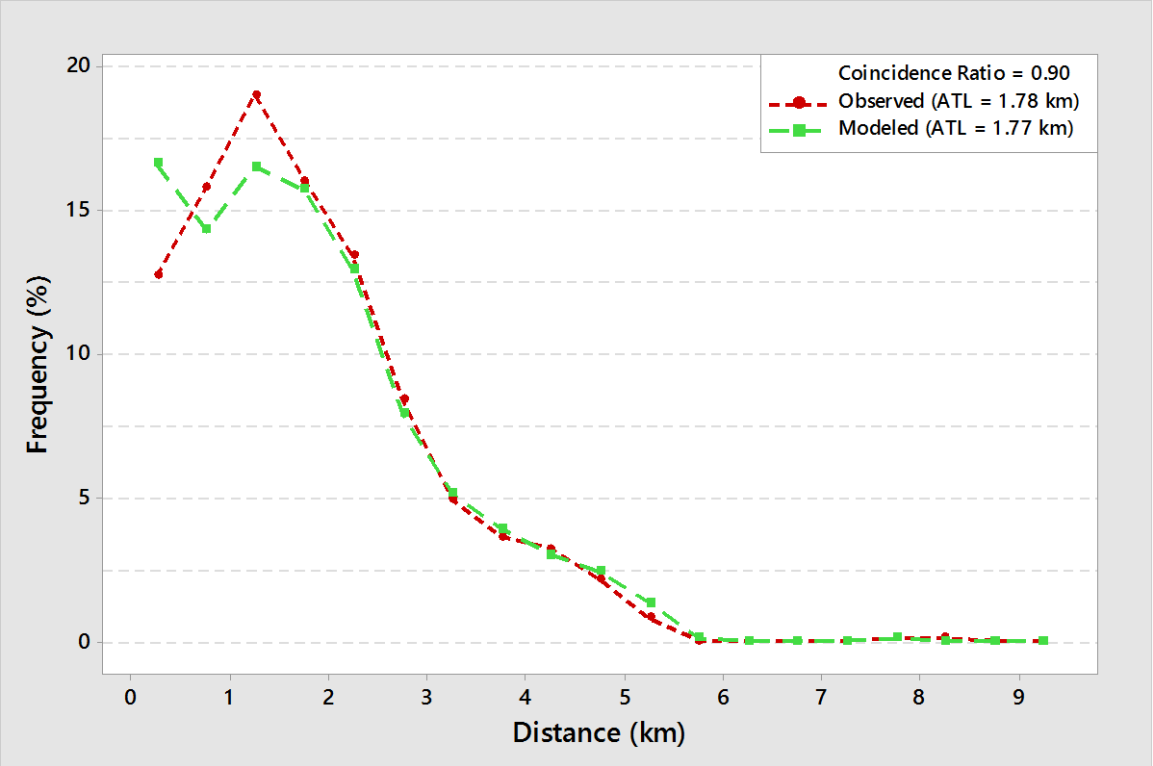

Figure 3.13: TLFD for HBS trips by car owners

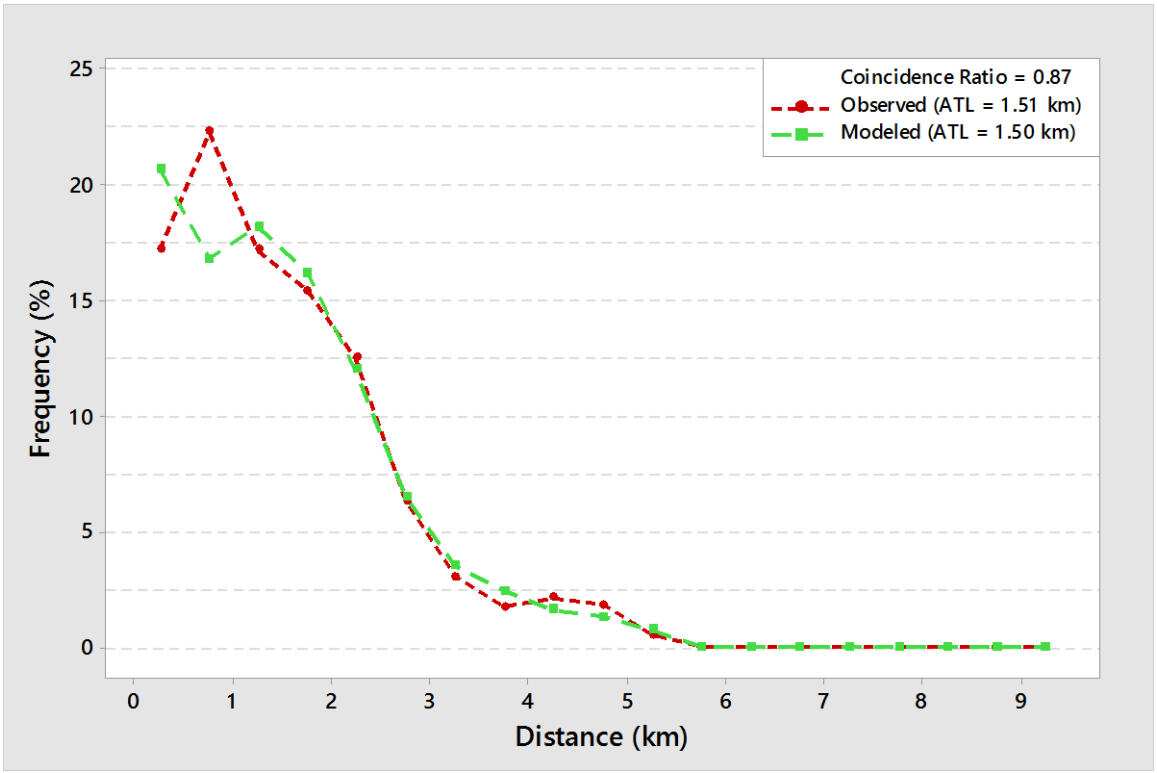

Figure 3.14: TLFD for HBS trips by non-owners

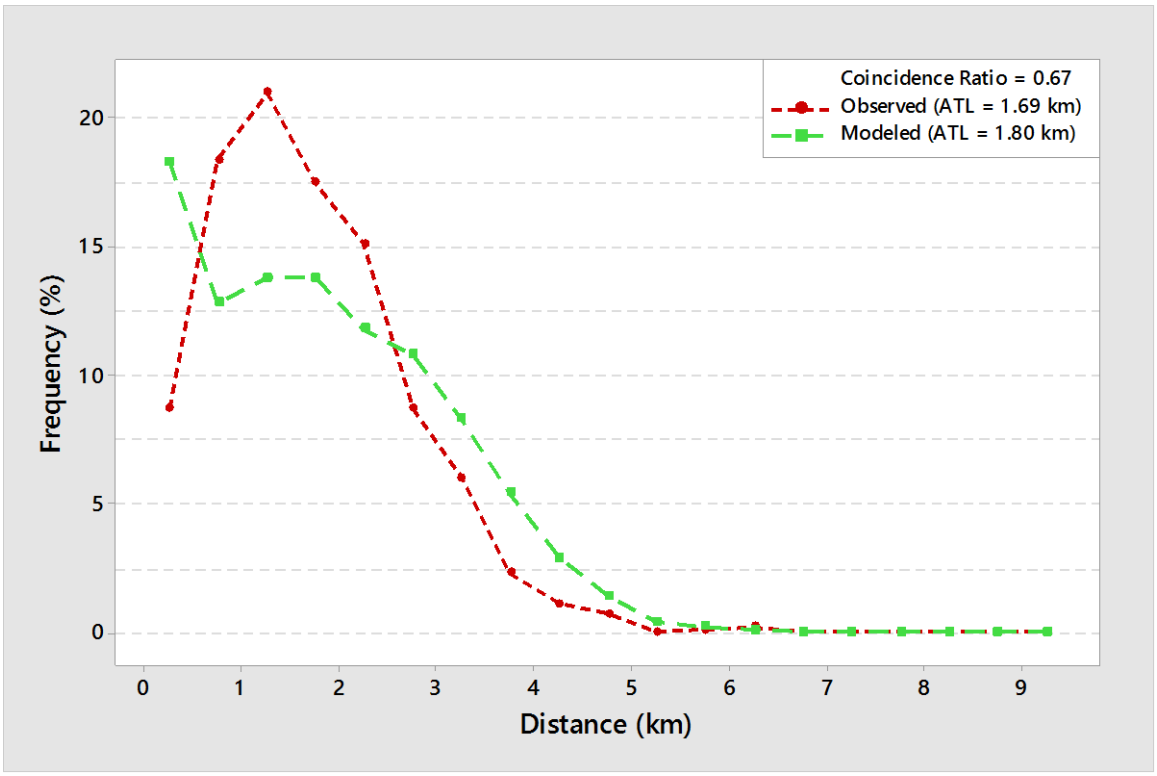

Figure 3.15: TLFD for HBE trips

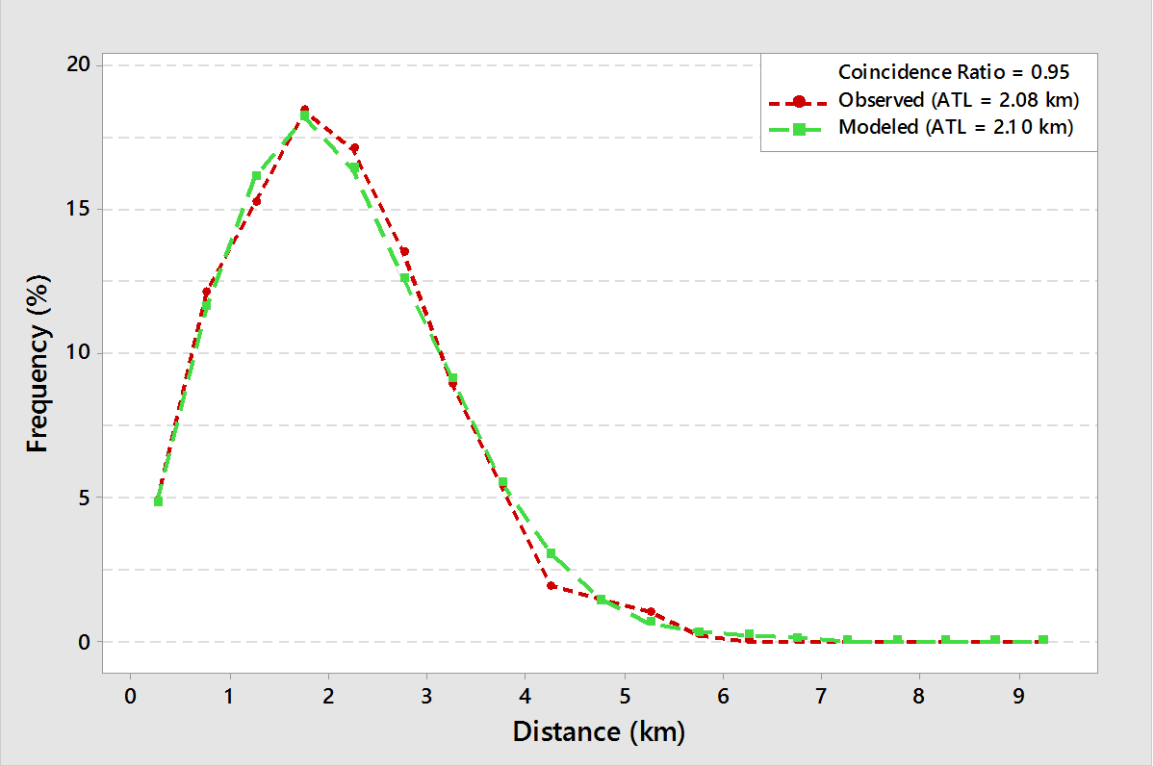

Figure 3.16: TLFD for HBR trips by car owners

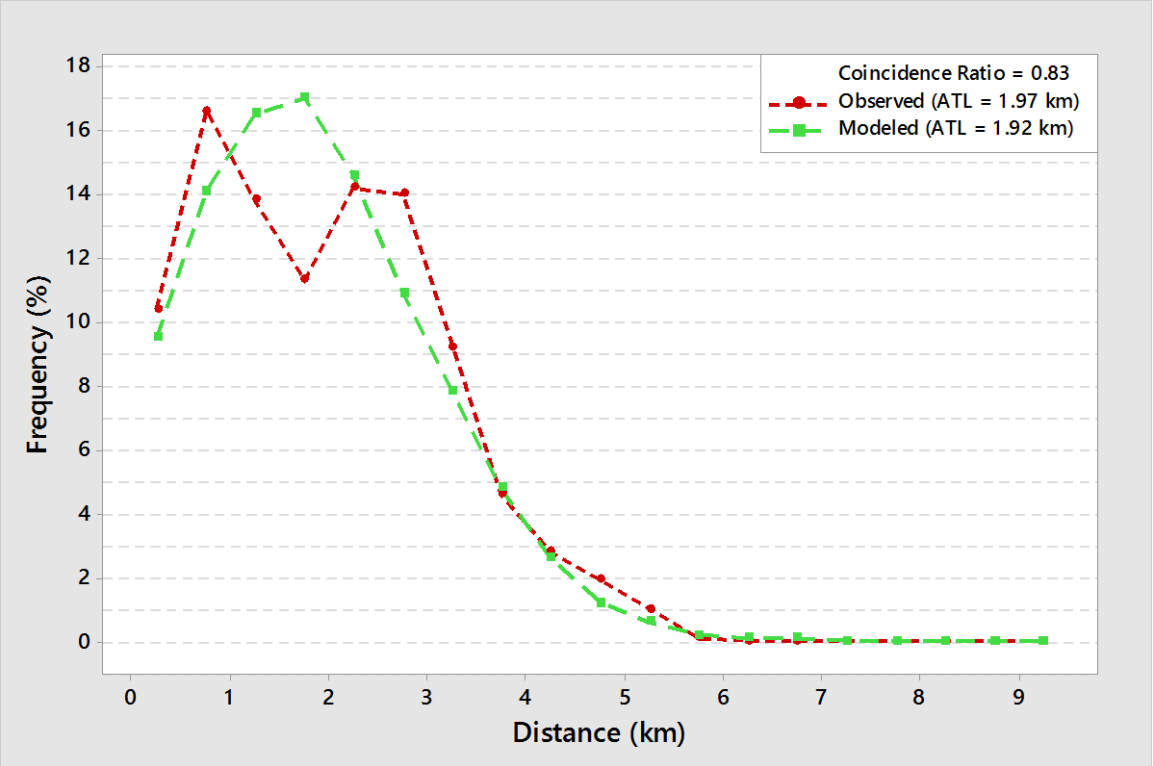

Figure 3.17: TLFD for HBR trips by non-owners

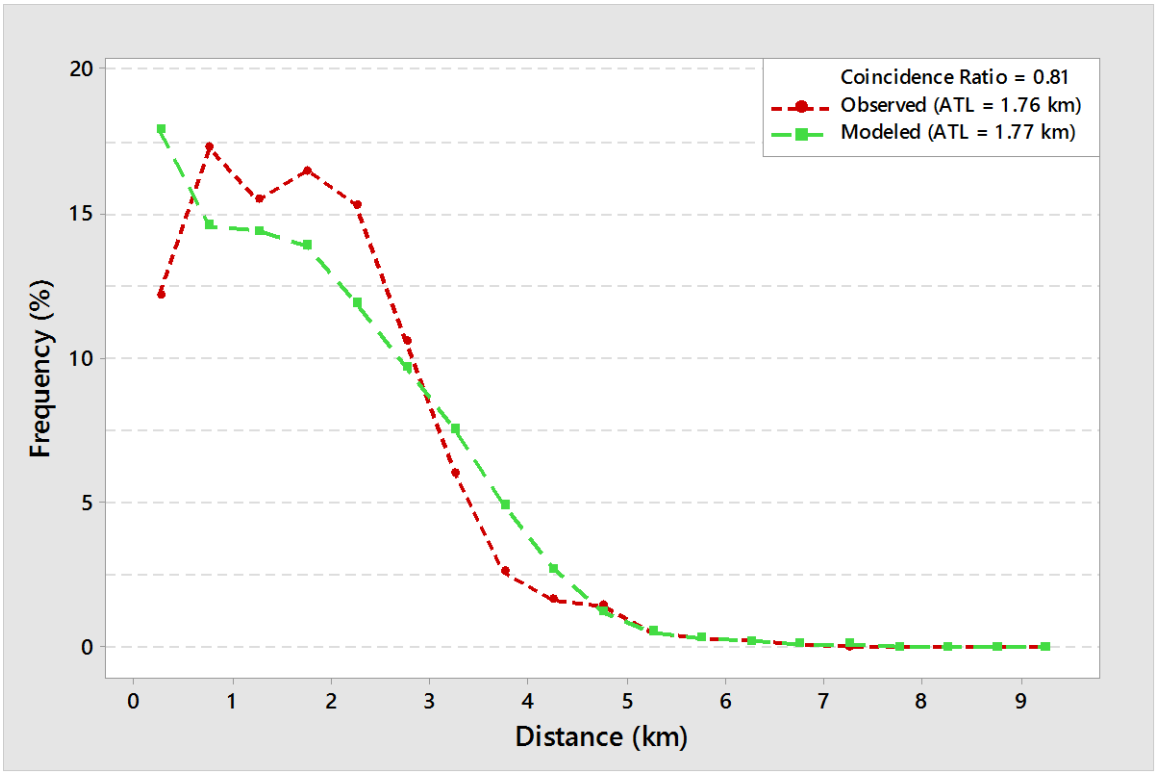

Figure 3.18: TLFD for HBO trips by car owners

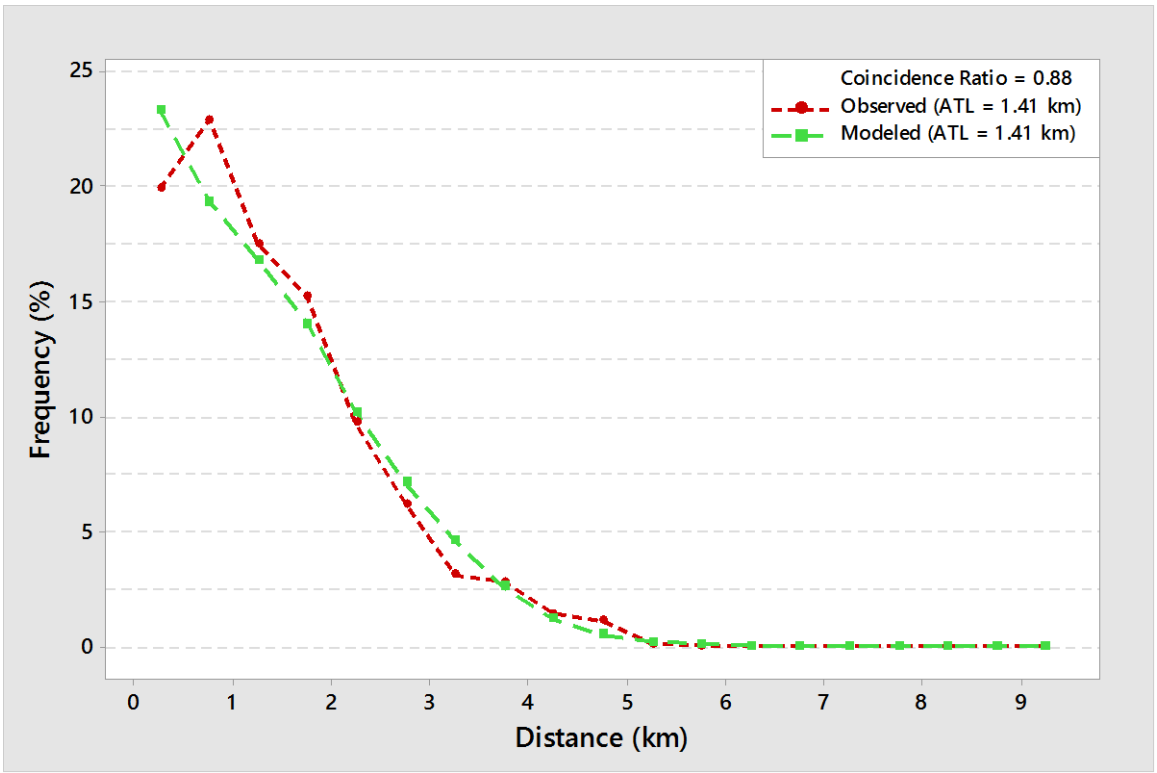

Figure 3.19: TLFD for HBO trips by non-owners

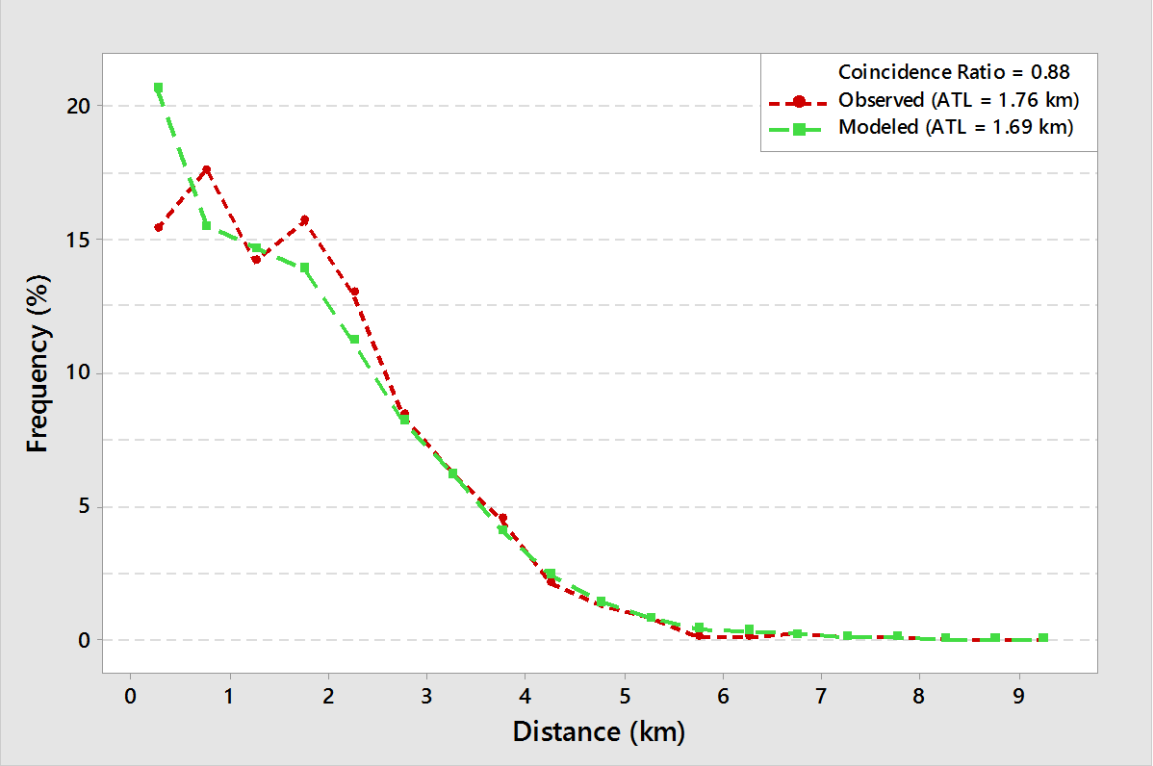

Figure 3.20: TLFD for NHB trips by car owners

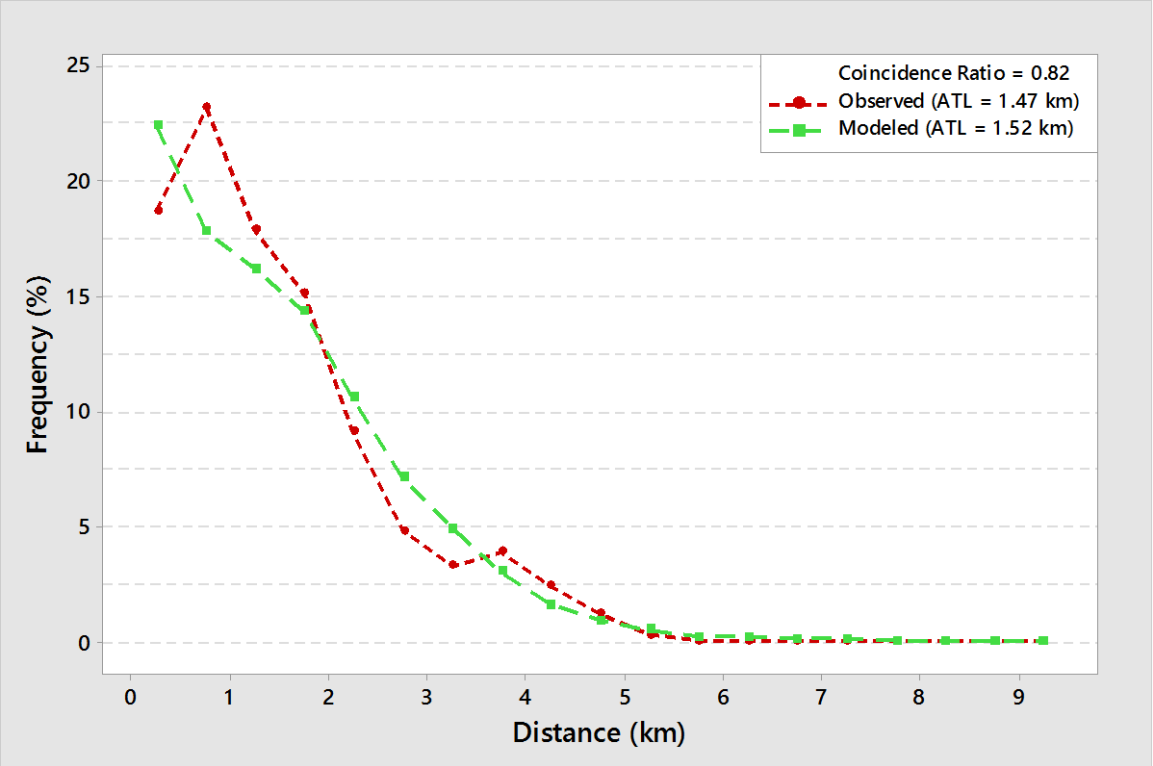

Figure 3.21: TLFD for NHB trips by non-owners

Table 3.11: Trip distribution results summary

Demand Groups	Difference in Average Trip Length (%)	Coincidence Ratio	Intrazonal Trip Share (%)	
			Observed	Modeled
HBWa	-7.07	0.78	1.23	0.87
HBWb	4.37	0.78	0.93	1.85
HBSa	-0.39	0.90	1.11	1.99
HBSb	-0.73	0.87	1.19	2.51
HBE	6.33	0.67	0.58	2.51
HBRa	1.11	0.95	0.52	0.37
HBRb	-2.29	0.83	1.46	1.02
HBOa	0.97	0.81	1.37	2.54
HBOb	0.12	0.88	4.42	3.30
NHBa	-3.79	0.88	2.00	3.51
NHBb	3.32	0.82	3.07	3.71

According to Cambridge Systematics (2010), the modeled average trip length for each purpose should generally be within 5% of observed average trip length for each trip purpose. From Table 3.11, it can be seen that this condition is satisfied for all but the HBE and HBWa demand groups. Besides the HBE demand group, the coincidence ratios exceed 70% for all other demand groups indicating a reasonably good fit between the modeled and observed TLFD for all but the HBE trips.

Using the guideline described in Cambridge Systematics (2010), which recommends that modeled intrazonal trip shares lie within three percentage points of observed intrazonal trip shares, it can be seen that the difference between the observed and modeled intrazonal trip shares lie within three percentage points for all demand groups. Intrazonal trips constitute only a small trip share for all demand groups implying very little loss of information when building blocks are used as spatial units for modeling.

3.4 Chapter Summary and Conclusion

This chapter described the study area as well as the sources, the assembly process, and the characteristics of the data to be used throughout the research. The choice of Dachau was influenced by its high share of non-motorized trips. Data assembly involved the collection of existing secondary data as well as checks and corrections to the collected data. Specifically, the household survey data needed to be corrected

using the returned questionnaires. In the end, the final trip table for subsequent analysis contained 2,186 records expanded to 56,018 trips.

The chapter also described the process involved in developing initial trip tables to be used as input to the approaches explored in this research. To develop the trip tables at the building block level to achieve a relatively finer level of spatial resolution, the TAZ level data were disaggregated to building block level. Trip tables were developed for 11 different demand groups and with the exception of the HBE demand group, all other models performed reasonably well.

Having developed the initial trip tables, the next chapter which identifies the most suitable method for calculating intrazonal impedances will use the trip tables to calculate reference values against which comparisons will be made.

4 Calculating Intrazonal Travel Impedances

4.1 Introduction

Because non-motorized trips are generally short trips, and many of them end up in the same TAZ in macroscopic models, improving the modeling of intrazonal trips in macroscopic models invariably improves the modeling of non-motorized trips. Since the size of the intrazonal impedance is thought to entirely control the number of intrazonal trips within the gravity model for trip distribution (Center for Urban Transportation Studies, 1999), good estimates of intrazonal impedances are required to improve the modeling of intrazonal trips.

The representation of a TAZ by a single centroid makes it impossible to measure intrazonal impedances by the centroid-to-centroid approach used to measure interzonal impedances. Although a number of methods are used to approximate intrazonal impedances, these methods are based on various assumptions related to zone shape and population distribution, which according to Kordi et al. (2012), are not applicable under all circumstances. Whereas Batty (1976) provides a consistent way of defining intrazonal impedances by disaggregating trip and impedance data within individual zones and finding the average trip impedance, the lack of data for the process makes the method practically difficult to use (Batty, 1976; Kordi et al., 2012). The calculation of intrazonal impedance in macroscopic models is thus an ongoing challenge.

This chapter focuses on finding a suitable method for calculating intrazonal impedances. The chapter first describes a proposed method for calculating intrazonal impedances whose development started as part of a master thesis by the author and detailed by Okrah (2012). In finding a suitable method for calculating intrazonal impedances, the research considers the proposed method along with the existing methods, and compares both calculated intrazonal impedances and modeled number of intrazonal trips.

4.2 Proposed Method for Calculating Intrazonal Travel Impedances

In view of the great care with which intrazonal impedances must be calculated (Center for Urban Transportation Studies, 1999), the potential of network representations providing insights into spatial problems (Daganzo, 1980), and the important role of nodes in a network, the proposed method adapts measures of node centrality to the most consistent way of defining intrazonal trip impedance where trip and impedance data are disaggregated within each individual zone and the average trip impedance is computed.

4.2.1 Measures of Node Centrality

ln developing methods for generating connectors in travel demand models, Friedrich and Galster (2009) highlighted the importance of determining weights for network nodes within a TAZ. They related the weight of a node to the share of trips which in reality start or terminate in the vicinity of the node. The centrality of a node therefore determines the relative importance of the node in a network. Different methods exist for measuring node centrality but Borgatti (2005) cautions against the application of measures that assume a given set of flow characteristics to flows with different characteristics. The importance of a node in a network, according to Borgatti, (2005), can therefore not be determined without reference to how traffic flows through the network.

Freeman, (1978) used the structural properties of the center of a star to come up with three different measures of node centrality. To illustrate his idea, he used a network consisting of five nodes and four links as shown in Figure 4.1.

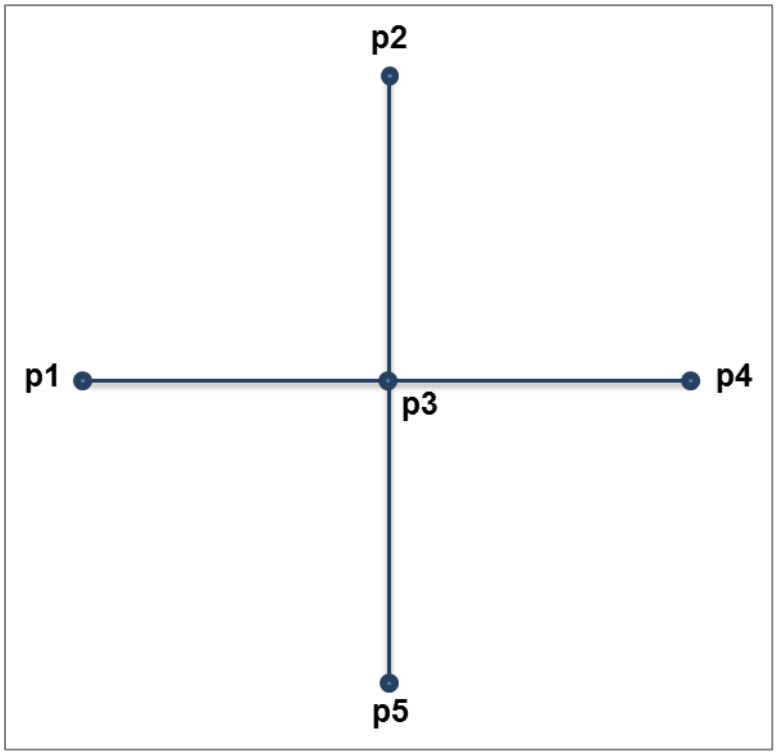

Figure 4.1: A star network (Source: Freeman, 1978)

As can be seen from Figure 4.1, the central node (p3) has the following properties:

1. It has the highest number of connected links;
2. It is located at the minimum distance from all other points; and
3. It falls on the shortest path between the largest possible pairs of other nodes.

Based on these properties, Freeman (1978) formalized three different measures of node centrality namely: degree, closeness and betweenness.

4.2.1.1 Degree Centrality

The degree of a node is viewed as an index of its potential communication activity and is defined as the count of the number of other nodes that are adjacent to it and with which it has direct contact (Freeman, 1978). In a directed graph, like a transport network, the degree of a node can further be classified into indegree and outdegree (Larson and Odoni, 1981). Whereas indegree represents the number of links that lead into a node, outdegree represents the number of links that lead away from it. In relation to weighted networks, Newman (2004) defines the degree of a node as the sum of the weights of the connected links. If the link weights are considered, the

degree C_D of a node *i* is termed node strength (Opsahl et al., 2010) and expressed as:

$$C_D(i) = \sum_{j}^{N} w_{ij}$$

where *N* is the total number of nodes and w_{ij} is the weight of link *ij* if and only if *i* is connected to *j* by a link, otherwise 0. To make the degree measure comparable across networks of different sizes, Freeman (1978) suggests a divisor that removes the effect of network size. Since a node can be connected to at most one less the total number of nodes, the value of the degree centrality is divided by *N-1*. An application of the degree centrality measure in transport studies described in Friedrich & Galster (2009), relates the weight of a node to the link lengths of all connected links of the node.

4.2.1.2 Closeness Centrality

Freeman (1978) defines closeness as the degree to which a node is close to all other nodes in a graph. Accordingly, determining the closeness of a node requires the identification and measurement of the length of the shortest paths between the node and all other nodes in the graph. Equating the closeness of a node to the sum of the shortest distances to all other nodes, nodes that are closer to all other nodes will have low closeness values and nodes that are far from all other nodes will have high closeness values. In order to establish a direct relationship between closeness values and centrality, closeness centrality is expressed as the inverse sum of shortest distance to all other nodes from a focal node. This results in high centrality for nodes with high closeness values and vice-versa. However, as the limit of 1 divided by infinity is 0, Opsahl et al. (2010) recommend that the inverse distances are summed up instead of finding the inverse of the sum. Closeness centrality C_C of a node *i* can thus be expressed as:

$$C_C(i) = \sum_{j}^{N} [d(i,j)]^{-1}$$

where *d(i,j)* is the distance from node *i* to node *j*. Like the degree measure, Freeman (1978) suggests a divisor to make the closeness measure comparable across networks of different sizes. Since the closeness measure is based on distances to at

most one less the total number of nodes, the value of the closeness centrality is divided by *N-1*.

4.2.1.3 Betweenness Centrality

Betweenness, as defined by Freeman (1978), is the frequency with which a node lies between pairs of other nodes on the shortest or geodesic paths connecting them. Like the closeness measure, betweenness requires the identification of shortest paths between all node pairs. The betweenness centrality of a node is then calculated as the number of shortest paths that pass through the node.

Betweenness measures the amount of network flow that a given node controls (Borgatti, 2005). With the assumption that traffic flows along the shortest paths, if each pair of nodes is connected by only one shortest path, the nodes that lie on these paths absolutely control the amount of network flow. However, in the identification of shortest paths, it is possible to find more than one shortest path between two nodes. This reduces the extent to which the nodes on the shortest paths control the amount of network flow. Freeman (1978) caters for this reduction in the potential for control by defining partial betweenness in terms of probability. The betweenness centrality C_B of a node *k* is thus expressed as:

$$C_B(k) = \sum_{i}^{N} \sum_{j}^{N} \frac{g_{ij}(k)}{g_{ij}}; i \neq k \neq j$$

where g_{ij} is the number of shortest paths from node *i* to node *j*. As in the case of the degree and closeness measures, Freeman (1978) suggests a divisor that removes the effect of network size. Using the upper limit of betweenness described in Freeman (1977), the value of the betweenness centrality is divided by *(N2 - 3N + 2) / 2*.

4.2.2 The Proposed Method

In keeping with the most consistent way of defining intrazonal trip distances, the proposed method uses network nodes as trip ends, elicits weights using node centrality measures, and computes the weighted average travel impedance within a zone. Figure 4.2 summarizes the method.

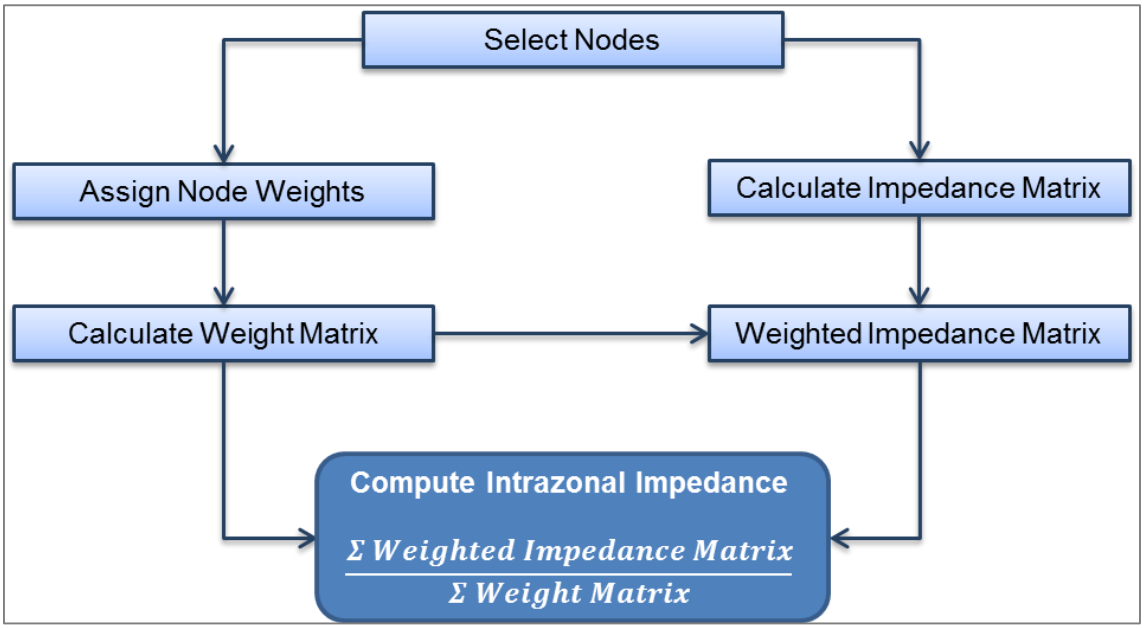

Figure 4.2: Proposed intrazonal impedance calculation method

To calculate intrazonal impedance for a zone, the method begins with the selection of nodes within the zone to serve as intrazonal trip origins and destinations. In order to consider only nodes that provide access to activity locations, nodes that lie on high-speed links such as highways are excluded from the selection.

After the node selection, each selected node is assigned an origin and destination weight based on their centrality in the zone's network. The weight elicitation is a proxy trip generation where the origin weight of a node represents the volume of trips produced by the node, and the destination weight represents the volume of trips attracted to the node. To distribute these trips among the nodes within the zone, the corresponding origin and destination weights for each node pair are multiplied to create a weight matrix. The travel impedances between the selected node pairs are also used to create an impedance matrix.

With a weight matrix and an impedance matrix available for the intrazonal node pairs, their respective values are multiplied together to create a weighted impedance matrix. Intrazonal impedance is then computed as the sum of the weighted impedance matrix divided by the sum of the weight matrix. Using different weight elicitation approaches, different forms of the method can be specified.

4.3 Comparison of Intrazonal Travel Impedances

To test the suitability of the proposed and existing intrazonal impedance calculation methods, the various methods were used to compute intrazonal walking, cycling and driving times, and their values were compared against reference intrazonal times. With walking speed being constant, intrazonal walking times represented impedances that have direct relationship with travel distances. Intrazonal cycling times, on the other hand, represented impedances that change with elevation, while intrazonal driving times represented impedances that vary with other link-specific attributes.

4.3.1 Aggregation of TAZ

To compare intrazonal times at different levels of spatial aggregation, the 102 TAZ of Dachau were aggregated into 2-, 5-, 10-, 25-, and 50-zone systems. The aggregation involved the manual combination of two or more adjacent TAZ into single zones depending on the zone system. For the 2-zone system, each new zone required a combination of 51 original TAZ. Similarly, each new zone of the 50-zone system required a combination of approximately 2 original TAZ.

Using different TAZ combinations, three variants were generated for each zone system, bringing the total number of zone systems to 15. The letters a, b, and c are used to distinguish between the three variants of each zone system. Thus, 2a, 2b, and 2c are the three variants of the 2-zone system. Since TAZ are generally variably sized, the heterogeneity in zone sizes was maintained in the aggregated zone systems.

4.3.2 Reference Intrazonal Times

An important step in this part of the research was determining reference intrazonal time values against which the calculated intrazonal walking, cycling and driving times would be compared. Three different options were considered and these included: (1) using average times between building block pairs within the same zone; (2) using average times between building block pairs within the same zone weighted by their corresponding trips; and (3) using average times from the surveyed intrazonal trips.

While options 1 and 2 were explored further, option 3 was excluded for a couple of reasons. First of all, the surveyed intrazonal trips did not have sufficient records to determine intrazonal times for every TAZ. There were instances of TAZ with no surveyed intrazonal trip, so for such TAZ, no intrazonal reference time could be determined. In addition, because reported times do not provide true reflections of actual times, the observed times would have had to be computed by applying the skimmed times to the respective origins and destinations. However, since the surveyed trips were provided at the TAZ level, there would be no paths along which intrazonal times could be skimmed.

Options 1 and 2 were therefore used to define two different reference values for each intrazonal time considered. Using option 1, reference intrazonal walking, cycling and driving times were defined by finding the average walking, cycling and driving times respectively between building block pairs within the same zone. For option 2, the average walking, cycling and driving times between building block pairs within the same zone were weighted by their corresponding modeled trips to get reference intrazonal walking, cycling and driving times respectively. The modeled trips used for the weighting were based on the sum of the initial trip tables described in Section 3.3.

4.3.3 Calculated Intrazonal Times

For each zone in the aggregated zone systems, the proposed and existing intrazonal impedance calculation methods were used to compute intrazonal walking, cycling and driving times. Table 4.1 summarizes the calculation methods considered and their characteristics.

Table 4.1: Intrazonal impedance calculation methods

Calculation Method	Approach	Notes
Base	1. Select nodes within a zone to serve as trip ends 2. Assign weights to nodes 3. Get time matrix between node pairs 4. Compute weight matrix between node pairs by multiplying origin weights by destination weights 5. Compute weighted average time within zone	Node weight = 1 for all nodes
Degree		Node weights by degree centrality
Closeness		Node weights by closeness centrality
Area-Based	1. Calculate intrazonal distance as $d_{ii} = \sqrt{\frac{A}{2\pi}}$ 2. Apply intrazonal speed of: a. 5 km/h to get intrazonal walking time b. 15.5 km/h to get intrazonal cycling time c. 30 km/h to get intrazonal driving time	A = Area of zone
Nearest Neighbor	1. Find average time to 3 nearest zones 2. Divide average time by 2	

As can be seen from Table 4.1, the calculation methods considered included the base, degree, and closeness forms of the proposed method, the simplest form of the area-based methods suggested by Batty (1976), and the nearest neighbor technique. Because of the high time requirement as well as its failure to calculate intrazonal impedance when no nodes lie on shortest paths (Okrah, 2012), the betweenness form of the proposed method was not considered. The other average trip length methods were also not considered since the proposed method offered a theoretically better approach to calculating average trip lengths than the existing practicable average trip length methods.

Whereas the PTV Visum software provided a direct function to calculate intrazonal times by the nearest neighbor technique, a python script shown in Appendix 1 was written to calculate intrazonal times by the base, degree, closeness and area-based methods. Intrazonal walking, cycling, and driving times by the nearest neighbor method was calculated by finding the average of the walking, cycling and driving times respectively to the three nearest zones and halving the values. The area-based method required an initial calculation of intrazonal distance d_{ii} as:

$$d_{ii} = \sqrt{\frac{A}{2\pi}}$$

where *A* is the area of the zone. Subsequently, an intrazonal speed of 5 km/h, 15.5 km/h, and 30km/h were subsequently applied to get intrazonal walking, cycling and driving times respectively.

The intrazonal time calculation by the base, degree, and closeness methods followed the same approach, with the only difference being the node centrality measure used to assign weights. The first step involved the selection of nodes to serve as intrazonal trip origins and destinations. Nodes that lay on links open to pedestrians, bicycles and cars were selected, with the assumption that such links provided direct access to activity locations. Secondly, the selected nodes were assigned origin and destination weights based on their centrality in the network. After assigning weights to the nodes, the corresponding origin and destination node weights for each node pair were multiplied to create a weight matrix. The walking, cycling and driving times between the node pairs were also used to create walking, cycling and driving matrices respectively.

Subsequently, the walking, cycling and driving time matrix values were multiplied by their corresponding weight matrix values to create weighted walking, cycling and driving time matrices respectively. Intrazonal walking time was then calculated as the sum of the weighted walking time matrix divided by the sum of the weight matrix. Similarly, intrazonal cycling time was calculated as the sum of the weighted cycling time matrix divided by the weight matrix, and intrazonal driving time was computed as the sum of the weighted driving time matrix divided by the sum of the weight matrix.

4.3.4 Comparing Intrazonal Walking Times

This sub-section assesses the suitability of the various intrazonal impedance calculation methods in calculating intrazonal walking times, and in effect, other impedances that have direct relationship with travel distances. Figure 4.3 shows the distributions of the two reference intrazonal walking times, as well as the intrazonal walking times calculated with the different calculation methods. The distributions include intrazonal walking times computed for the three variants of each of the five zone systems resulting from the TAZ aggregation.

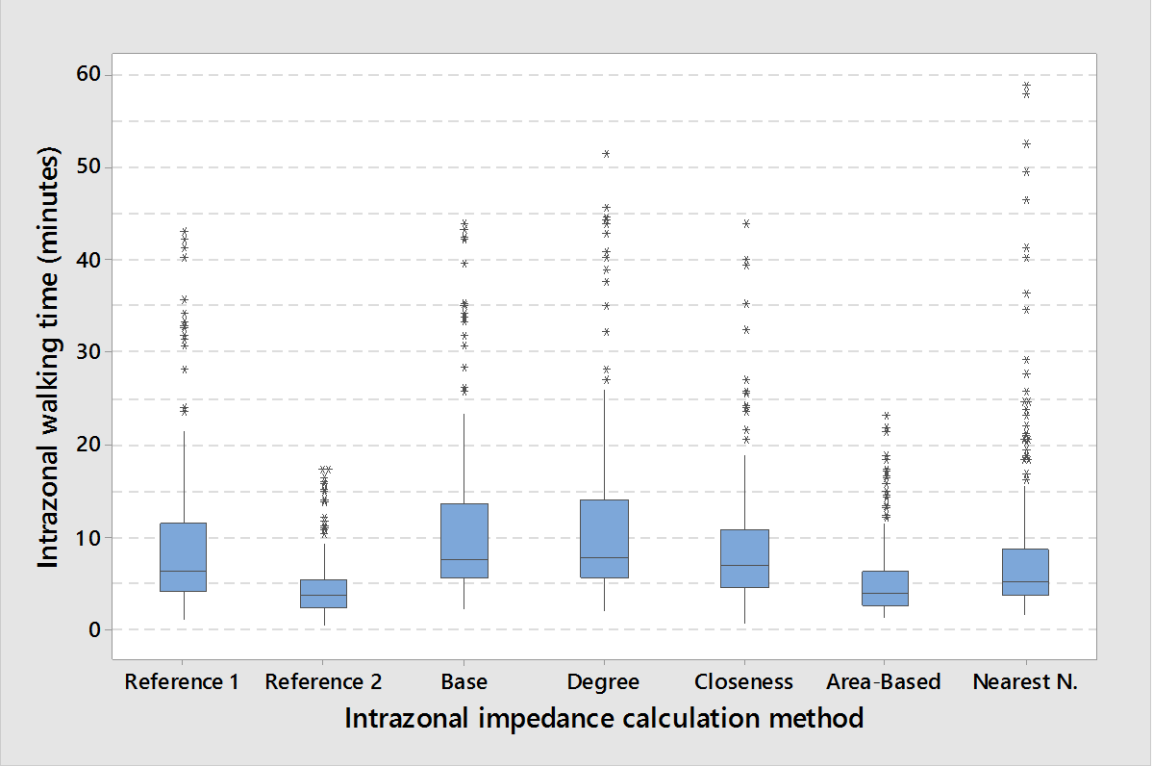

Figure 4.3: Distribution of reference and calculated intrazonal walking times

The box plots in Figure 4.3 show dissimilar spread characteristics among the different walking time distributions. The proposed methods produce higher values of intrazonal walking times than the existing methods. Whereas the area-based method produces the smallest values of intrazonal walking times among the calculation methods, the nearest neighbor technique produces the widest range of intrazonal walking times. Among the proposed methods, the closeness method produces the lowest values of intrazonal walking times whereas the degree method produces slightly higher values than the base method.

References 1 and 2 represent the reference walking times computed using options 1 and 2 respectively, and the two can be seen to produce significantly different distributions indicating that the choice of reference values has a huge impact on the suitability or otherwise of the methods. Whereas the proposed methods produce distributions that are closer to reference 1, it is the area-based method that produces the closest distributions to reference 2. Depending on which reference distribution is considered the better representation of actual intrazonal walking times, the area-

based or the proposed methods can be deemed to provide the best estimates of intrazonal walking times.

Using references 1 and 2 as benchmarks to measure how well the different intrazonal impedance calculation methods compute intrazonal walking times, Figures 4.4 and 4.5 show the deviations in the computed intrazonal walking times from references 1 and 2 respectively.

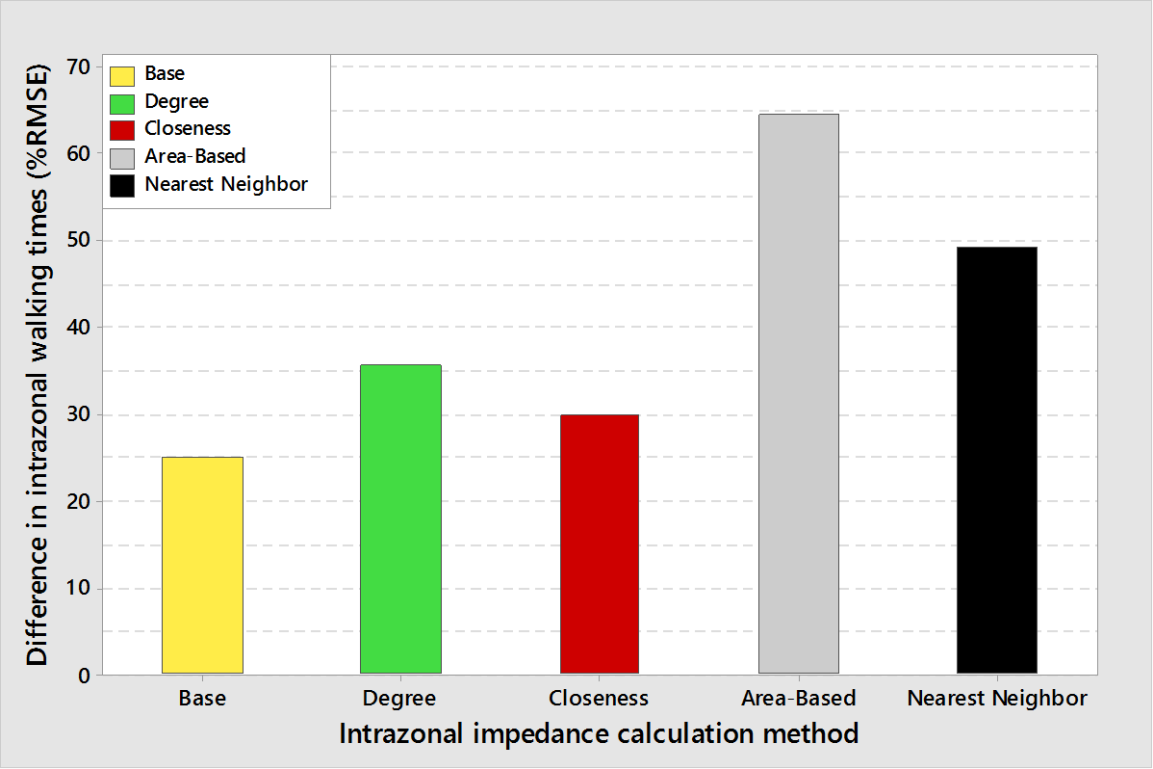

Figure 4.4: Deviations from reference 1 intrazonal walking times

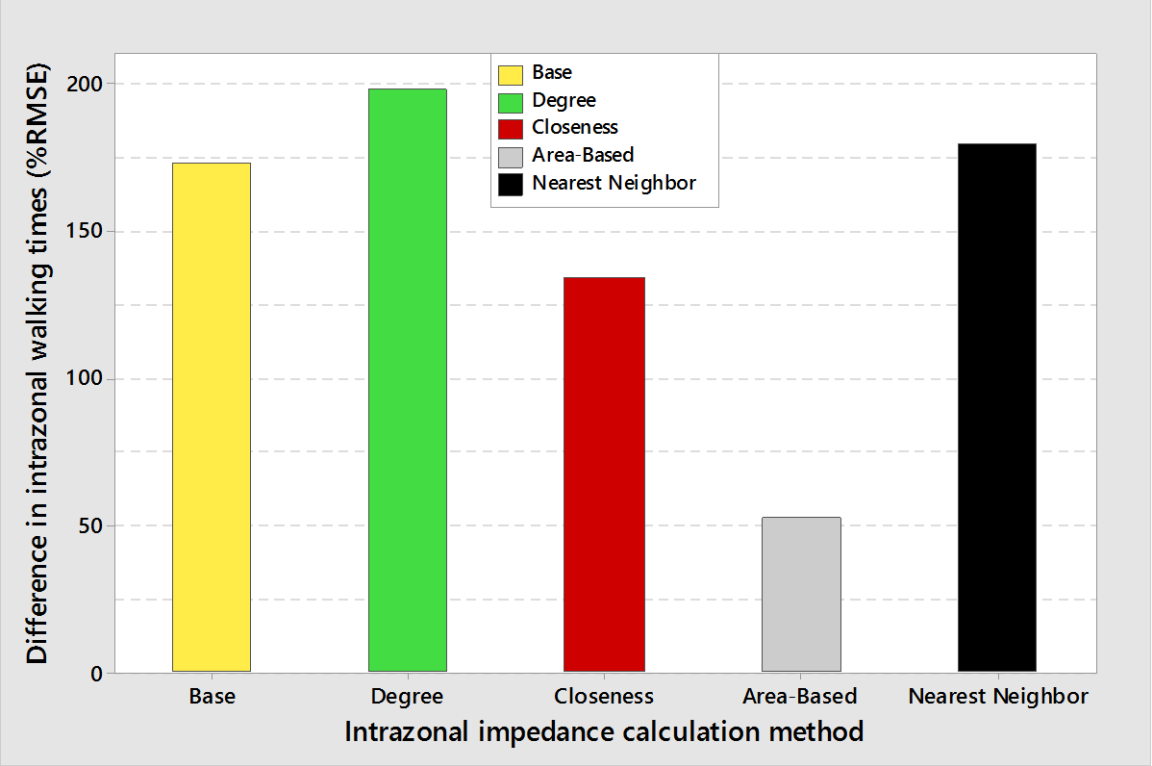

Figure 4.5: Deviations from reference 2 intrazonal walking times

From Figures 4.4 and 4.5, it can be seen that none of the methods produce accurate estimates of intrazonal walking times using either of the references as benchmarks. Nevertheless, the walking times produced by the methods have lower deviations from reference 1 than from reference 2. Whereas the deviations from reference 1 lie between 25% and 65%, the deviations from reference 2 fall between 52% and 199%. With the exception of the area-based method that results in 53% deviation from reference 2, all other methods result in deviations from reference 2 exceeding 130%.

By comparing the bars in Figures 4.4 and 4.5, the base method provides the best estimates of intrazonal walking times when reference 1 is used as the benchmark closely followed by the closeness and degree methods whereas the area-based method provides the worst estimates. On the other hand, when reference 2 is used as the benchmark, the area-based method provides the best and only reasonable estimates of intrazonal walking times.

Figures 4.6 and 4.7 show the deviations from references 1 and 2 respectively for each of the zone systems resulting from the TAZ aggregation.

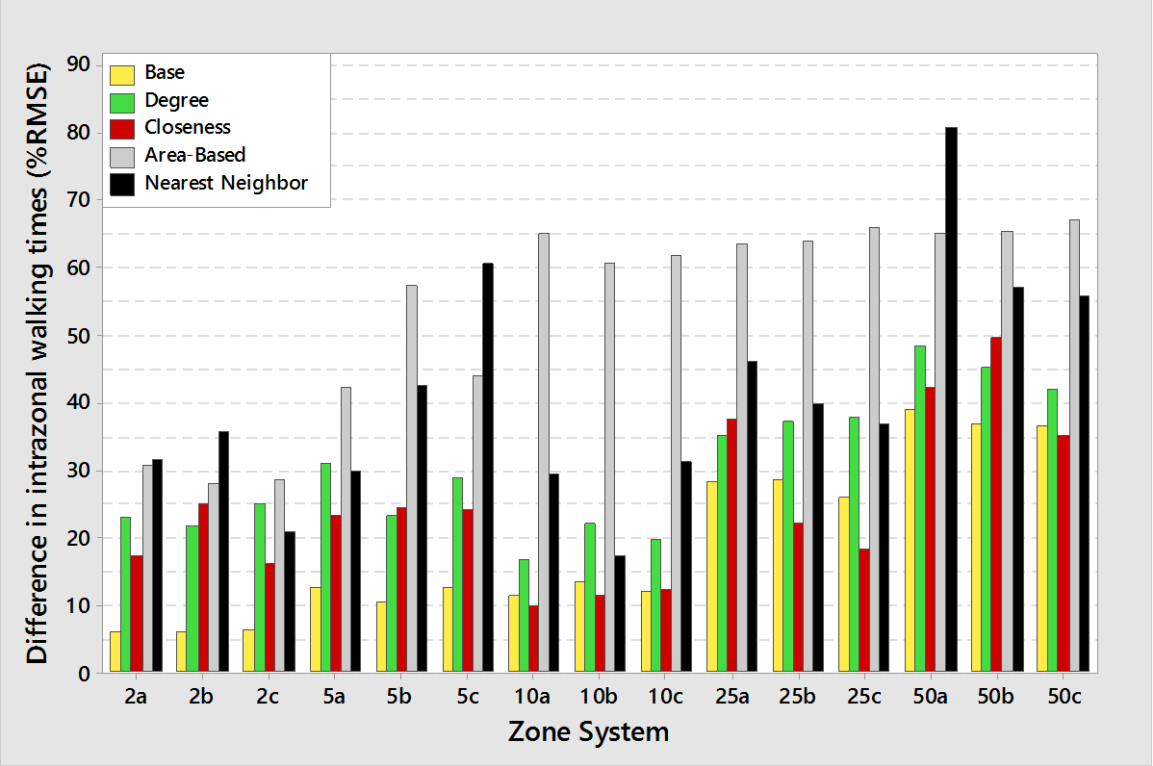

Figure 4.6: Deviations from reference 1 walking times by zone system

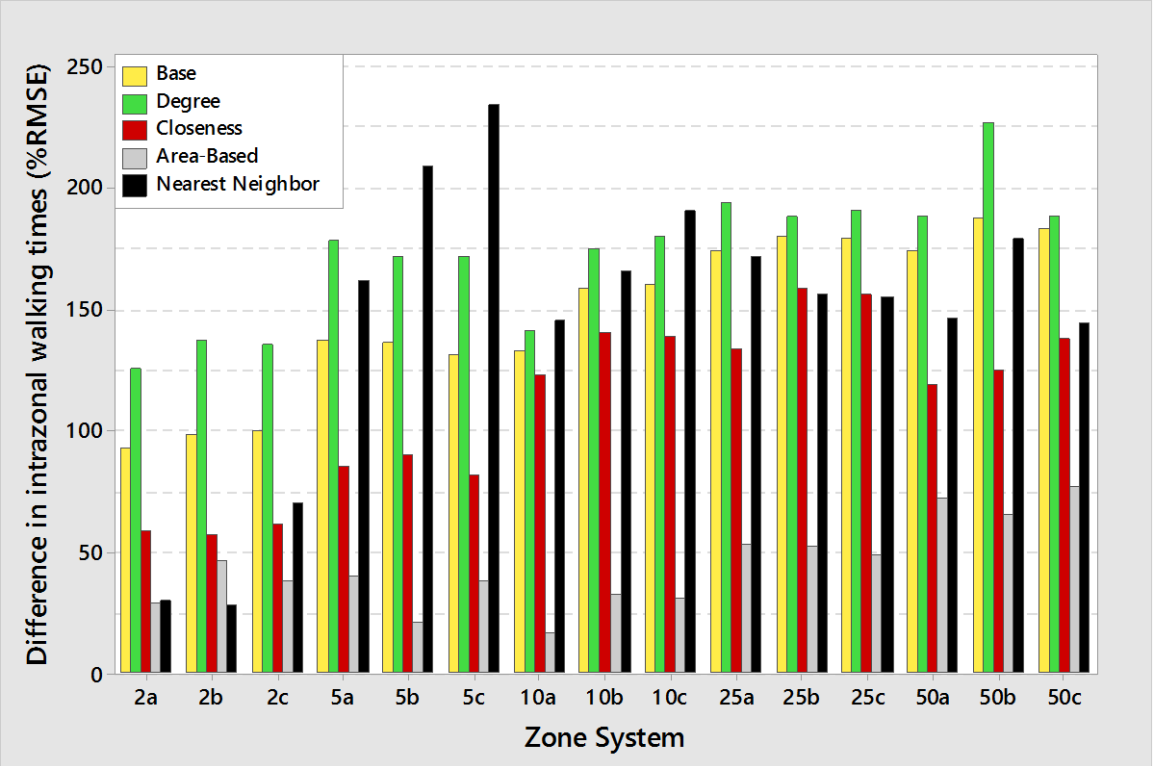

Figure 4.7: Deviations from reference 2 walking times by zone system

A comparison of the deviations in Figures 4.6 and 4.7 shows that the performance of the proposed methods for reference 1 and the area-based method for reference 2 is consistent across the different zone systems. In the case of reference 1, the best performance alternates between the base and the closeness methods across the different zone systems. In the case of reference 2 however, the area-based method provides the best estimate for all but the 2b zone system, where the nearest neighbor technique provides the best estimate. The area-based method still provides a good estimate for this zone system.

Although there are different levels of disparity involved, the deviations are comparable across the three variants of each zone system, and the deviations generally get larger as zone systems get finer.

4.3.5 Comparing Intrazonal Cycling Times

This sub-section assesses the suitability of the various intrazonal impedance calculation methods in calculating intrazonal cycling times, and in effect, other impedances that change with elevation. Figure 4.8 shows the distributions of the two reference intrazonal cycling times as well as the intrazonal cycling times calculated with the different calculation methods. The distributions include intrazonal cycling times computed for the three variants of each of the five zone systems resulting from the TAZ aggregation.

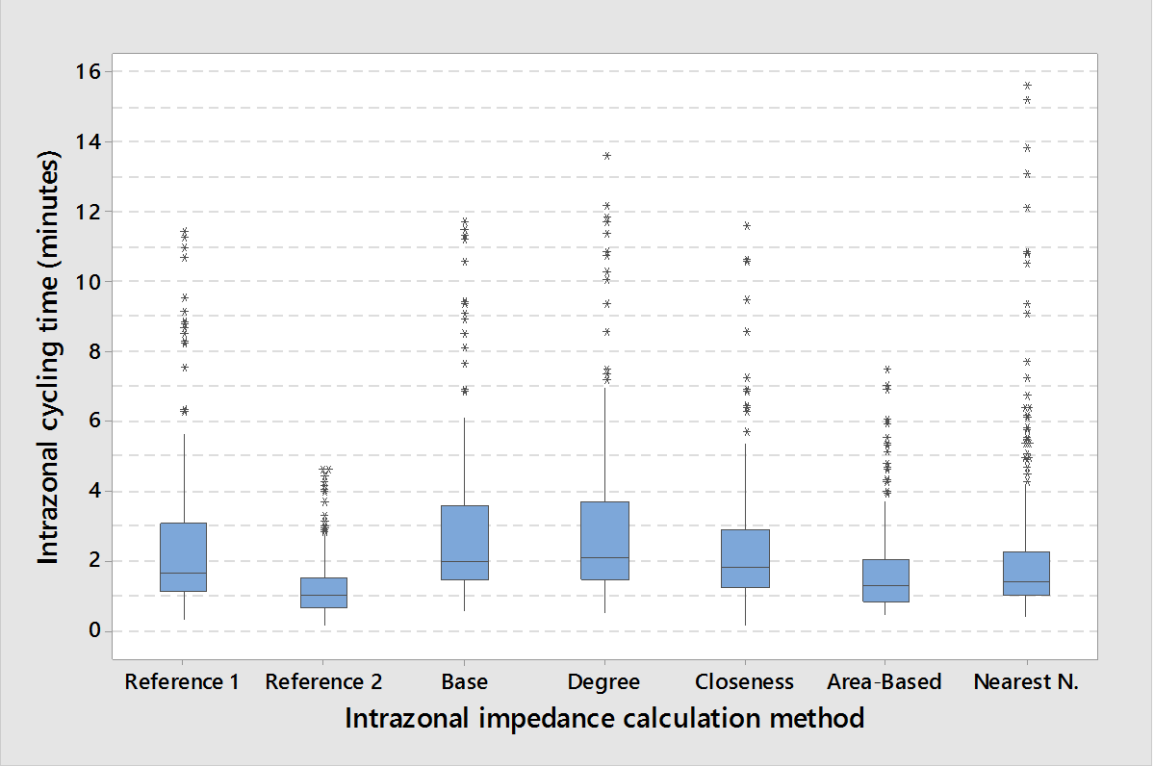

Figure 4.8: Distribution of reference and calculated intrazonal cycling times

The box plots in Figure 4.8 show dissimilar spread characteristics among the different cycling time distributions. The proposed methods produce higher values of intrazonal cycling times than the existing methods. Whereas the area-based method produces the smallest values of intrazonal cycling times among the calculation methods, the nearest neighbor technique produces the widest range of intrazonal cycling times. Among the proposed methods, the closeness method produces the lowest values of intrazonal cycling times whereas the degree method produces slightly higher values than the base method.

References 1 and 2 represent the reference cycling times computed using options 1 and 2 respectively, and the two can be seen to produce significantly different distributions indicating that the choice of reference values has a huge impact on the suitability or otherwise of the methods. Whereas the proposed methods produce distributions that are closer to reference 1, it is the area-based method that produces the closest distributions to reference 2. Depending on which reference distribution is considered the better representation of actual intrazonal cycling times, the area-

based or the proposed methods can be deemed to provide the best estimates of intrazonal cycling times.

Using references 1 and 2 as benchmarks to measure how well the different intrazonal impedance calculation methods compute intrazonal cycling times, Figures 4.9 and 4.10 show the deviations in the computed intrazonal cycling times from references 1 and 2 respectively.

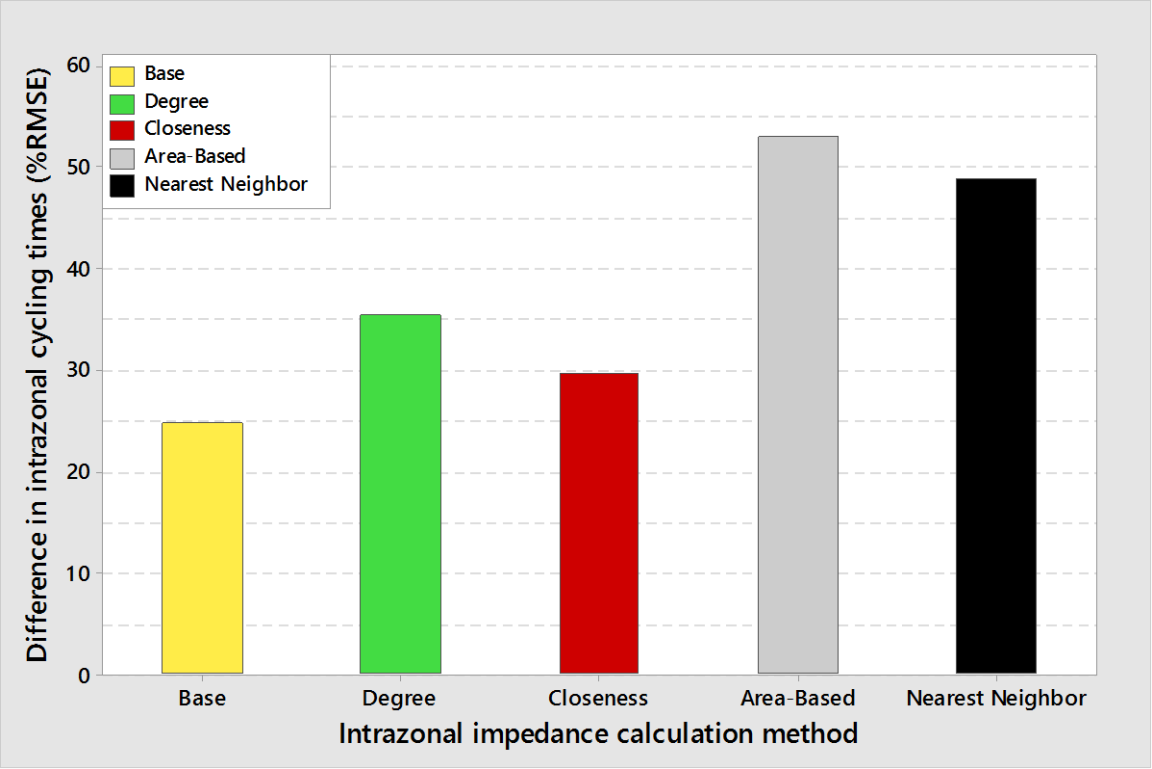

Figure 4.9: Deviations from reference 1 intrazonal cycling times

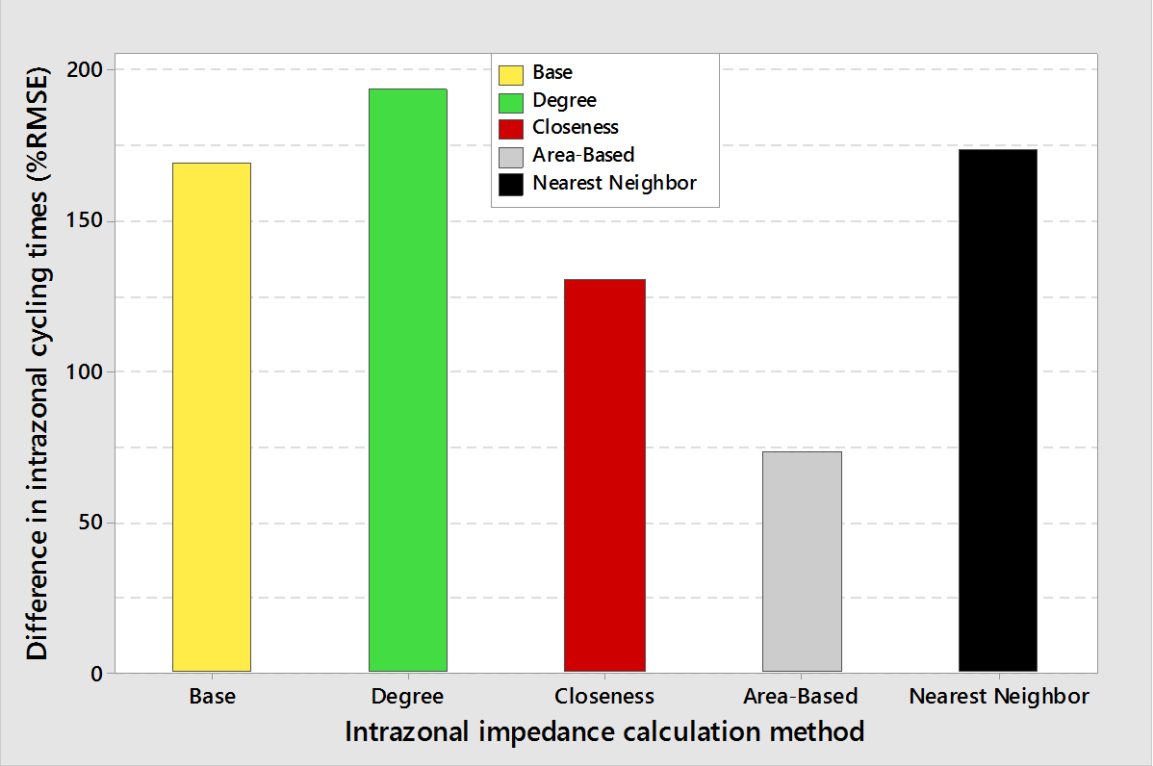

Figure 4.10: Deviations from reference 2 intrazonal cycling times

From Figures 4.9 and 4.10, it can be seen that none of the methods produce accurate estimates of intrazonal cycling times using either of the references as benchmarks. Nevertheless, the cycling times produced by the methods have lower deviations from reference 1 than from reference 2. Whereas the deviations from reference 1 lie between 24% and 53%, the deviations from reference 2 fall between 73% and 194%. With the exception of the area-based method that results in 74% deviation from reference 2, all other methods result in deviations from reference 2 exceeding 130%.

By comparing the bars in Figures 4.9 and 4.10, the base method provides the best estimates of intrazonal cycling times when reference 1 is used as the benchmark closely followed by the closeness and degree methods whereas the area-based method provides the worst estimates. On the other hand, when reference 2 is used as the benchmark, the area-based method provides the best but poor estimates of intrazonal cycling times.

Figures 4.11 and 4.12 show the deviations from references 1 and 2 respectively for each of the zone systems resulting from the TAZ aggregation.

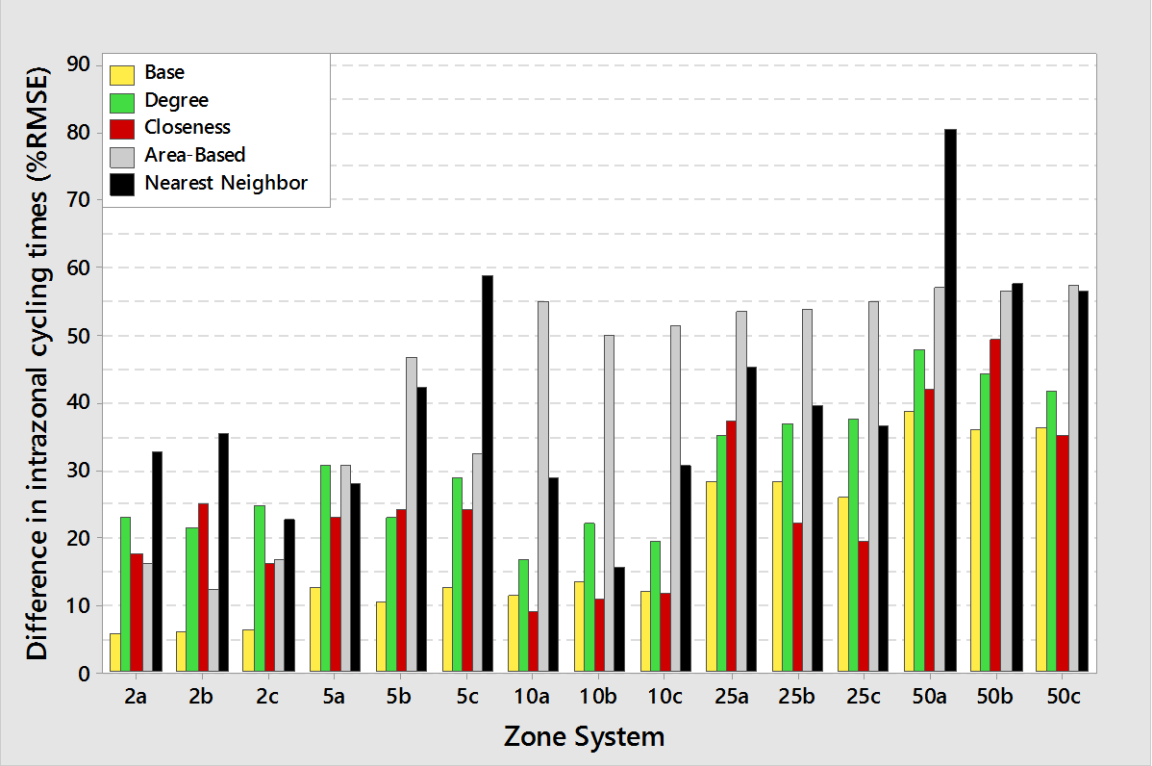

Figure 4.11: Deviations from reference 1 cycling times by zone system

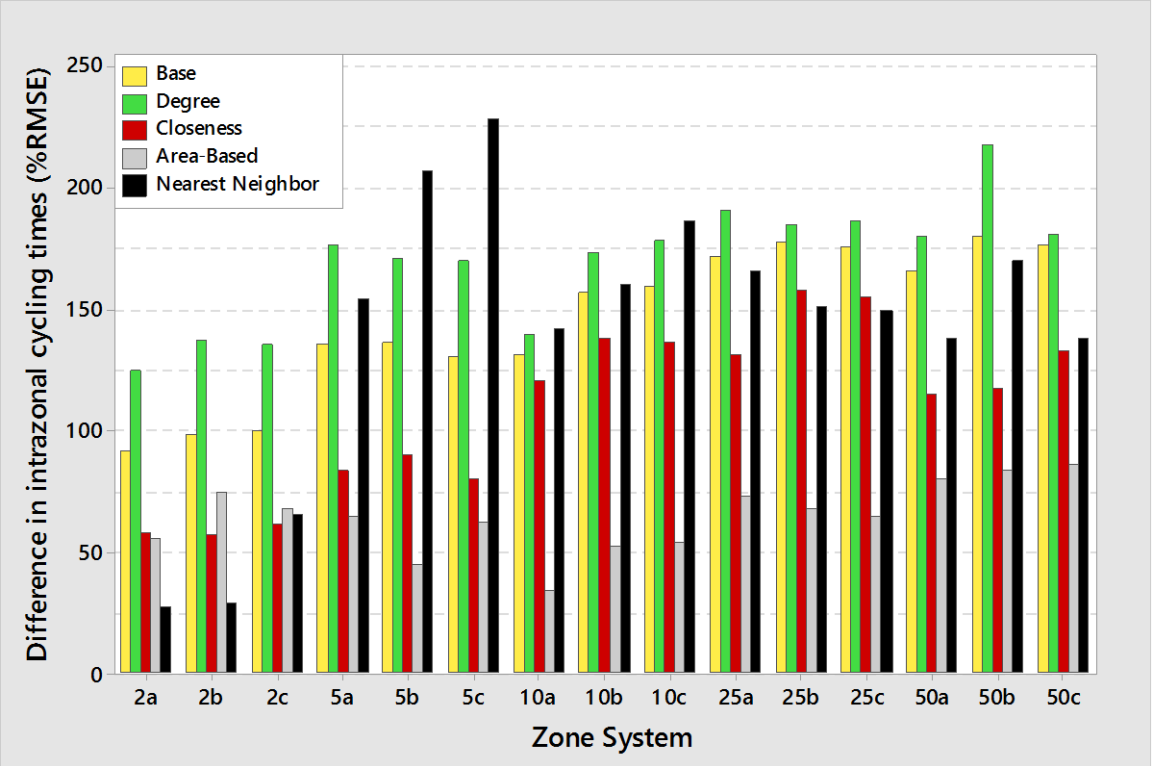

Figure 4.12: Deviations from reference 2 cycling times by zone system

A comparison of the deviations in Figures 4.11 and 4.12 shows that, the performance of the proposed methods for reference 1 and the area-based method for reference 2 is consistent across the different zone systems. In the case of reference 1, the best performance alternates between the base and the closeness methods across the different zone systems. In the case of reference 2 however, the area-based method provides the best estimate for all but the variants of the 2-zone system.

Although there are different levels of disparity involved, the deviations are comparable across the three variants of each zone system, and the deviations generally get larger as zone systems get finer.

4.3.6 Comparing Intrazonal Driving Times

This sub-section assesses the suitability of the various intrazonal impedance calculation methods in calculating intrazonal driving times, and in effect, other impedances that vary with other link-specific attributes. Figure 4.13 shows the distributions of the two reference intrazonal driving times as well as the intrazonal driving times calculated with the different calculation methods. The distributions include intrazonal driving times computed for the three variants of each of the five zone systems resulting from the TAZ aggregation.

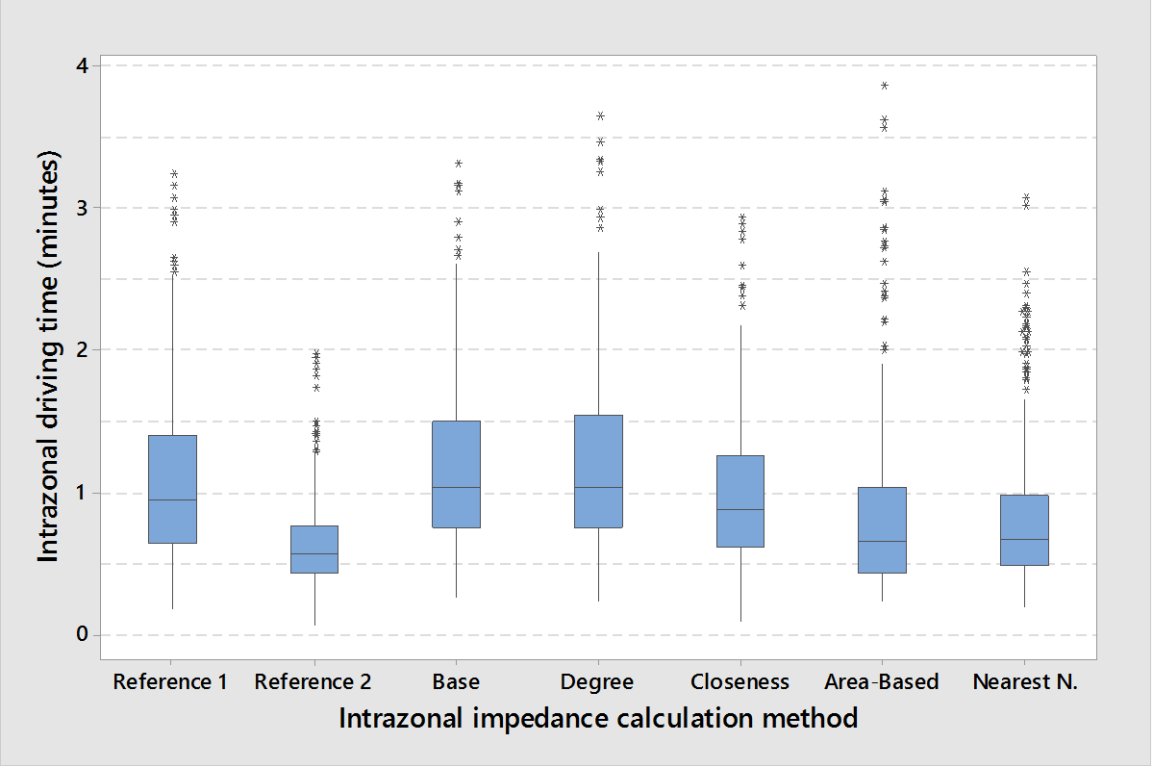

Figure 4.13: Distribution of reference and calculated intrazonal driving times

The box plots in Figure 4.13 show dissimilar spread characteristics among the different driving time distributions. The proposed methods produce higher values of intrazonal driving times than the existing methods with the area-based method producing the widest range of intrazonal driving times. Among the proposed methods, the closeness method produces the lowest values of intrazonal driving times whereas the degree method produces slightly higher values than the base method.

References 1 and 2 represent the reference driving times computed using options 1 and 2 respectively, and the two can be seen to produce significantly different distributions indicating that the choice of reference values has a huge impact on the suitability or otherwise of the methods. Whereas the proposed methods produce distributions that are closer to reference 1, none of the methods tend to have distributions close to reference 2. Depending on which reference distribution is considered the better representation of actual intrazonal driving times, the area-based, nearest neighbor technique or the proposed methods can be deemed to provide the best estimates of intrazonal driving times.

Using references 1 and 2 as benchmarks to measure how well the different intrazonal impedance calculation methods compute intrazonal driving times, Figures 4.14 and 4.15 show the deviations in the computed intrazonal driving times from references 1 and 2 respectively.

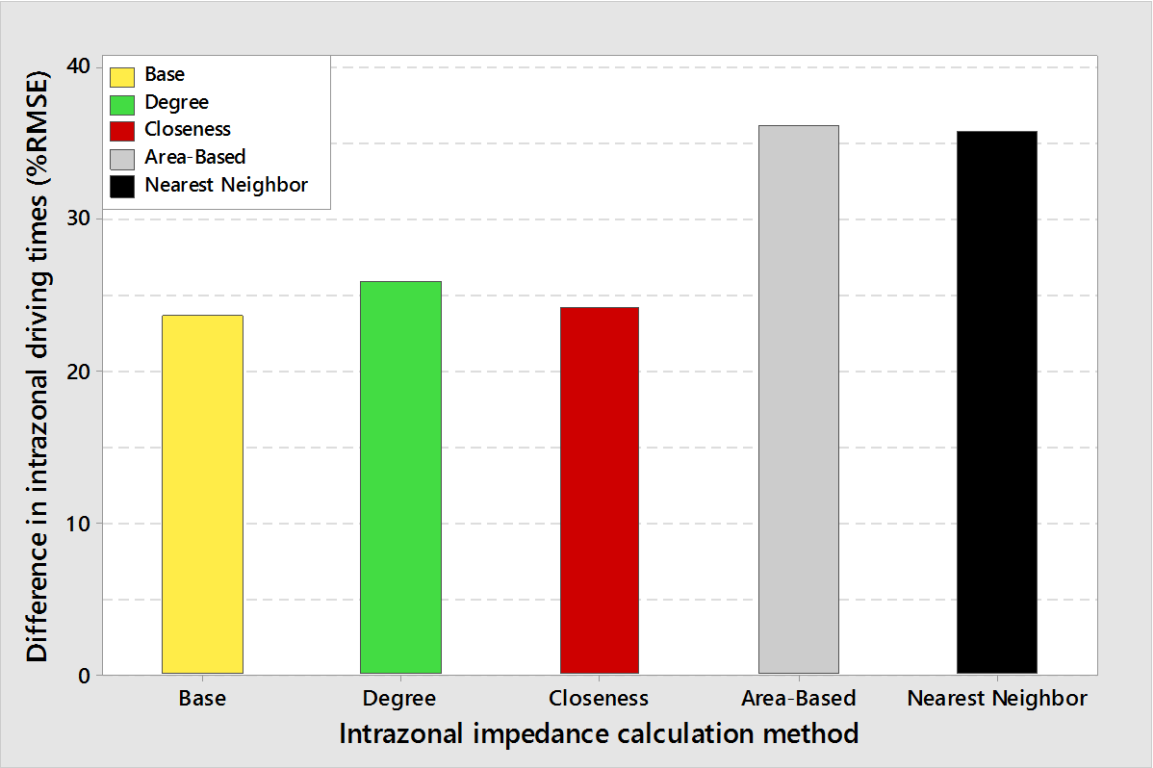

Figure 4.14: Deviations from reference 1 intrazonal driving times

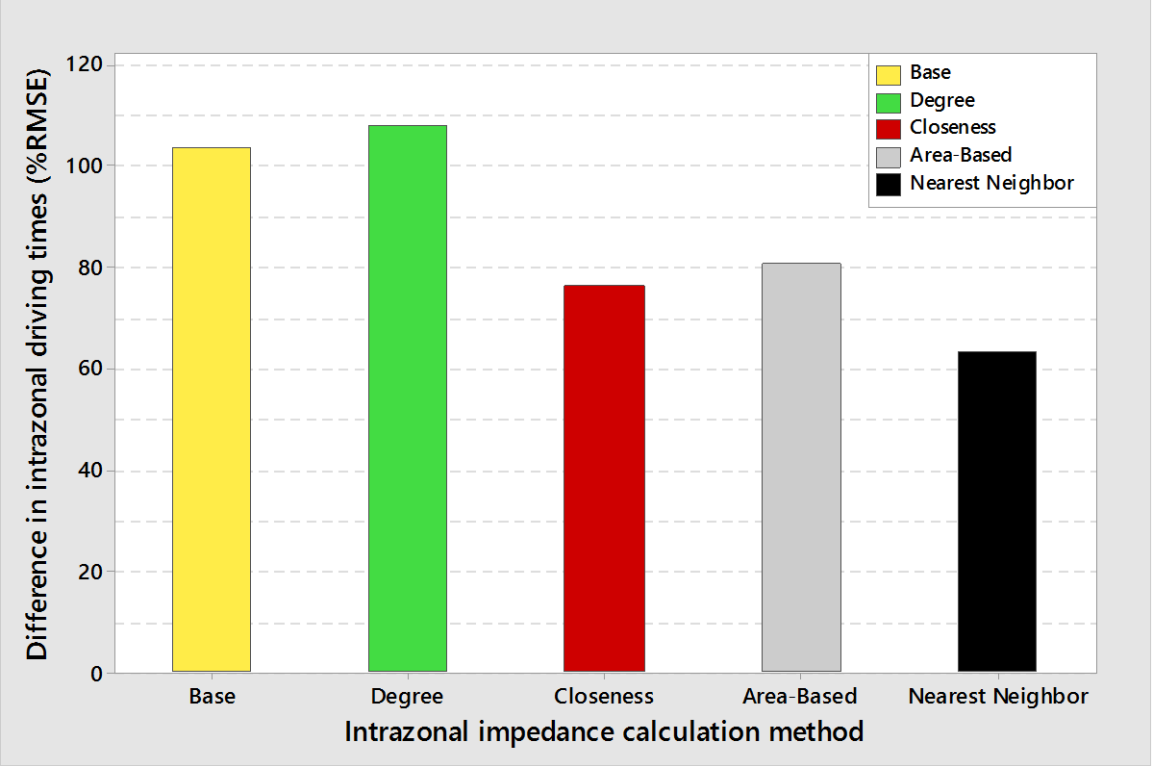

Figure 4.15: Deviations from reference 2 intrazonal driving times

From Figures 4.14 and 4.15, it can be seen that none of the methods produce accurate estimates of intrazonal driving times using either of the references as benchmarks. Nevertheless, the driving times produced by the methods have lower deviations from reference 1 than from reference 2. Whereas the deviations from reference 1 lie between 23% and 37%, the deviations from reference 2 fall between 63% and 109%.

By comparing the bars in Figures 4.14 and 4.15, the base method provides the best estimates of intrazonal driving times when reference 1 is used as the benchmark closely followed by the closeness and degree methods whereas the area-based method provides the worst but reasonable estimates. On the other hand, when reference 2 is used as the benchmark, the nearest neighbor technique provides the best but poor estimates of intrazonal driving times.

Figures 4.16 and 4.17 show the deviations from references 1 and 2 respectively for each of the zone systems resulting from the TAZ aggregation.

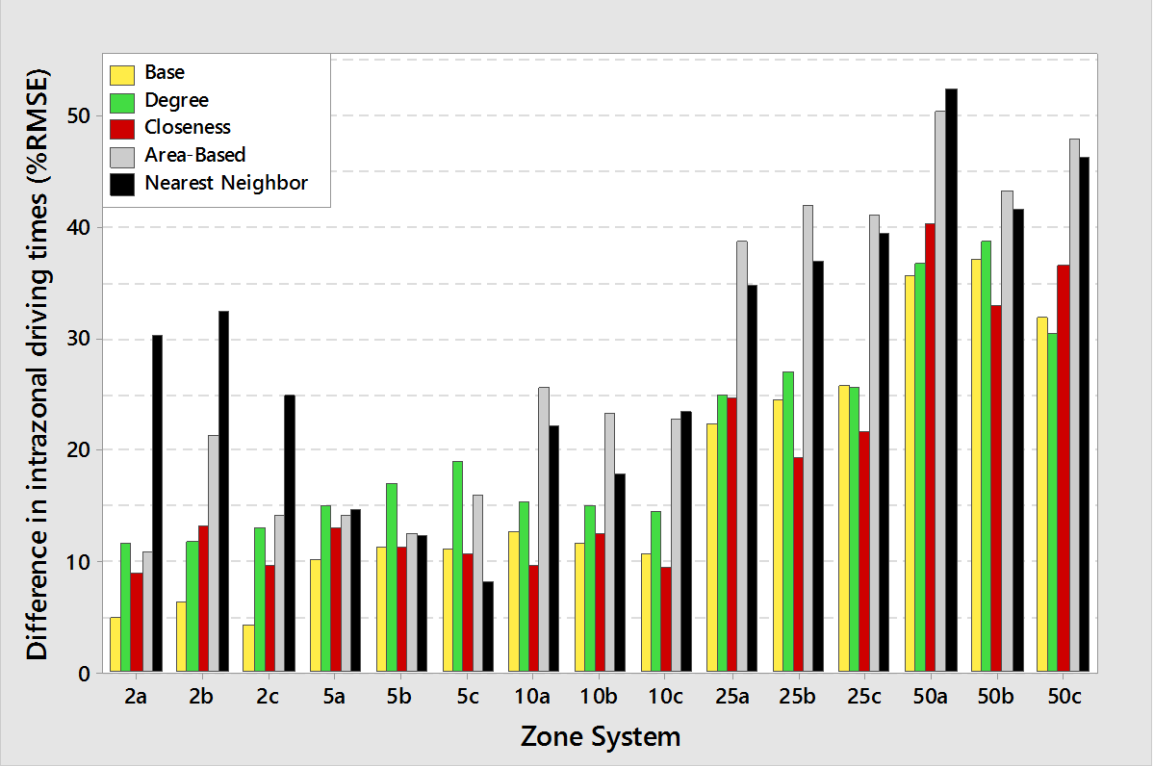

Figure 4.16: Deviations from reference 1 driving times by zone system

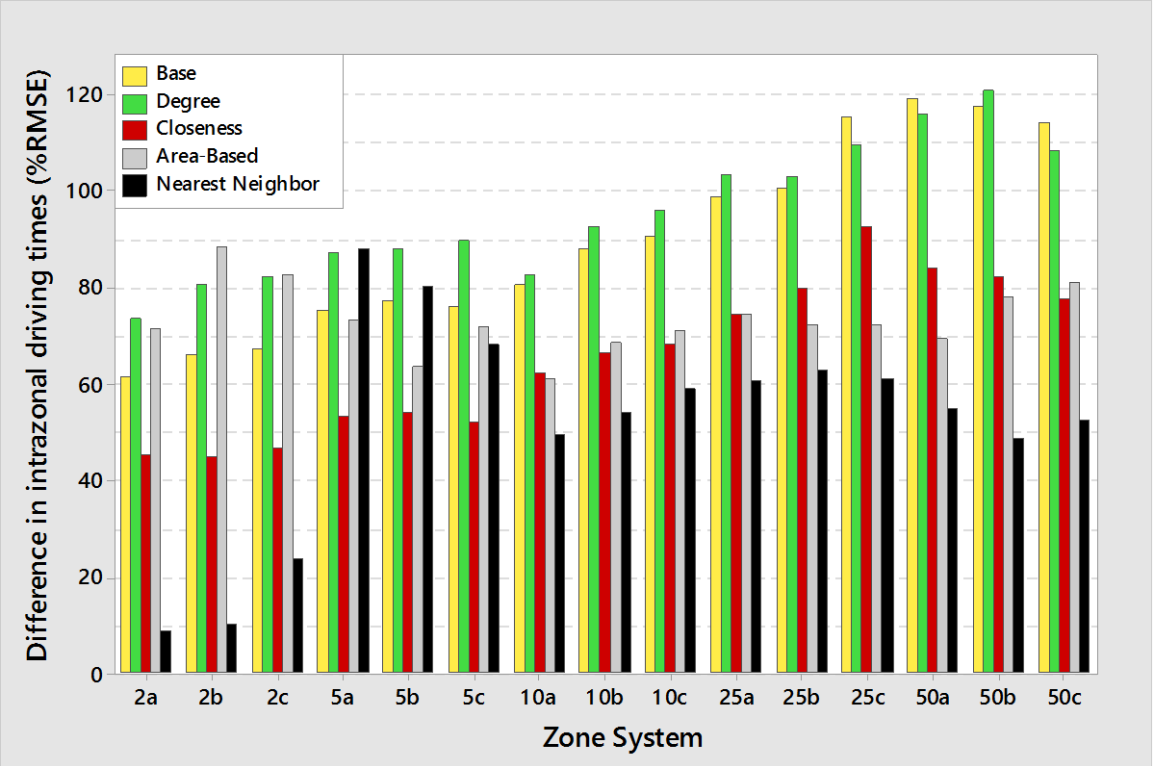

Figure 4.17: Deviations from reference 2 driving times by zone system

A comparison of the deviations in Figures 4.16 and 4.17 shows that, the performance of the proposed methods for reference 1 and the nearest neighbor technique for reference 2 is consistent across the different zone systems. In the case of reference 1, the best performance alternates between the base and the closeness methods across the different zone systems. In the case of reference 2 however, the nearest neighbor technique provides the best estimate for all but the variants of the 5-zone system.

Although there are different levels of disparity involved, the deviations are comparable across the three variants of each zone system, and the deviations generally get larger as zone systems get finer.

4.3.7 Discussion of the Intrazonal Travel Impedance Comparison

Figure 4.18 gives an overview of the deviations in the calculated intrazonal times from the two reference options for the different modes considered.

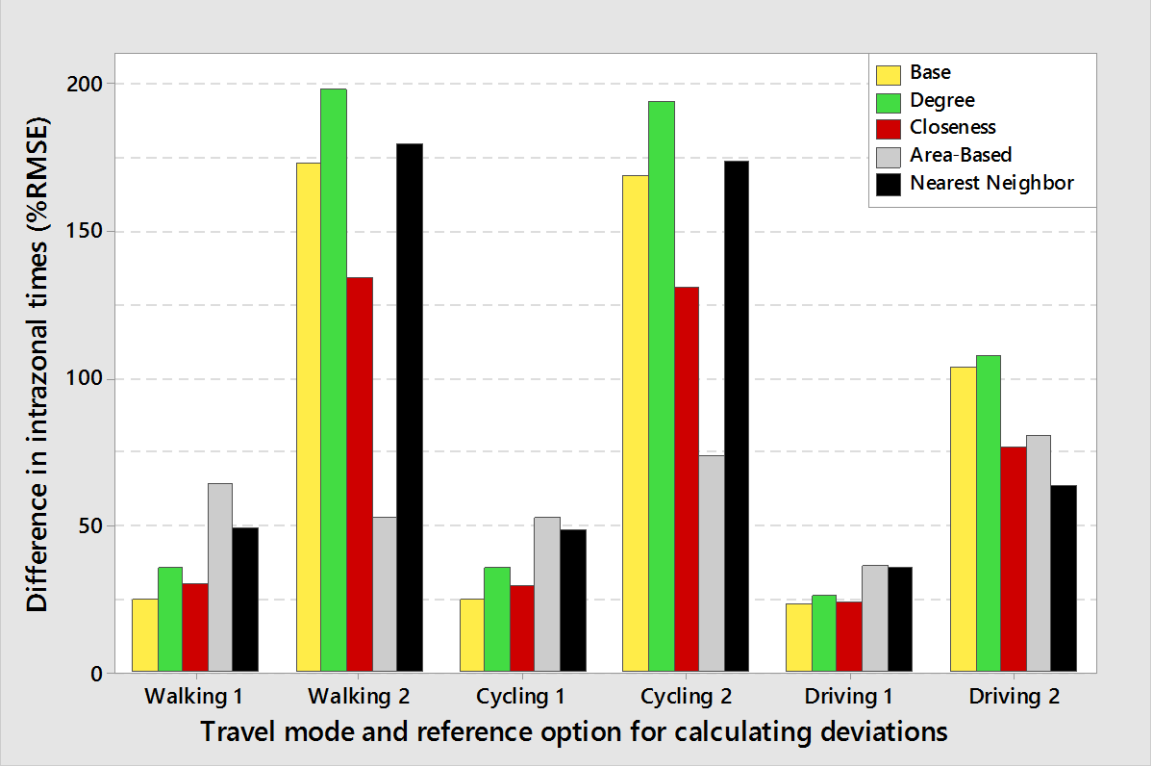

Figure 4.18: Summary of deviations from reference intrazonal times

In Figure 4.18, Walking 1 represents the reference intrazonal walking times computed using reference option 1 while Driving 2 represents the reference intrazonal driving times computed using reference option 2. Apart from the intrazonal times calculated with the area-based method, the deviations in intrazonal walking and cycling times are similar and higher than the deviations in intrazonal driving times calculated with the other methods for each of the reference options considered. This pattern is not observed for the area-based method because, unlike the other methods, the area-based method does not consider transport network in the calculation of intrazonal times. Whereas most of the network links were multimodal and permitted pedestrians, bicycles and cars, the network included links that permitted cars but were closed to pedestrian and bicycles. Essentially, the walking and cycling network were identical but not as connected as the car network, and as such involved a wider range of distance than the driving network. The relatively lower deviations in the driving times are therefore as a result of the small range of intrazonal driving time values.

It can also be seen in Figure 4.18 that the choice of reference values has a huge impact on the suitability or otherwise of the methods. Whereas the base variant of the proposed method is identified as the best method when reference option 1 is considered, the use of reference option 2 favors the area-based method for the calculation of intrazonal walking and cycling times, and the nearest neighbor method for the calculation of intrazonal driving times. The deviations resulting from the use of reference option 1 are also lower than the deviations resulting from the use of reference option 2. In that regard, the methods can be deemed to provide reasonable estimates of intrazonal impedances when reference option 1 is used. On the other hand, the use of reference 2 as a benchmark renders the methods unsuitable for calculating intrazonal impedances since the least deviation is as high as 63%.

Although reference option 2 offers a theoretically sound approach by considering the influence of trips in determining average times within a zone, it necessitates the calculation of different intrazonal times for each demand group since trips are generally categorized into groups. Given the fact that interzonal times do not change with demand group, the calculation of different intrazonal times for every demand group is an unnecessary task which will introduce inconsistencies in the model.

Moreover, the use of building blocks as spatial unit overestimates the number of trips at very short distances thereby adding more weight to very short trips in the calculation of average times within a zone, and in effect resulting in small intrazonal time values for reference option 2 as can be seen in Figures 4.3, 4.8, and 4.13. On the other hand, reference option 1 provides a measure that is consistent with interzonal impedance, does not change with demand group, and is not affected by over- or under-estimation of trips.

Admitting reference 1 as the appropriate reference option, the proposed method provides better estimates of intrazonal times than the existing methods. Among the different forms of the proposed method, the base method provides the best estimate closely followed by the closeness method, and the degree method. The fact that the base method provides the best estimate among the proposed methods can be explained by the fact that the reference times are not weighted. This is evident in the case of the reference 2 times where the closeness method provides better estimates than the base method for all intrazonal times considered. While weighting intrazonal times by trips gives a true average travel time within a zone, the multiplicity of intrazonal times for a single zone makes the effort unnecessary.

With the proposed method providing better estimates than the existing methods and the base method providing the best estimates of intrazonal times, the next section seeks to find out whether better estimates of intrazonal times necessarily result in better estimates of intrazonal trips.

4.4 Comparison of Model Results

This section describes a second approach explored to test the suitability of the various intrazonal impedance calculation methods where model results were compared. Here, trips were generated and distributed at the TAZ level, and using each of the intrazonal impedance calculation methods for the calculation of intrazonal distances, five different trip distribution scenarios were developed for each demand group. Subsequently, modeled trip lengths and intrazonal trips were compared against observed data.

Despite the fact that building blocks provide finer level of spatial resolution than TAZ, TAZ was chosen as the spatial unit for this exploratory work mainly because the input data for modeling had been provided at the TAZ level. Modeling at the building block-level would require the use of data disaggregated from the TAZ level. However, since data disaggregation is based on various assumptions and there are errors inherent in disaggregated data, modeling at the TAZ level avoided the potential transfer of such errors to model results.

4.4.1 Development of Scenarios

With the socio-economic data of the TAZ and the estimated trip rates described in Section 3.3.2, the number of trips produced by and attracted to each TAZ was computed and balanced for the 11 different demand groups.

At the trip distribution step which follows the description in Section 3.3.3, the different intrazonal impedance calculation methods were applied in the calculation of intrazonal distances to create five different scenarios for each demand group. Table 4.2 shows the impedance function parameters for the different scenarios of each demand group.

Table 4.2: Impedance function parameters

Demand Group	Base		Degree		Closeness		Area-Based		Nearest Neighbor	
	b	c	b	c	b	c	b	C	b	c
HBWa	-1.04	0.27	-1.04	0.27	-1.03	0.27	-1.01	0.26	-1.03	0.27
HBWb	-0.97	0.27	-0.97	0.27	-0.95	0.26	-1.11	0.33	-1.12	0.33
HBSa	-1.18	-0.14	-1.18	-0.14	-1.18	-0.14	-1.16	-0.14	-1.16	-0.14
HBSb	-1.37	-0.29	-1.37	-0.29	-1.39	-0.29	-1.37	-0.29	-1.37	-0.29
HBE	-2.81	1.25	-2.81	1.25	-2.82	1.28	-2.81	1.28	-2.81	1.28
HBRa	0.55	-0.77	0.55	-0.77	0.57	-0.77	0.52	-0.75	0.51	-0.75
HBRb	-0.80	0.00	-0.80	0.00	-0.78	0.00	-0.78	0.00	-0.79	0.00
HBOa	-0.95	0.05	-0.95	0.05	-0.95	0.05	-0.91	0.03	-0.90	0.03
HBOb	-1.33	0.05	-1.33	0.05	-1.38	0.08	-1.30	0.02	-1.30	0.02
NHBa	-0.86	-0.09	-0.85	-0.09	-0.97	0.01	-0.90	-0.03	-0.83	-0.10
NHBb	-0.82	-0.25	-0.82	-0.25	-0.89	-0.20	-0.84	-0.22	-0.86	-0.21

As can be seen from Table 4.2, there is little difference in the parameter values across the different distribution scenarios of the same demand group. The parameter b which should generally be negative is negative for all but the HBRa trips, and this is consistent across the different distribution scenarios. Likewise, the sign of the parameter c is the same across the different scenarios.

4.4.2 Trip Length Checks

Trip length checks involve comparing average trip lengths and trip length frequency distributions. Figure 4.19 shows the deviations in modeled average trip lengths from observed average trip lengths for the different scenarios of each demand group.

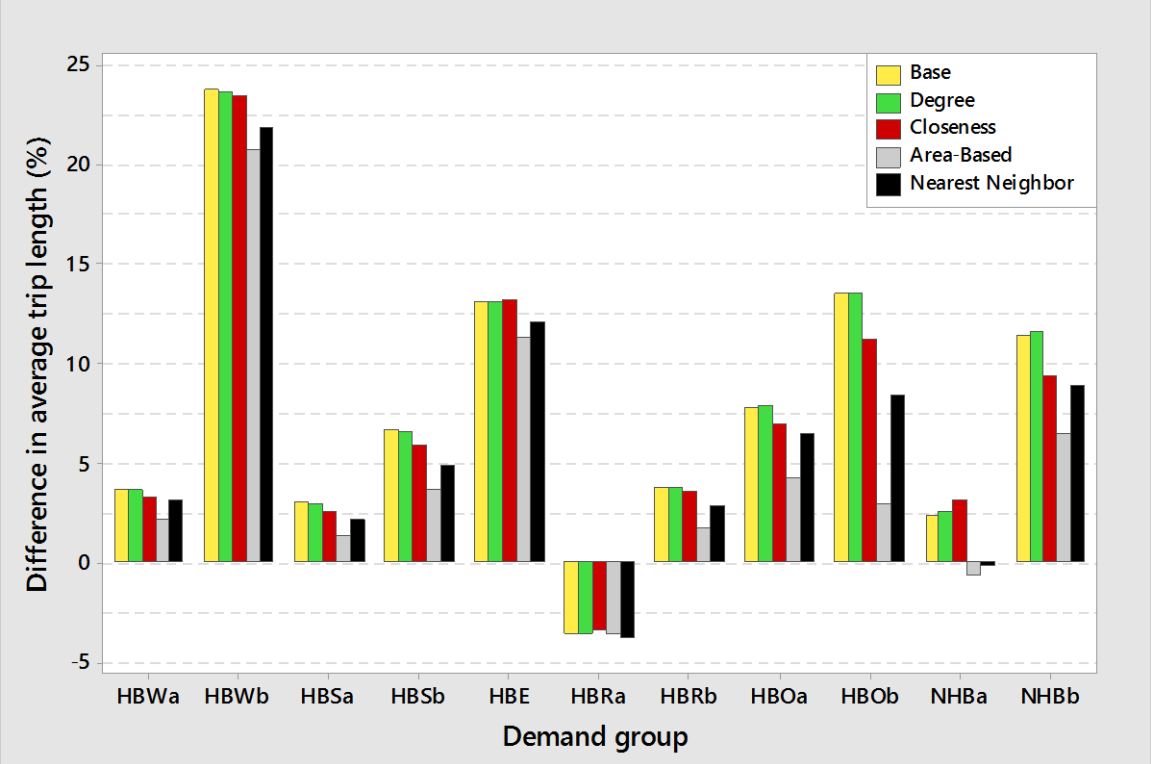

Figure 4.19: Deviations from observed average trip lengths

According to Cambridge Systematics (2010), the modeled average trip length for each purpose should generally be within 5% of observed trip length for each trip purpose. From Figure 4.19, it can be seen that the area-based method satisfies this criterion for eight out of the 11 demand groups whereas the nearest neighbor technique satisfies the criteria for six demand groups, with the proposed methods

satisfying the criterion for five demand groups. Overall, the area-based method produces the least deviation from observed average trip lengths.

To get a better view of how close the modeled trip length frequency distributions match the observed trip length frequency distributions, Figure 4.20 shows the coincidence ratios between modeled and observed TLFD for the different scenarios of each demand group.

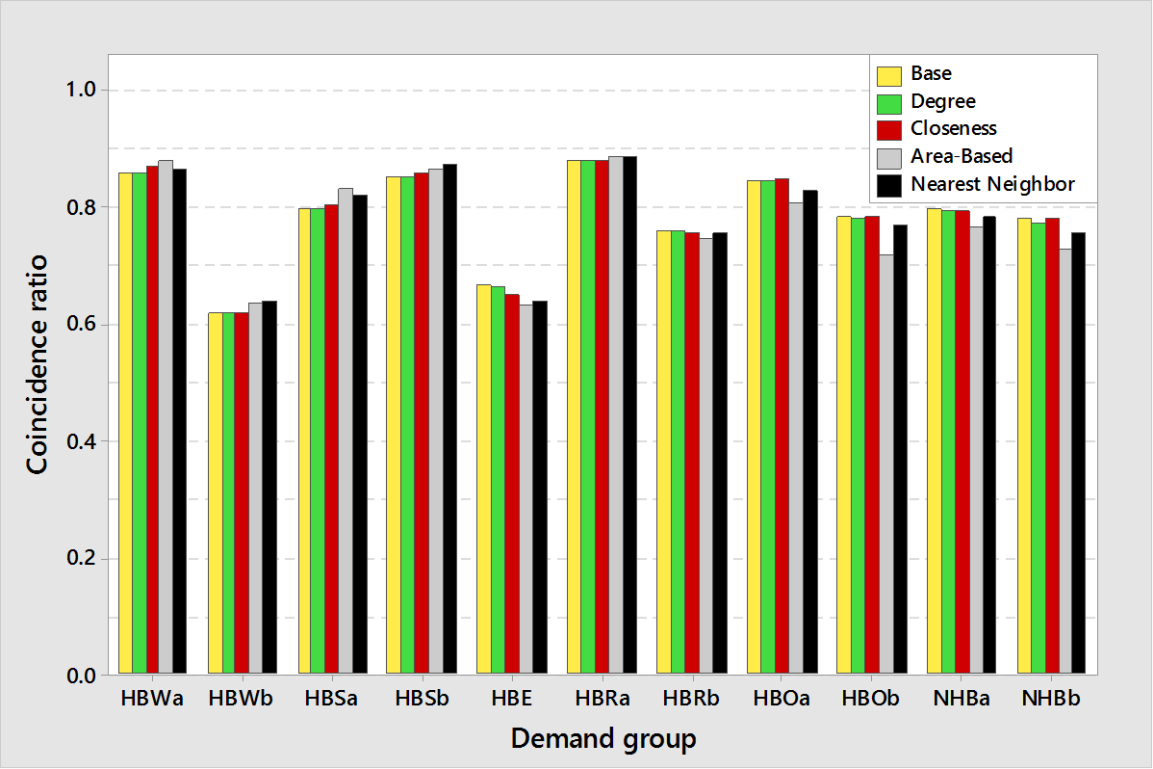

Figure 4.20: Coincidence ratios between modeled and observed TLFD

As seen in Figure 4.20, there is not much difference between the coincidence ratios across the different scenarios of the same demand group, and besides the HBE and HBWb, the coincidence ratios of all other demand strata exceed 70%, indicating a reasonably good fit between the modeled and observed TLFD.

Whereas there is not much difference between the coincidence ratios across the different scenarios of the same demand group, the deviations from observed average trip lengths exhibit differences across scenarios of the same demand group. Average trip lengths are computed from individual records whereas coincidence ratios are

calculated from aggregated values. For an interval of 5 minutes, the difference between 1 and 4 minutes is concealed in the calculation of coincidence ratios. However, this difference is noticeable in the calculation of average trip lengths. Since the differences among the scenarios lie in the number of intrazonal trips, the differences stem from the lowest interval and this has a higher effect on average trip length than on coincidence ratios.

4.4.3 Comparing Intrazonal Trips

To check whether better estimates of intrazonal impedances produce better estimates of intrazonal trips, Figure 4.21 shows the deviations in the modeled intrazonal trips from the observed intrazonal trips for the different demand groups. The observed intrazonal trips together with their shares are shown in Table 4.3 for each demand group.

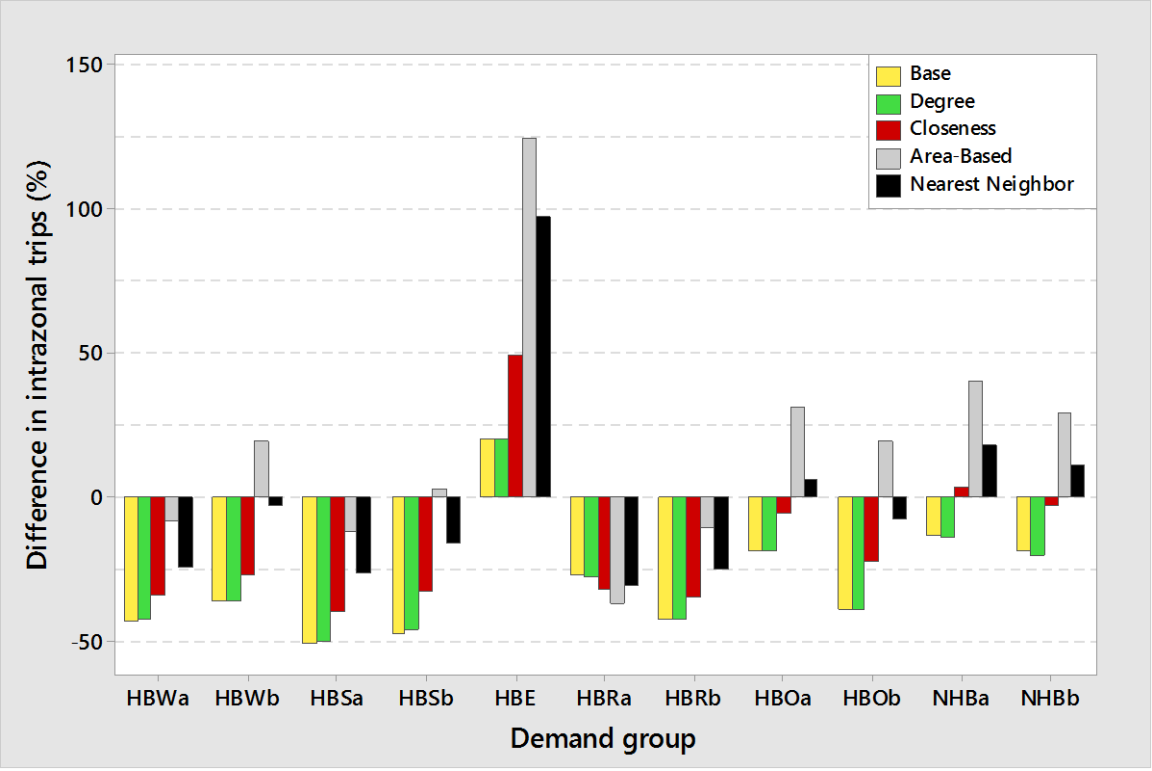

Figure 4.21: Deviations from observed intrazonal trips

Table 4.3: Intrazonal trips and shares

Demand Group	Observed Intrazonal Trips	Observed Intrazonal Trip Share
HBWa	259	7.6
HBWb	91	6.3
HBSa	698	8.1
HBSb	331	9.9
HBE	176	3.9
HBRa	147	3.6
HBRb	266	8.6
HBOa	700	8.6
HBOb	490	17.6
NHBa	1254	11.4
NHBb	795	14.2

From Figure 4.21, it can be seen that there is no single method that provides the best intrazonal trip estimates for all demand groups. Whereas the area-based method provides the best estimate for four demand groups, it is the closeness variant of the proposed method that provides the best estimates in the three demand groups with the highest number of observed intrazonal trips. The nearest neighbor method also provides the best estimates for the HBOb and HBWb demand groups, and apart from the HBE group where it provides poor estimates, the deviations involved in all other demand groups do not exceed 30%.

Among the proposed methods, the closeness variant produces the best intrazonal trip estimate for all but the HBE and HBRa demand groups. For both groups, the base and degree variants provide better estimates than the closeness methods. The base and degree variants of the proposed method tend to produce similar levels of error for each demand group.

Using the guideline described in Cambridge Systematics (2010), where modeled intrazonal trip shares should be within three percentage points of observed intrazonal trip shares, Figure 4.22 shows the deviations in the modeled intrazonal trip shares from the observed intrazonal trip shares for the different demand groups.

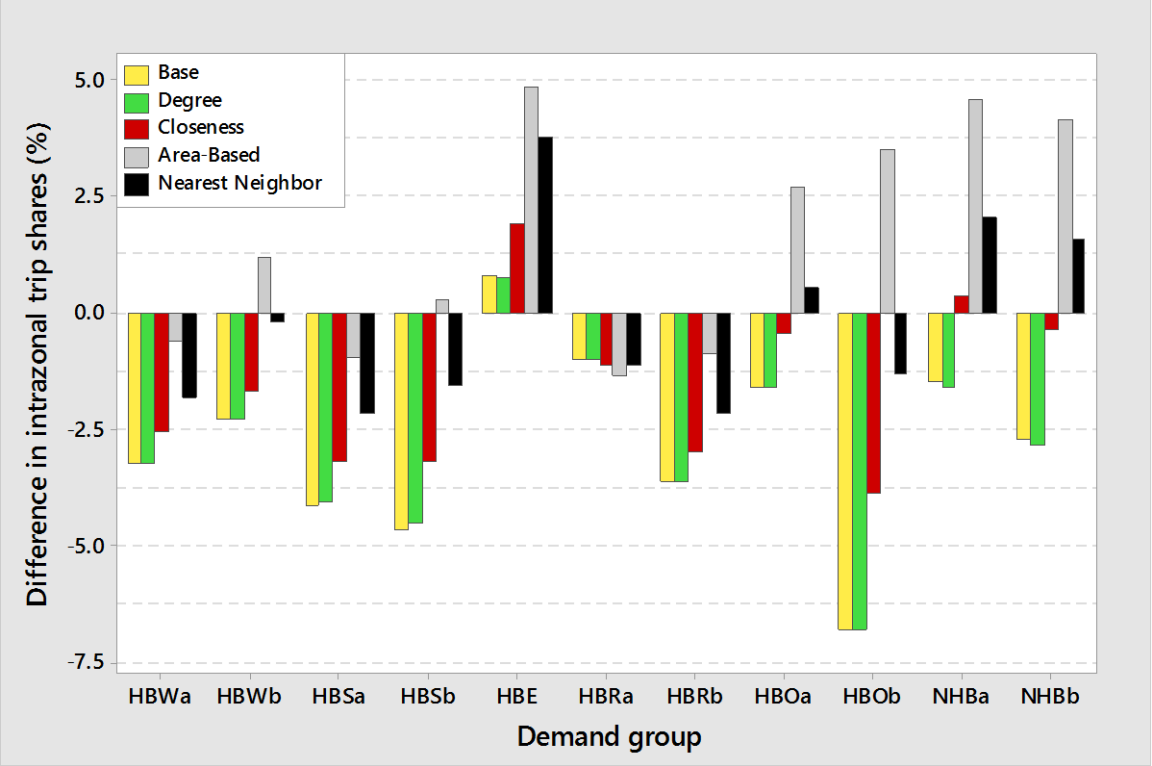

Figure 4.22: Deviations from observed intrazonal trip shares

From Figure 4.22, it can be seen that the nearest-neighbor method provides estimates of intrazonal trip shares that fall within three percentage points for all but the HBE trips, and even for this exception, the deviation is only slightly above the three percentage points. The closeness variant also provides similar results for all but three demand groups, with the three exceptions having deviations only slightly above the three percentage points.

4.5 Chapter Summary and Conclusion

This chapter focused on finding a suitable method for calculating intrazonal impedances. After describing a proposed method for calculating intrazonal impedances, the research considered the proposed method along with existing methods, and compared both calculated intrazonal times and modeled number of intrazonal trips.

In comparing the calculated intrazonal times, the study defined two reference values for each intrazonal time considered using two reference options. Whereas option 1 defined reference intrazonal time as average time between building block pairs within

the same zone, option 2 considered the number of trips between building block pairs in the definition of reference intrazonal time. The results show that the choice of reference values has a huge impact on the suitability or otherwise of the methods. Whereas reference option 2 offers a theoretically sound approach by considering the influence of trips in determining average times within a zone, reference option 1 provides a measure consistent with interzonal impedance which does not require multiple intrazonal times for a single zone and is not affected by over-or under-estimation of trips.

Admitting reference 1 as the appropriate reference option, the study finds that the proposed methods provide better estimates of intrazonal impedances than the existing methods, with the base method providing the best estimates of intrazonal impedances.

With the proposed method providing better estimates than the existing methods and the base method providing the best estimates of intrazonal times, the study sought to find out whether better estimates of intrazonal times results in better estimates of intrazonal trips. Using each of the intrazonal impedance calculation methods for the calculation of intrazonal distances, five different trip distribution scenarios were developed for each demand group, and their resultant modeled trip lengths and intrazonal trips were compared against observed data.

The comparison of the calculated number of intrazonal trips indicates that no single method provides the best intrazonal trip estimate for all demand groups. Whereas the proposed method provides better intrazonal impedance estimates than the existing methods, they provide the worst estimates of intrazonal trips for some demand groups. With the nearest neighbor technique producing estimates of intrazonal trip share that falls within three percentage points of observed intrazonal trip shares for all but the HBE trips, the nearest neighbor technique can be deemed to provide good estimates of intrazonal trips.

The results show that better estimates of intrazonal impedances do not necessarily result in better estimates of intrazonal trips. The need for values of intrazonal impedance should therefore be treated as the need for a value big enough to capture

intrazonal trips but small enough to avoid the misallocation of interzonal trips within the same zone. Considering the logic and the ease of measurement as well as its good performance regarding the calculation of intrazonal trips, the nearest neighbor technique can be deemed sufficient for calculating intrazonal impedances.

Since improving the calculation of intrazonal impedances will not necessarily improve intrazonal trip estimates, non-motorized trips cannot be adequately handled in macroscopic models by improvements to the calculation of intrazonal impedances. There is therefore the need to explore the second approach for mitigating the intrazonal problem which involves reducing the need to model intrazonal trips, and that is the focus of the next chapter.

5 Identifying an Appropriate Level of Spatial Resolution

5.1 Introduction

Because intrazonal trips could not be dealt with adequately by improvements to the calculation of intrazonal impedances, the other option to mitigate the intrazonal problem which sought to reduce the need to model intrazonal trips was explored. To reduce the need to model intrazonal trips, models should be made compatible with the scale of short trips by reducing the sizes of TAZ and in effect limiting the frequency of intrazonal trips.

Whereas different approaches have been employed to redefine TAZ to achieve finer levels of spatial resolution to ensure that models are compatible with the scale of short trips which are mainly non-motorized, there are conceptual and computational issues associated with the use of more detailed TAZ for modeling. Viegas et al. (2009) point out the loss of statistical precision as more TAZ are used, and according to Moeckel & Donnelly (2015), destination choice models become unstable when the number of alternatives is too large while the increased size of trip matrices slows down traffic assignment. Detailed information is also not available for most areas, either for privacy reasons or because of infrequency of full censuses (Wegener, 2011). Ortúzar and Willumsen (2011) also draw attention to the difficulty in forecasting at the same level of detail, changes at the individual household level affecting demand. A balanced level of resolution is thus recommended for modeling (Moeckel and Donnelly, 2015; Wegener, 2011).

This chapter focuses on identifying an appropriate level of spatial resolution for handling non-motorized trips in macroscopic travel demand models. The objective is to improve model results while limiting the number of TAZ. The study compares model results from 24 different zone systems defined with raster cells to find an appropriate level of spatial resolution. Raster cells were selected for the definition of zone systems because they offered a systematic approach to quickly generate zone systems that are exclusive, complete and unique. Whereas a manual approach would have been time consuming and introduced inconsistencies in the zone redefinition, other automatic procedures would have allowed the generation of

irregular shaped zones which should be avoided in modeling (Ding, 1998; Martínez et al., 2009; Moeckel and Donnelly, 2015).

5.2 Test Area and Reference Raster Cell System

5.2.1 Rasterization of Test Area

To identify an appropriate level of spatial resolution for TAZ, a 23 km^2 section of Dachau extending beyond the inner city was used. Figure 5.1 shows the test area with a dotted boundary overlaid on the building blocks in Dachau.

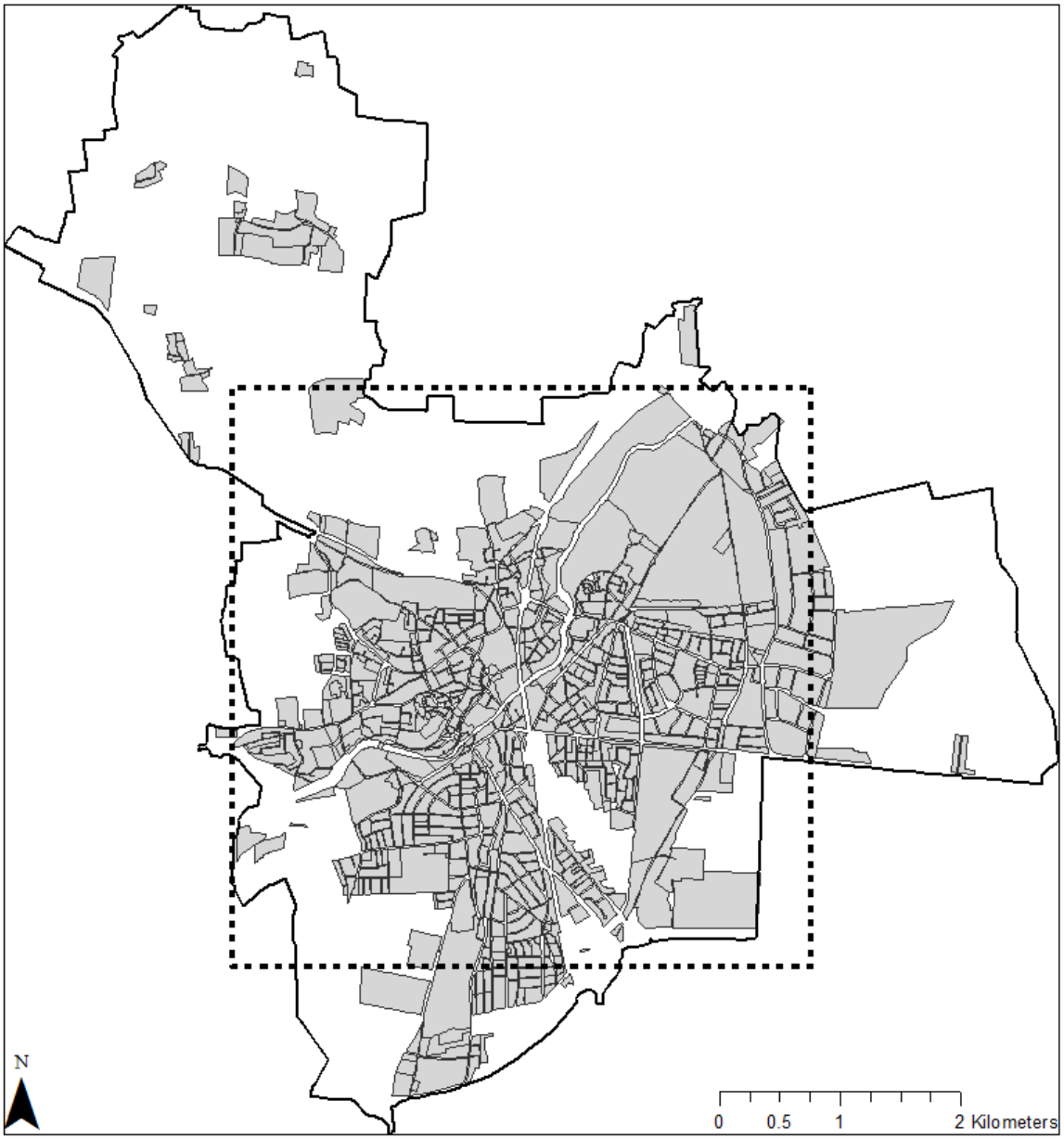

Figure 5.1: Dachau and the test area

The size of the test area was limited by the maximum number of zones permitted by the software license obtained for the study. Whereas the study required a reference system of fine raster cells, the software license permitted a maximum of 5,000 zones. The methodology also required that the number of fine raster cells be a power of 2 so considering the zone limit imposed by the software license, the reference system could only have a maximum of 4,096 (2^{12}) raster cells.

For the reference raster cells, a system consisting of 75 m × 75 m raster cells was chosen to achieve a very detailed level of spatial resolution at which non-motorized trips could be analyzed. A system consisting of 25 m × 25 m raster cells was considered since it would have provided a much finer resolution comparable to the sizes of land parcels. However, this would have required the use of a smaller test area since the maximum number of raster cells could only be 4,096. Using 25 m × 25 m raster cell over the 23 km^2 area would have resulted in 36,864 raster cells. Apart from the limit imposed by the software license, the resultant trip matrices would have slowed down the assignment step substantially, since the size of trip matrices increases exponentially with increases in the number of zones. Besides, the 75-meter cell dimension represents less than a minute walking distance at 5 km/h, and provides a finer resolution than the 264 ft. × 264 ft. (80 m × 80 m) described by Clifton et al. (2013) as small enough for capturing and representing short walking trips. Figure 5.2 shows the fine raster cells that served as the reference raster cell system.

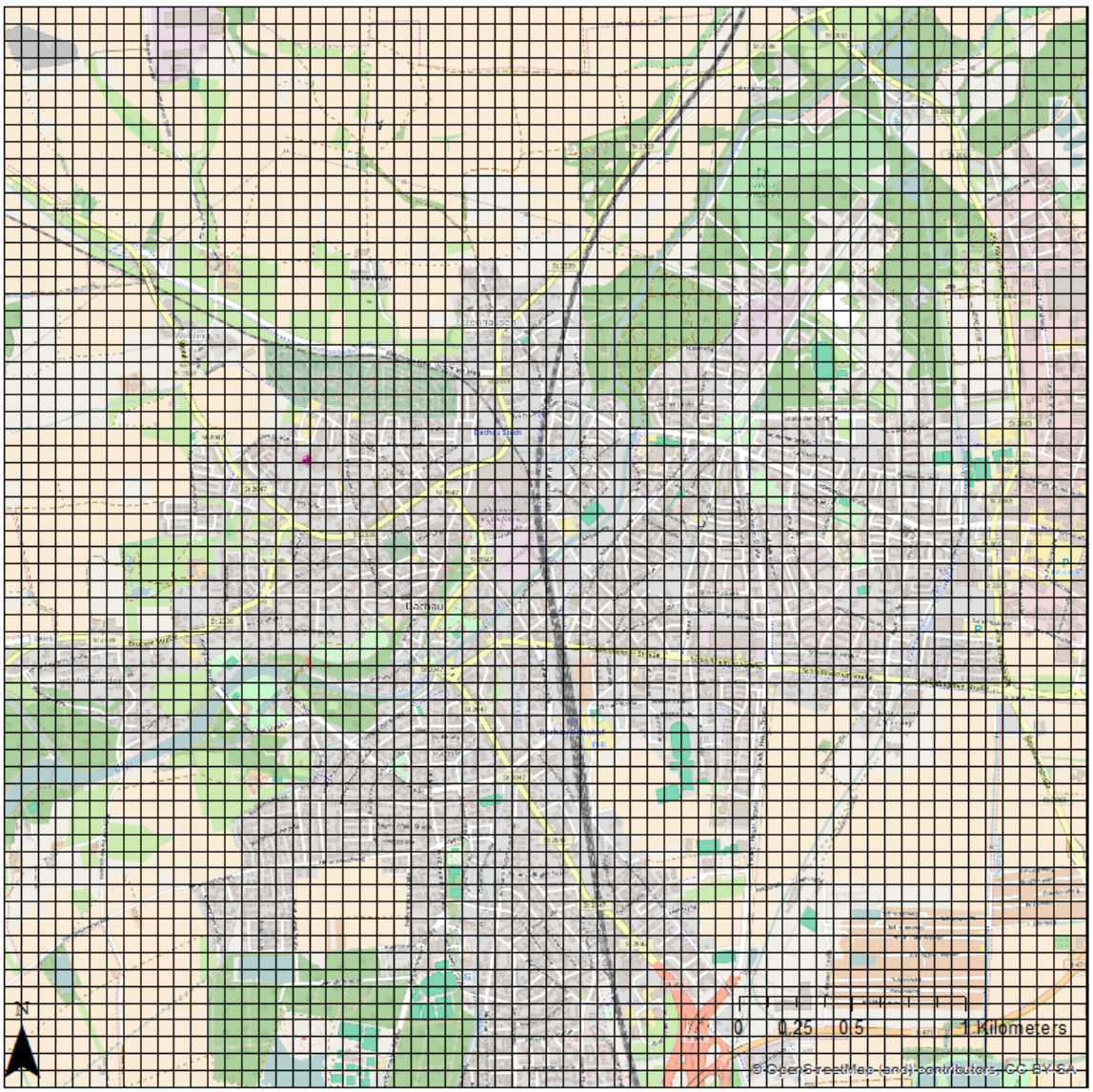

Figure 5.2: Reference raster cells (Background image: OpenStreetMap contributors, 2016)

5.2.2 Disaggregation of Initial Trip Tables to Reference Raster Cells

The identification of an appropriate level of spatial resolution required the comparison of assignment results from different raster cell systems. The initial trip tables developed at the building block level and described in Section 3.3 were added together, and the resultant trip table was disaggregated to the reference raster cell system.

Since the test area did not cover the whole of Dachau, the building blocks were assigned weights based on the share of their total area that fell within the test area.

For example, if a building block had a total area of 5,000 m^2, and out of that 4,000 m^2 fell within the test area, the building block was assigned a weight of 0.8. These weights were used to reduce the number of trips between building block pairs that had sections of their blocks outside the study area. For each building block pair, the number of trips was multiplied by the weight of the origin block and the weight of the destination block to get an adjusted demand value.

The disaggregation from the building block level to the reference raster cell system followed the same approach used to disaggregate the TAZ level data to building blocks described in Section 3.3.1. The output of the disaggregation process was a reference trip table used for subsequent analysis.

5.2.3 Reference Trip Length Frequency Distributions

To enable the calculation of travel impedance between pairs of reference raster cells, the reference raster cells were connected to the network by centroid connectors, using one two-way connector for each raster cell. The centroid connector for each raster cell was connected to the closest node on a multimodal link that provided access to pedestrians, bicycles and cars. The total connector times presented in Table 3.5 were used for the calculation of travel times. In the case of travel time by car, the total connector time for moderate activity areas was used for all raster cell pairs.

Using the reference trip table and the mode-specific travel times between pairs of raster cells, TLFD was computed for pedestrians, bicycles and cars at intervals of 5, 2, and 1 minute respectively. This was done to get reference TLFD against which TLFD from different raster cell system would be compared.

5.2.4 Assignment of Reference Trip Table

Using an all-or-nothing assignment, the reference trip table was assigned to the network via shortest paths to get reference volumes against which comparisons would be made. To analyze the effect of spatial resolution on different modal networks, the same reference trip table was assigned separately to pedestrian,

bicycle and car networks to get reference volumes for pedestrians, bicycles and cars respectively.

Although an all-or-nothing assignment does not consider congestion effects, the study sought to identify the response of network volumes to changes in levels of spatial resolution when all other things are held constant, and for that matter an all-or-nothing assignment was appropriate. An all-or-nothing assignment ensured that the scale effect is singled out and analyzed rather than being mixed up in a pool of effects. A different form of assignment that considers congestion effects would have made it difficult to identify the extent of influence of the scale effect on network volumes.

5.3 Gradual Rasterization and Different Raster Cell Systems

To generate different raster cell systems at different levels of spatial resolution, the study adopted a process of creating gradual raster cells using the quadtree concept. Moeckel & Donnelly (2015) applied this approach to the model of Georgia to refine zones where they used population and employment as threshold to subdivide raster cells. Whereas population and employment data is a good proxy for the density of trips being generated, this requires robust and disaggregated data set which is not easily available.

In this study, total network length per raster cell was used to define threshold values. This worked on the premise that, since trip ends are connected by transport network, the lack of network in an area indicates a lack of trip generator. Correspondingly, areas with higher network densities are expected to have more trip origins and destinations, and as such deserve finer resolution. Whereas the lack of network in an area indicates a lack of trip generator, network links that are a few meters long can have very different number of trip origins and destinations depending on the urban function and density. Therefore, areas with higher network densities will not always have more trip origins and destinations. To minimize the error that this assumption may introduce, only network links providing direct access to trip origins and destinations were considered in the calculation of threshold values.

The definition of threshold values was based on an undirected link length calculation such that a two-way street covering a 100 m distance was assigned a total network length of 100 m and not 200 m. In order to ensure that threshold values considered only links that provide direct access to trip origins and destinations, the calculation of total network lengths excluded higher-level network links such as highways that do not provide direct access to activity locations. Therefore, the network links used for the calculation of network lengths were those open to pedestrians and cyclists in addition to cars. Using the Intersect tool in ArcGIS, the network links covering the study area were split into separate individual links at the reference raster cells' boundaries. This was done to ensure that each link had a one-to-one relationship with a reference raster cell in order to avoid conflicts during the calculation of total network length per raster cell.

5.3.1 Gradual Rasterization Process

The gradual rasterization process is summarized in Figure 5.3 and it started with a single raster cell covering the test area. This raster cell was selected and its total network length calculated. If the total network length exceeded a pre-defined threshold value, the raster cell was split into four new raster cells. Next, total network length in each of the new raster cells was calculated and compared to the threshold value, and whenever a cell's total network length exceeded the threshold value, the cell was subdivided into four smaller raster cells. The process continued until the total network length in every cell was smaller than the pre-defined threshold value. Since the reference cells had dimensions of 75 m × 75 m, an additional condition was set to limit the smallest possible size of a generated raster cell to 75 m × 75 m. Therefore, raster cells of size 75 m × 75 m with total network length exceeding the pre-defined threshold were not split further in the rasterization process. The python script for the gradual rasterization process is shown in Appendix 2.

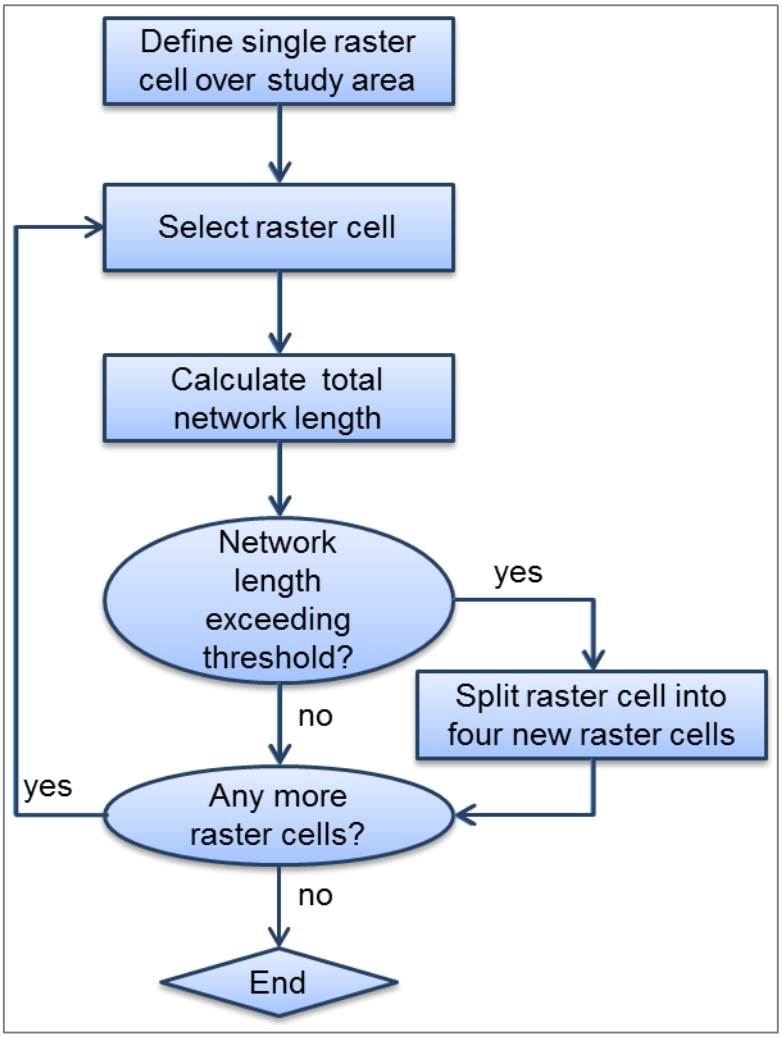

Figure 5.3: Gradual rasterization process

Defining threshold as network length per raster cell, 24 different threshold values were used to create 24 different raster cell systems. The threshold values considered were 50 m, 100 m to 2,000 m in increments of 100 m, as well as 3,000 m, 4,000 m, and 5,000 m. Figures 5.6 to 5.9 show the outputs from consecutive runs of the rasterization process with a threshold of 1,000 m network length per raster cell.

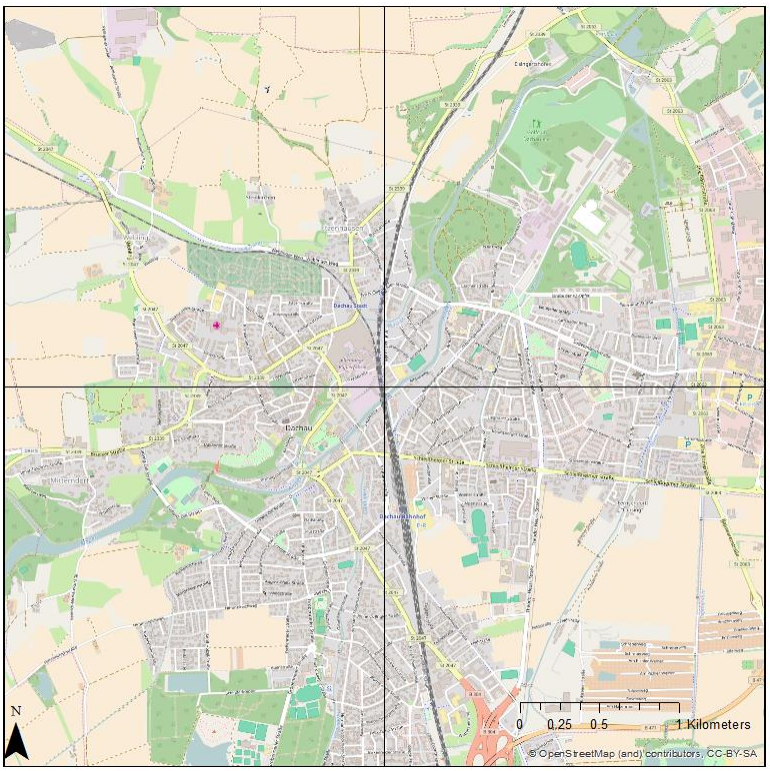

Figure 5.4: Gradual rasterization output 1 (Background image: OpenStreetMap contributors, 2016)

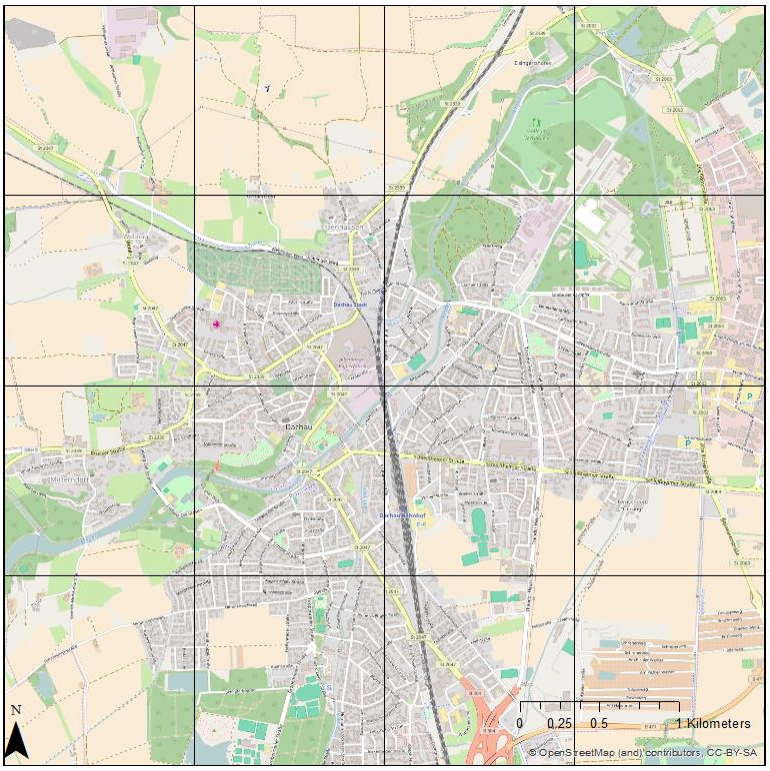

Figure 5.5: Gradual rasterization output 2 (Background image: OpenStreetMap contributors, 2016)

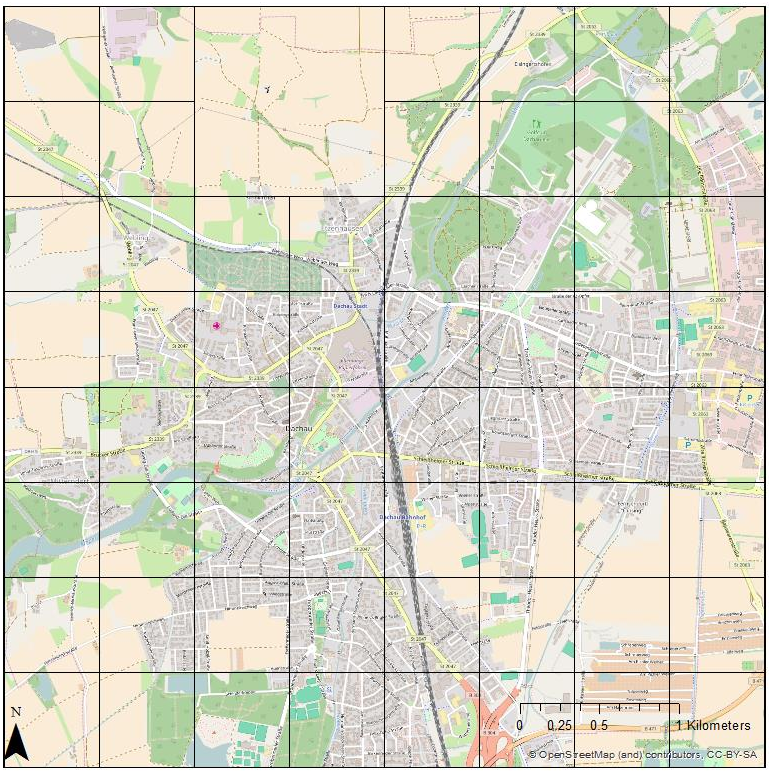

Figure 5.6: Gradual rasterization output 3 (Background image: OpenStreetMap contributors, 2016)

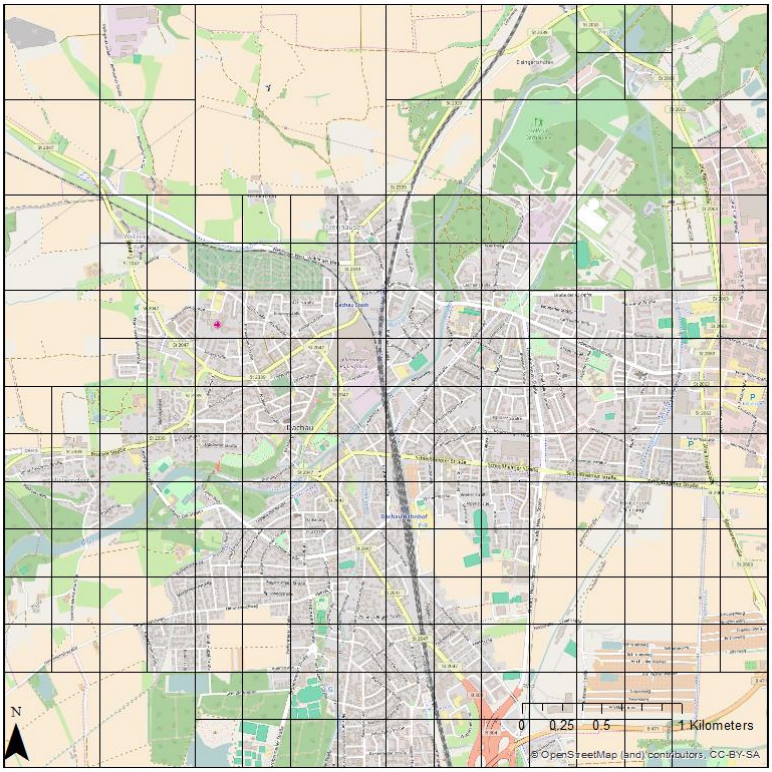

Figure 5.7: Gradual rasterization output 4 (Background image: OpenStreetMap contributors, 2016)

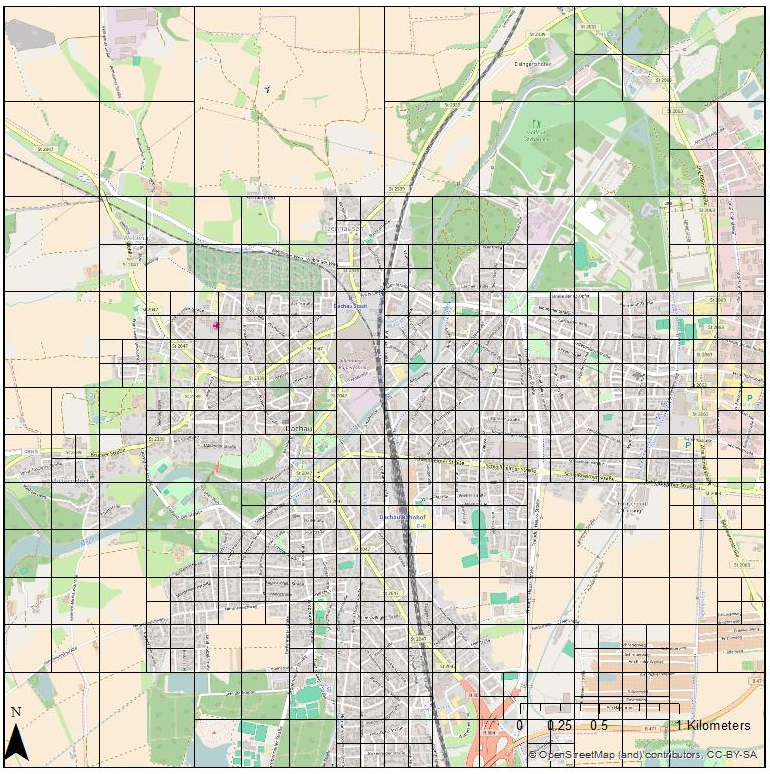

Figure 5.8: Gradual rasterization output 5 (Background image: OpenStreetMap contributors, 2016)

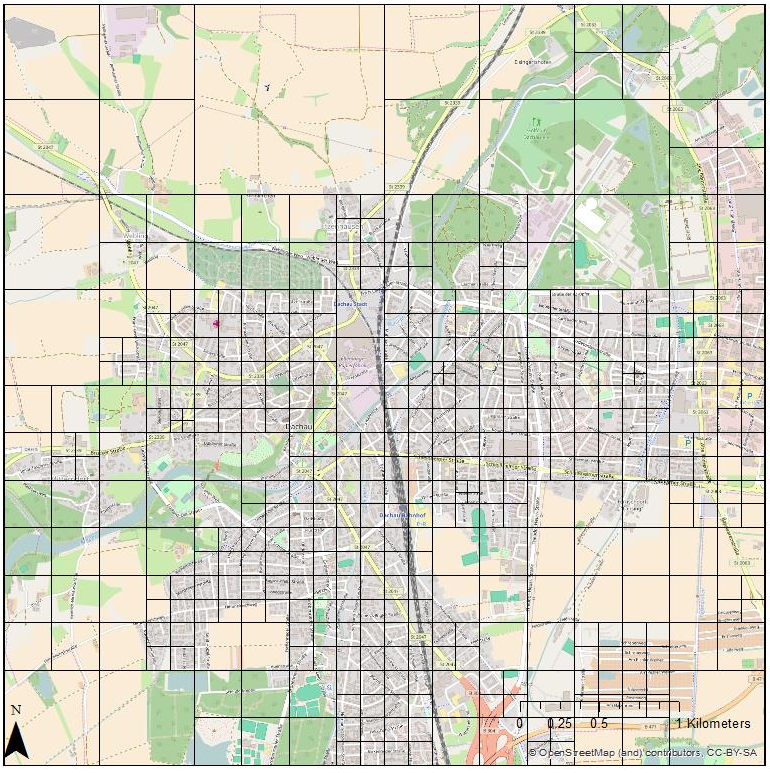

Figure 5.9: Gradual rasterization output 6 (Background image: OpenStreetMap contributors, 2016)

5.3.2 Aggregation of Reference Trip Table

The reference trip table that resulted from the disaggregation from building blocks to the reference raster cell system was aggregated for each of the 24 raster cell systems generated by the gradual rasterization process.

For each generated raster cell system, the Aggregate-Zone-by-Main Zone function in PTV Visum was used to sum up the matrix values of the reference trip table belonging to the same O-D pair to get trip tables for the generated raster cell systems.

5.3.3 Trip Length Frequency Distributions

To enable the calculation of travel impedance matrices for the generated raster cell systems, the raster cells were connected to the network by centroid connectors, using one two-way connector for each raster cell. The centroid connector for each raster cell was connected to the closest node on a multimodal link that provided access to pedestrians, bicycles and cars. As it was done for the reference raster cells, the total connector times presented in Table 3.5 were used for the calculation of travel times, with the connector time for moderate activity areas used in the case of travel time by car.

Using the trip table and the mode-specific travel times between pairs of raster cells for each generated raster cell system, TLFD was computed for pedestrians, bicycles and cars at intervals of 5, 2, and 1 minute respectively. This was done to get TLFD for the generated raster cell systems.

5.3.4 Traffic Assignment

An all-or-nothing assignment was subsequently used to assign the trip table of each generated raster cell system to get network volumes for the generated raster cell systems. As it was done for the reference raster cells, the same trip table was assigned separately to the pedestrian, bicycle and car networks to get network volumes for pedestrians, bicycles and cars respectively.

5.4 Comparison of Trip Length Distributions

For each generated raster cell system, the distributions of travel times by pedestrians, bicycles and cars were compared to their respective time distributions from the reference raster cell system. This was done to assess the effects of spatial aggregation on trip length distributions.

Figure 5.10 shows the deviations in average trip length relative to the reference average trip length, while Figure 5.11 shows the coincidence ratios between the computed and reference TLFD for each mode at different levels of spatial resolution.

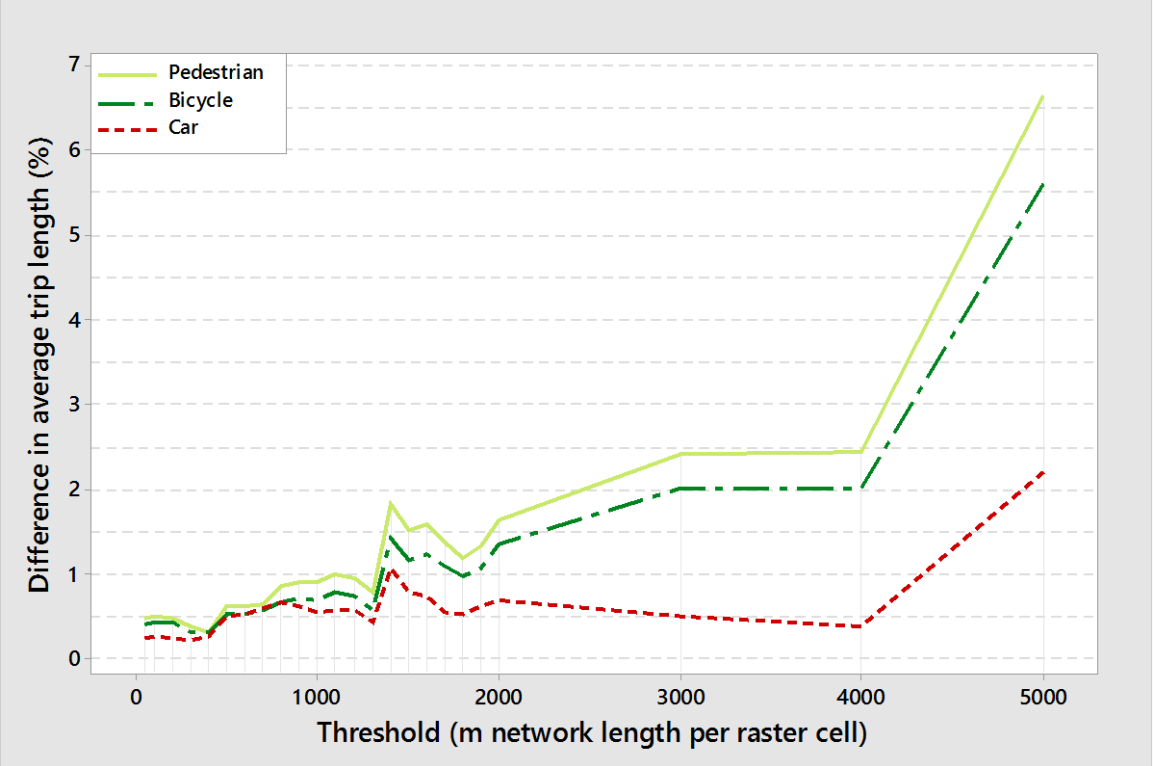

Figure 5.10: Deviations from reference average trip lengths

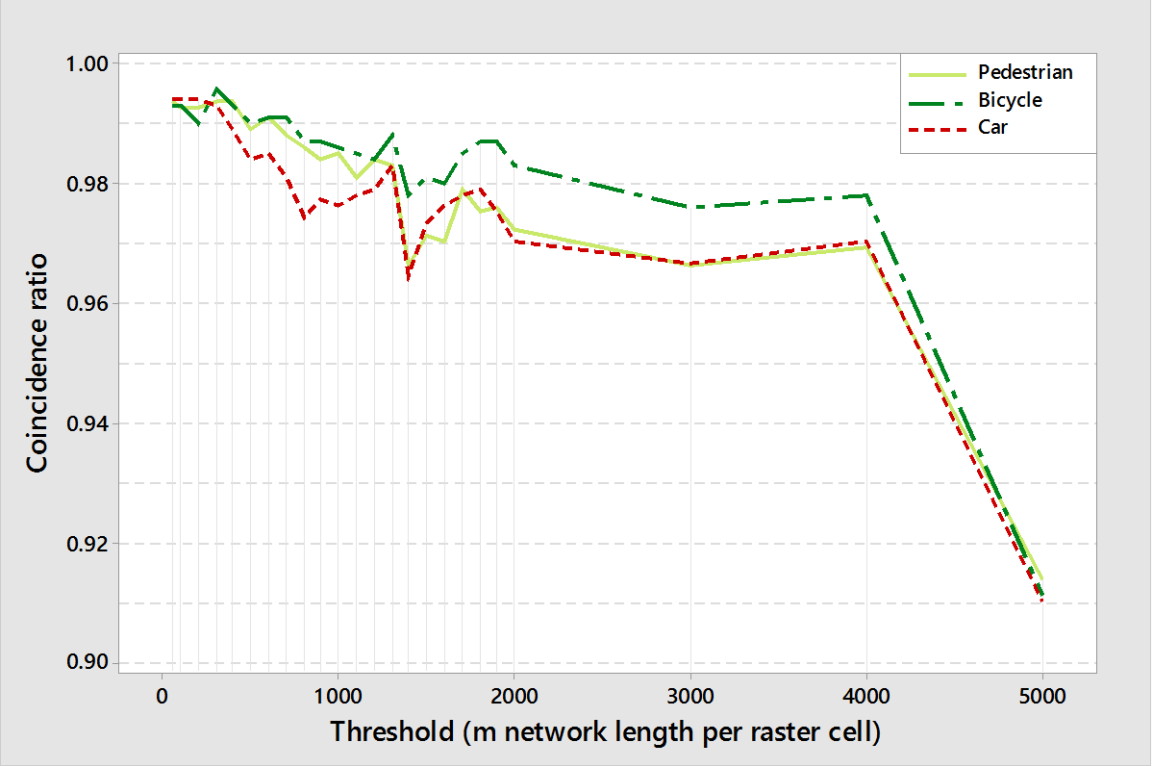

Figure 5.11: Coincidence ratio between reference and computed TLFD

As can be seen from Figures 5.10 and 5.11, levels of spatial resolution are represented by their threshold values. Since larger threshold values indicate coarser levels of spatial resolution, the horizontal axis shows decreasing levels of spatial resolution from left to right.

Figure 5.10 shows that reducing the spatial resolution of raster cells increases errors involved in the estimation of average trip lengths. Although the steepest increase in error occurs between the 1,300 m and 1,400 m threshold, the curves are generally gentle until the 4,000 m threshold. Further reduction in spatial resolution beyond the 4,000 m threshold results in relatively higher increases in errors. Despite the increase in errors associated with reduction in spatial resolution, the errors involved in the range considered in this study is within reasonable limits, apart from the bicycle and pedestrian travel times at the 5,000 m threshold that results in errors exceeding 5%.

The behavior of the average trip length error curves is also observed in Figure 5.11, where the steepest drop in coincidence ratio occurs between the 1,300 m and 1,400 m threshold, but then the curves are generally gentle until the 4,000 m threshold. It

can also be observed that further reduction in spatial resolution beyond the 4,000 m threshold results in relatively higher decreases in coincidence ratio. Nevertheless, the least value of coincidence ratio in the range considered indicates a good fit between the computed and reference TLFD even at the 5,000 m threshold.

5.5 Comparison of Number of Intrazonal Trips

Since intrazonal trips represent trips that cannot be adequately represented by macroscopic models, the intrazonal trip shares for each generated raster cell system were compared to identify the extent of information loss due to presence of intrazonal trips as spatial resolution gets coarser. Figure 5.12 looks at the number of intrazonal trip as a share of the total number of trips.

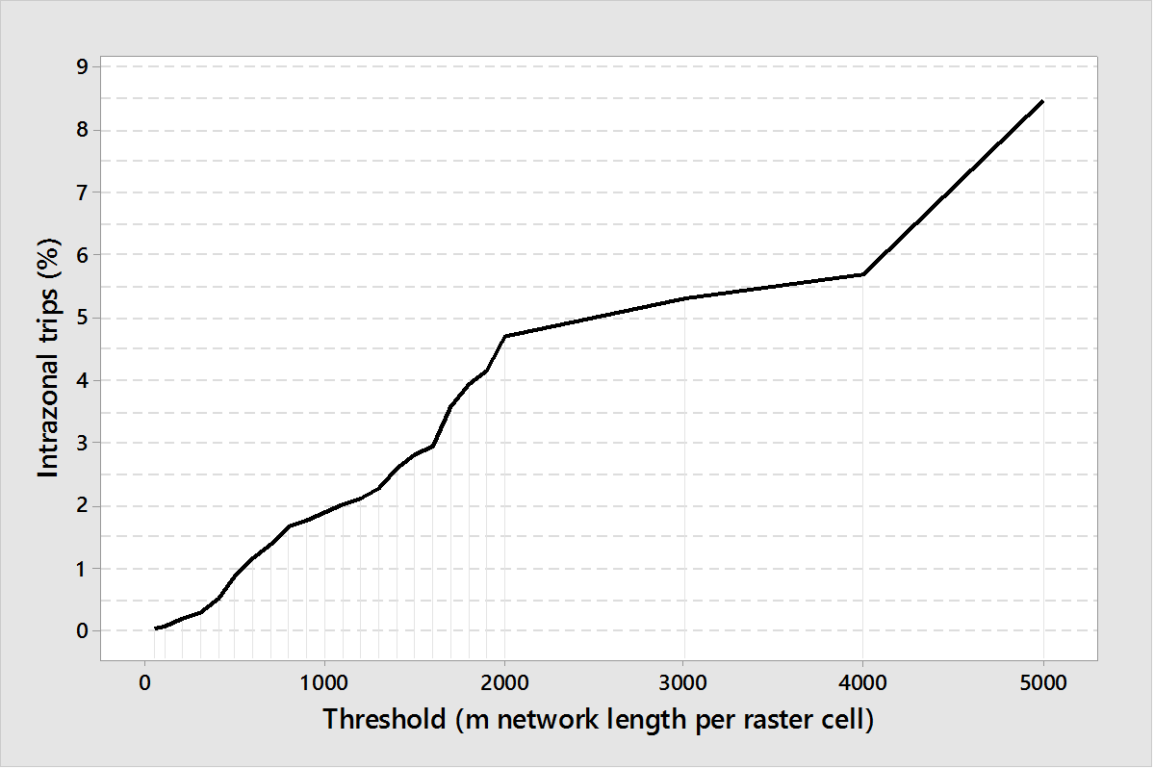

Figure 5.12: Intrazonal trips as a share of total trips

It can be seen from Figure 5.12 that the intrazonal trip share increase as spatial resolution gets coarser. The rise is steep before the 2,000 m threshold, and after the 4,000 m threshold, but increases gently between the two thresholds. Whereas the reduction in resolution before the 2,000 m threshold, or after the 4,000 m threshold will lead to huge loss of information due to presence of intrazonal trips, the reduction

in resolution between the 2,000 and 4,000 m thresholds is associated with relatively little loss of information.

Using the guideline that modeled intrazonal trip shares should be within three percentage points of observed intrazonal trip shares, coupled with the fact that the intrazonal trip share of the reference trip table was 0%, the levels of spatial resolution exceeding 1,600 m can be said to produce poor estimates of intrazonal trips.

5.6 Comparison of Network Volumes

For each generated raster cell system, the pedestrian, bicycle and car network volumes resulting from traffic assignment were compared to their respective network volumes from the reference raster cell system. This was done to check the extent to which traffic assignment results change as spatial resolution gets coarser. Figure 5.13 shows the deviations in the assigned network volumes relative to the reference volumes for each mode at the different levels of spatial resolution. The deviation was computed as percentage root mean square error (%RMSE) between the reference and assigned volumes on all network links of the respective modes.

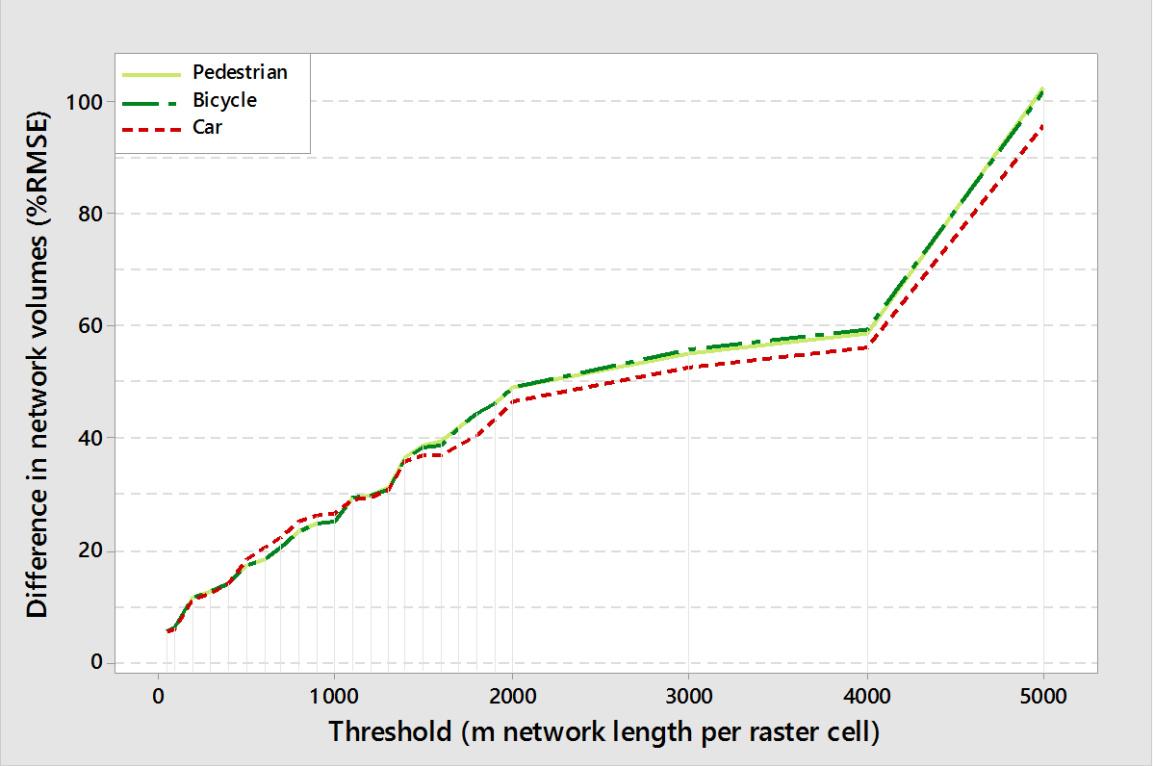

Figure 5.13: Deviations from reference network volumes

As seen in Figure 5.13, the deviations in assigned volumes increase as spatial resolution gets coarser. All three curves exhibit an identical pattern, a pattern similar to that of the intrazonal trip share curve, with the only difference being the part of the curve before the 2,000 m threshold which tends to have a steeper increase in the intrazonal trip share curve than the assignment deviation curves. Whereas a reduction in resolution before the 2,000 m threshold will lead to higher deviations in assigned volumes than a reduction between the 2,000 m and 4,000 m thresholds, a reduction beyond the 4,000 m threshold will result in the highest deviations in assigned volumes.

5.7 Comparison of Number of Raster Cells

Although the use of coarser levels of spatial resolution increases the number of intrazonal trips and increases the deviations in assignment results as well, the number of raster cells decreases with reduction in levels of spatial resolution. Figure 5.14 shows the number of raster cells generated at the different levels of spatial resolution.

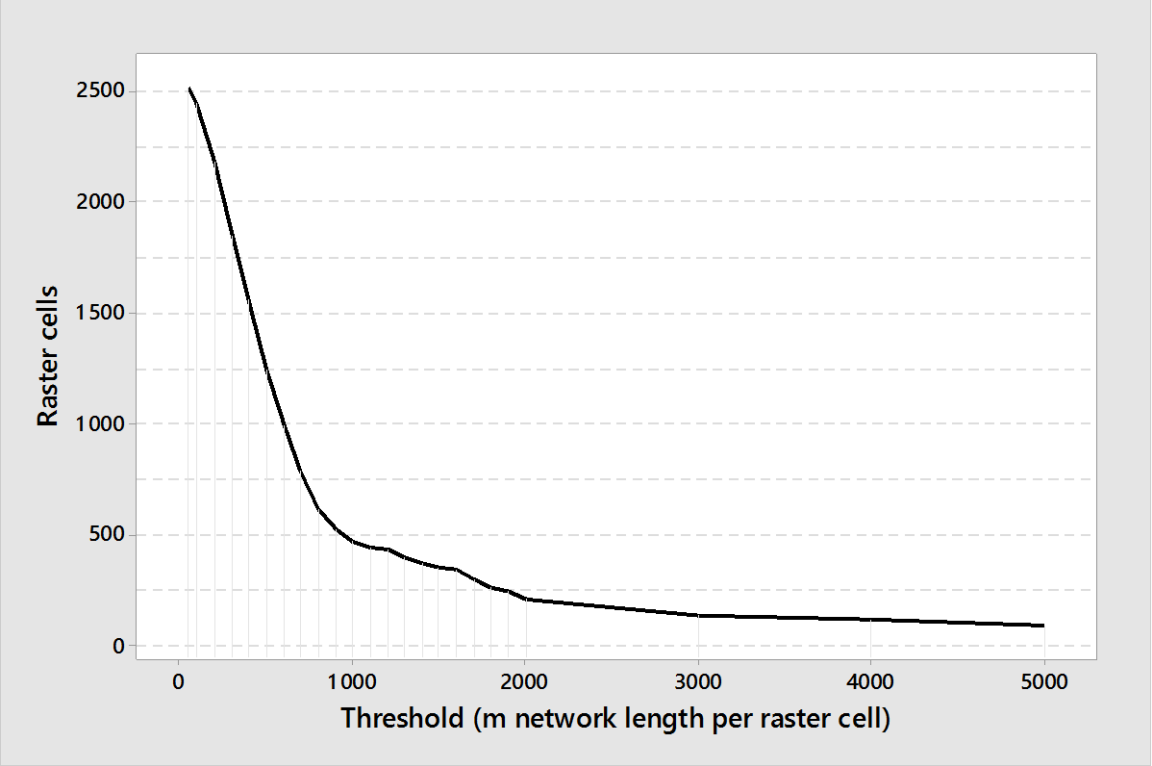

Figure 5.14: Number of raster cells

As seen in Figure 5.14, the number of raster cells decreases as the threshold value increases. However, this relationship is very steep before the 1,000 m threshold, gets fairly gentle between the 800 m and 2,000 m threshold, and is very gentle beyond the 2,000 m threshold. Although the maximum number of generated cells of 2,500 is not unusual for travel demand models, Figure 5.14 seeks to highlight the changes in number of raster cells with every change in the level of spatial resolution. Whereas an increase in resolution from 5,000 m to 2,000 m will have very little impact on the number of raster cells, an increase in resolution from 800 m to 50 m will lead to a substantial increase in the number of raster cells.

5.8 An Appropriate Resolution

From the foregoing, it is evident that the use of fine levels of spatial resolutions results in improved representation of network volumes and a reduction in information loss related to the presence of intrazonal trips. However, this comes with an increase in the number of raster cells. While higher computer speeds make large number of zones less of an issue, the implications for destination choice models, data collection,

as well as the need to forecast socio-demographic changes at very fine levels of detail make it worthwhile to limit the number of zones.

Identifying an appropriate level of spatial resolution involves a trade-off between improvements to model results and a reduction in the number of raster cells. An ideal solution is to keep the number of raster cells to the minimum possible while ensuring a close match between the assigned and reference volumes. Mathematically, the objective is to minimize a cost function with respect to the deviation in assignment results and the number of generated raster cells. Since the function variables are in different units, the values for each variable are normalized between 0 and 1 in order to analyze them in a single framework. For each of the travel modes considered, the cost function F_m is given as:

$$F_m(x_m, y) = \alpha[Norm(x_m)] + \beta[Norm(y)]\ ;\ \ \alpha + \beta = 1$$

where x_m represents the deviation in assignment results of mode m, y represents the number of raster cells, $Norm(x_m)$ and $Norm(y)$ represent the normalized values of variables x_m and y respectively, and α and β represent the relative participation of each variable.

In this study, the variables were treated equally with both α and β equaling 0.5. Figure 5.15 shows the normalized function variables for the different thresholds, and to determine the level at which the function is minimized, Figure 5.16 shows the function outputs at different levels of spatial resolution for the different modes considered.

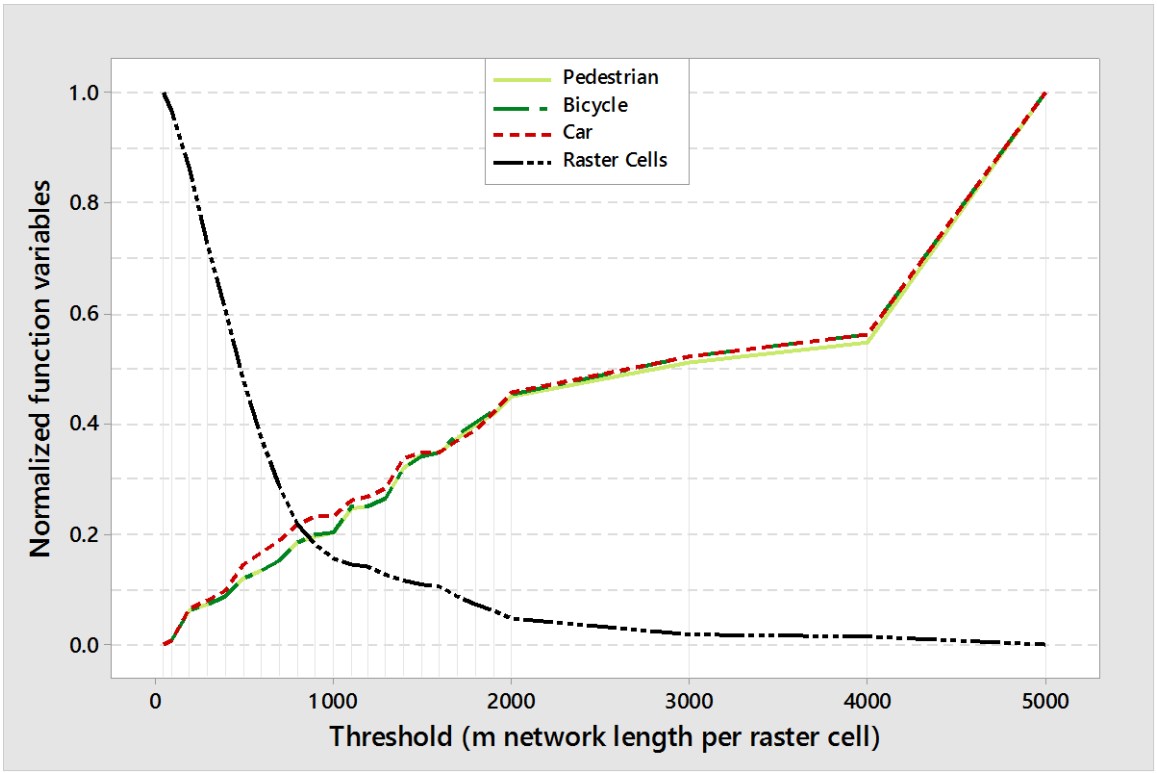

Figure 5.15: Cost function input variables

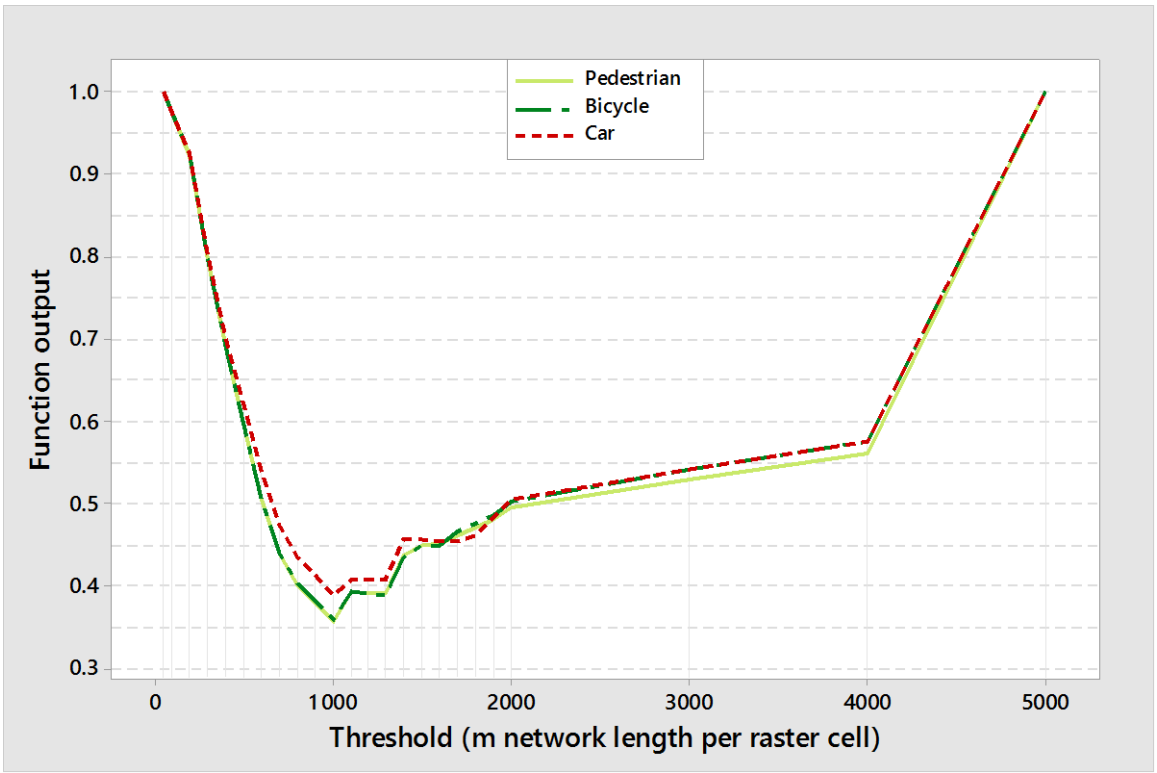

Figure 5.16: Cost function curves

As can be seen from Figure 5.15, the pedestrian, bicycle and car curves keep going up whereas the raster cells curve keeps dropping as spatial resolution gets coarser. The raster cells curve cuts the car curve at the 800 m threshold whereas it cuts the pedestrian and bicycle curves around the 860 m threshold. The drop in the number of raster cells before the meeting point is steep, and it is after the meeting point that the drop begins to get gentle. The pedestrian, bicycle and car curves however rise at the same rate before and after the meeting point. Network volume representation can be improved at low cost by increasing the level of spatial resolution from the 5,000 m threshold until the meeting point of the curves since the increase in the number of raster cells is relatively lower. However, any increase in spatial resolution beyond this point leads to extremely high increases in the number of raster cells.

From Figure 5.16, it can be seen that the minimum of the curves occurs at the 1,000 m threshold. At this point, the combined effect of the deviations in assigned volumes and the number of generated raster cells is at its minimum. Whereas the 800 m and 850 m thresholds for cars and the non-motorized modes respectively are reasonable levels of spatial resolution based on the deductions from Figure 5.15, Figure 5.16 shows that the reduced number of raster cells achieved by decreasing resolution up to the 1,000 m threshold is worth the cost associated with the increased deviation in assignment results.

5.9 Chapter Summary and Conclusion

This chapter focused on identifying an appropriate level of spatial resolution for handling non-motorized trips in macroscopic travel demand models. After creating 24 different raster cell systems for the test area, the study compared number of generated raster cells, intrazonal trip shares as well as deviations in network volumes of each raster cell system.

In creating the raster cell systems, the study applied the gradual rasterization process, and used different thresholds defined as the total length of network links in a raster cell. Despite the fact that macroscopic travel demand modeling involves interaction between TAZ and transport network, the definition and redefinition of TAZ have mostly been done without recourse to the represented transport network. By

using network length as threshold in the gradual rasterization process to define spatial resolution, the study offered a TAZ definition approach that considers the interdependence of zone and network detail.

Although assignment results will continuously improve with increases in spatial resolution, this comes with an increase in the number of raster cells which poses conceptual and computational problems for modeling. With an objective to keep the number of raster cells to the minimum possible while ensuring low deviations in network volumes, a cost function was defined which summed up the normalized number of generated raster cells and the normalized deviations in network volumes for each raster cell system.

Identifying the level where the cost function is minimized, a resolution of 1,000 m network length per raster cell was identified as appropriate. While the 1,000 m network length per raster cell might be applicable in other urban areas, the results should be interpreted as appropriate for the test area, given the range of resolutions considered, as well as the weights assigned to the input variables. Whereas the variables were treated equally in this study, they can be assigned different weights in other contexts to reflect the relative importance of each variable.

Although the study used raster cells to define an appropriate level of spatial resolution, the definition of zones is not restricted to raster cells. Raster cells offer a simplified structure that allows the automatic generation of zone systems at different resolutions and as such can be used to define context-specific appropriate levels of spatial resolution. Subsequently, the identified appropriate level can be used as a benchmark to refine existing zone systems while respecting administrative boundaries and physical separators.

6 Application in Dachau's Travel Demand Model

6.1 Introduction

As discussed in Section 1.2, the purpose of the research was twofold: (1) to find a suitable method for calculating intrazonal impedances; and (2) to identify an appropriate level of spatial resolution to enhance the modeling of non-motorized trips in macroscopic travel demand models. While chapter 4 focused on finding a suitable method for calculating intrazonal impedances, chapter 5 focused on identifying an appropriate level of spatial resolution.

In order to assess the enhancement to macroscopic modeling of non-motorized trips that the study sought to achieve, the outcome of the two parts of the study were applied to model travel demand in Dachau. While the first part of the study considered the nearest neighbor approach sufficient for calculating intrazonal impedances, a resolution of 1,000 m network length per raster cell was identified as an appropriate level of spatial resolution in the second part of the study.

This chapter describes the application of the research outcomes in the travel demand model of Dachau and the comparison of model results to results from a classical travel demand model of Dachau developed with the original TAZ system.

6.2 TAZ Redefinition

Using the 1,000 m network length per raster cell identified as an appropriate level of spatial resolution, the gradual rasterization process was applied with a 1,000 m threshold to redefine the TAZ in Dachau.

The rasterization process started with the definition of a single raster cell over Dachau. A single raster cell of size 9,600 m × 9,600 m was selected considering the 9,370 m length of Dachau along with the following factors:

1. In order to avoid conflicts during the calculation of threshold values, fine raster cells are needed to split network links;
2. The number of fine raster cells has to be a power of 2; and
3. The finest raster cell has to be 75 m × 75 m.

After defining the single raster cell over Dachau, the area was rasterized into 75 m × 75 m raster cells, and the network links were split at the boundaries of these raster cells. Subsequently, the gradual rasterization process was run using a threshold of 1,000 m network length per raster cell to achieve a raster cell system at the appropriate level of spatial resolution. The initial single raster cell and the final output of the rasterization process are shown in Figures 6.1 and 6.2 respectively.

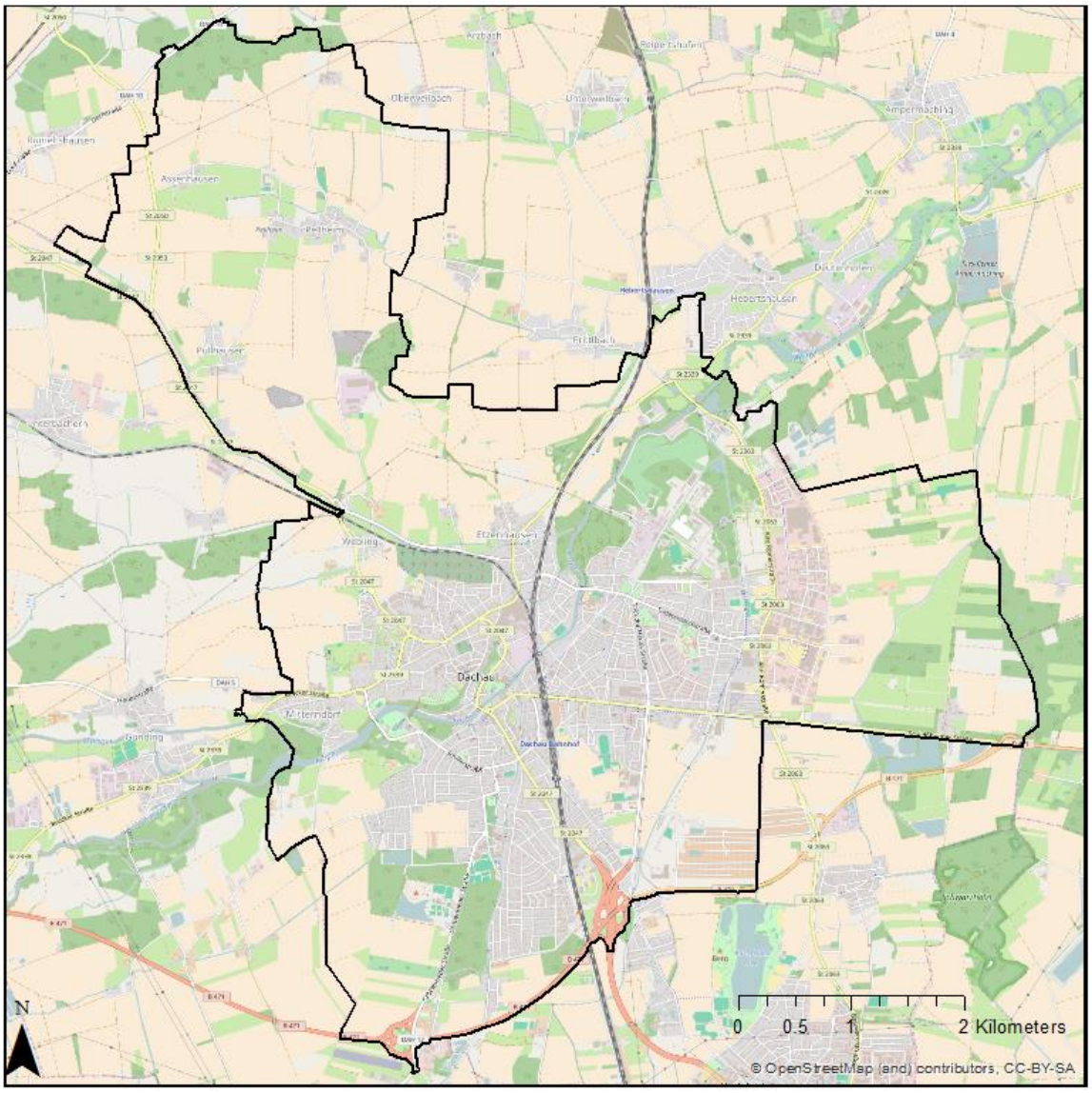

Figure 6.1: Initial single raster cell (Background image: OpenStreetMap contributors, 2016)

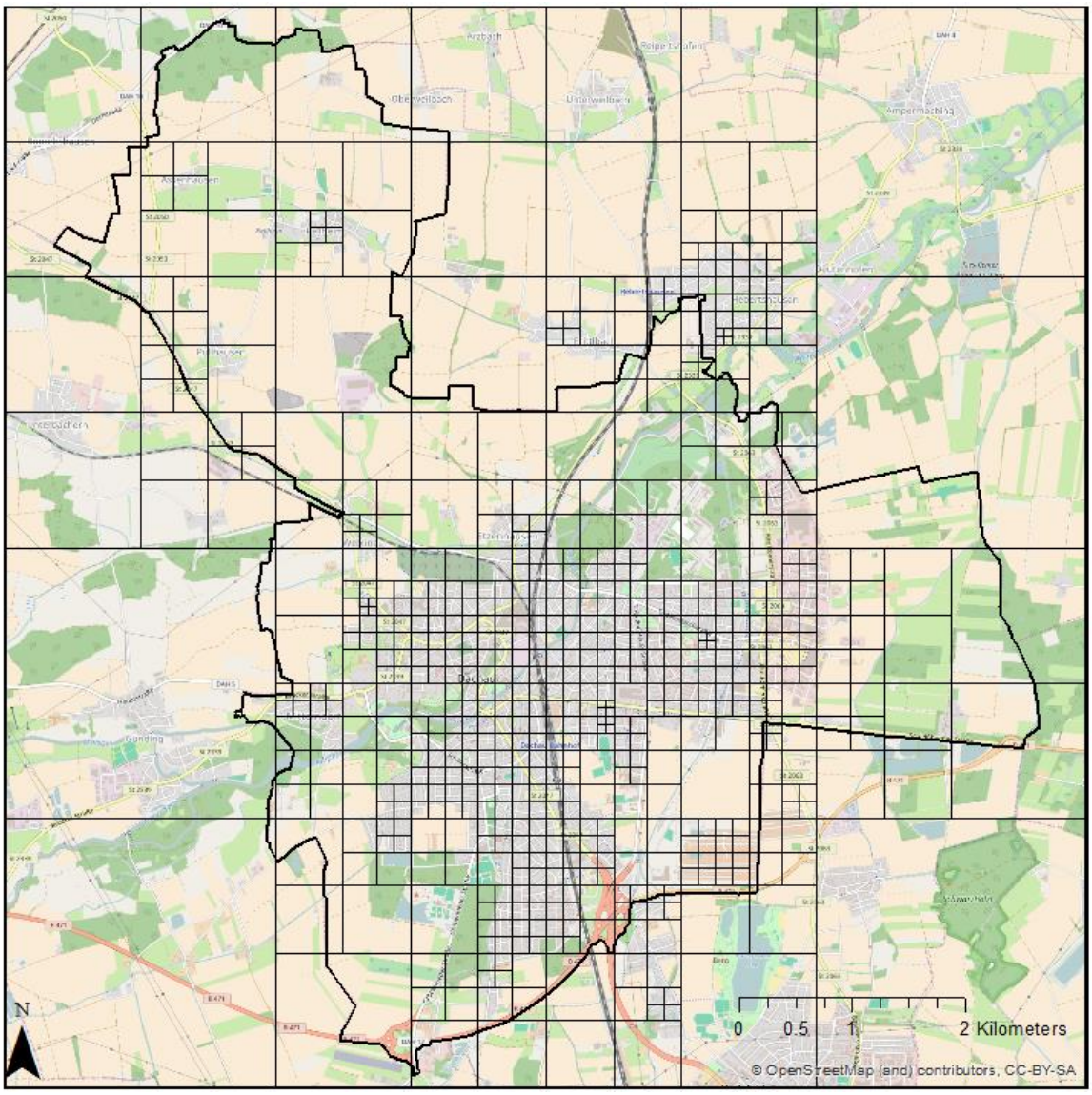

Figure 6.2: Final output (Background image: OpenStreetMap contributors, 2016)

As can be seen from Figure 6.2, the rasterization process resulted in varying sizes of raster cells extending beyond the boundary of Dachau. The boundary of Dachau was used to clip the raster cells to get the raster cells that fell within Dachau. The clipping resulted in instances along the boundary where some raster cells had been split into multiple faces. These were manually checked and corrected by treating the different faces as different cells or merging them to the closest cell depending on the sizes of the faces. Figure 6.3 shows the refined zone system which contains 587 zones.

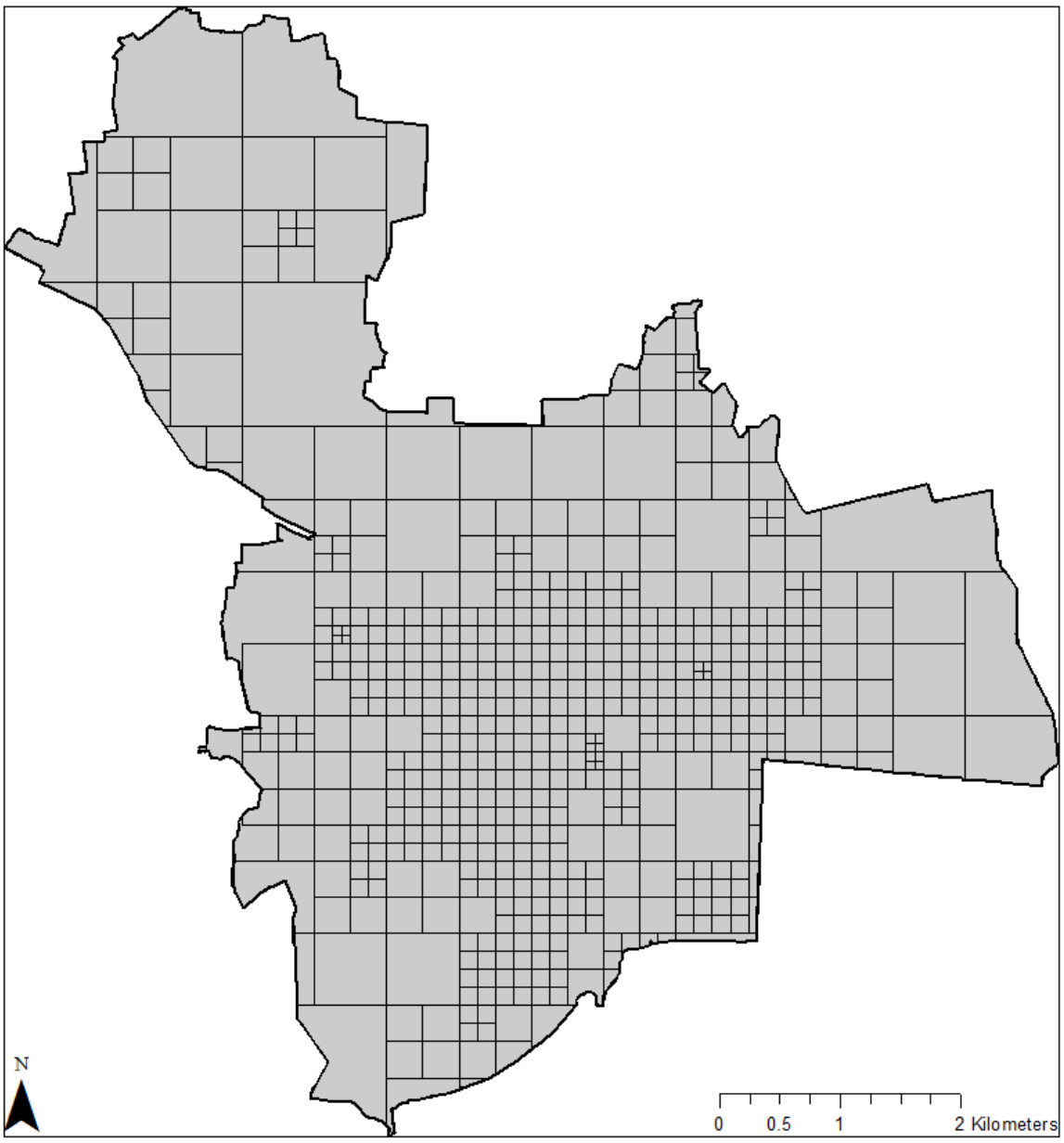

Figure 6.3: Refined zone system

6.3 Modeling Travel Demand with the Refined Zone System

In order to model travel demand with the refined zone system, the socio-economic data as well as the household survey data were disaggregated from the TAZ level to the level of the refined zones. The disaggregation followed the same process used to disaggregate TAZ level data to the building block level described in Section 3.3.1.

Using the disaggregated socio-economic data and the estimated trip rates described in Section 0, the number of trips produced by and attracted to each refined zone was

computed and balanced for the 11 different demand groups. Trip distribution followed the description in Section 3.3.3, with the nearest neighbor technique used in the calculation of intrazonal distances.

Since there were not enough records to do maximum likelihood estimation, mode-share-by-distance curves were developed for each demand group using the household survey data. Figures 6.4 to 6.14 show the mode-share-by-distance curves developed for the different demand groups.

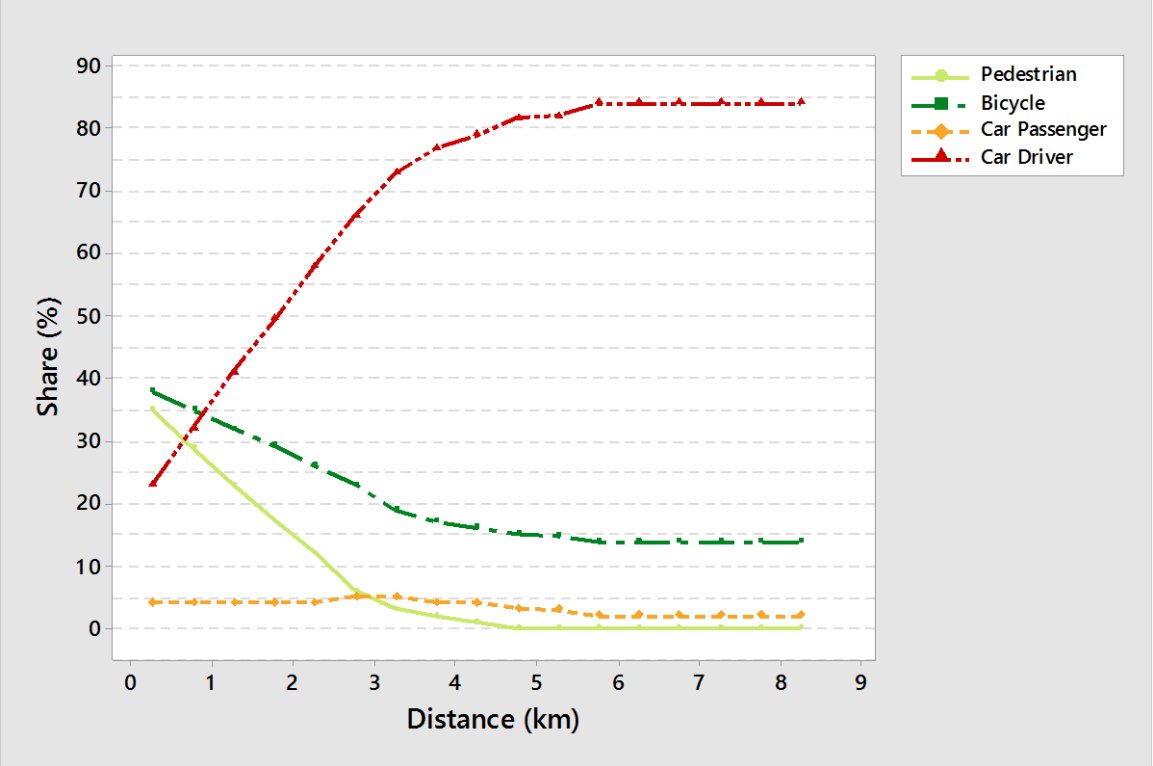

Figure 6.4: Mode shares for HBWa

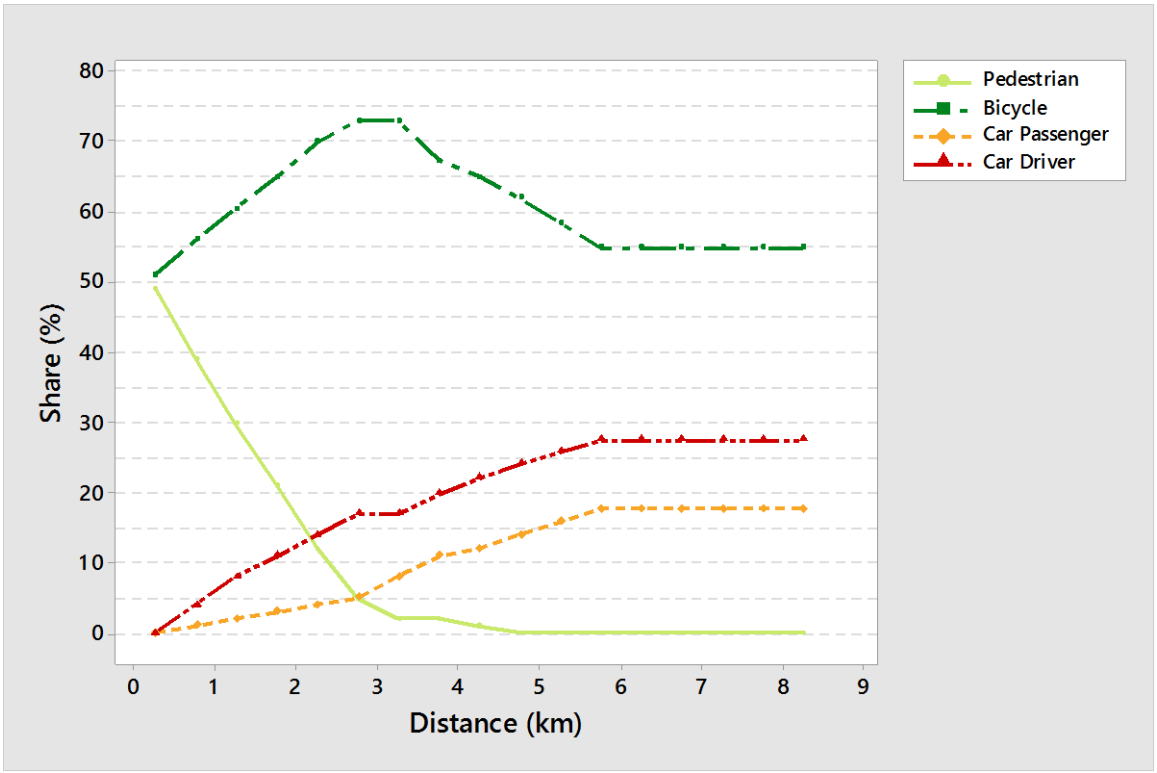

Figure 6.5: Mode shares for HBWb

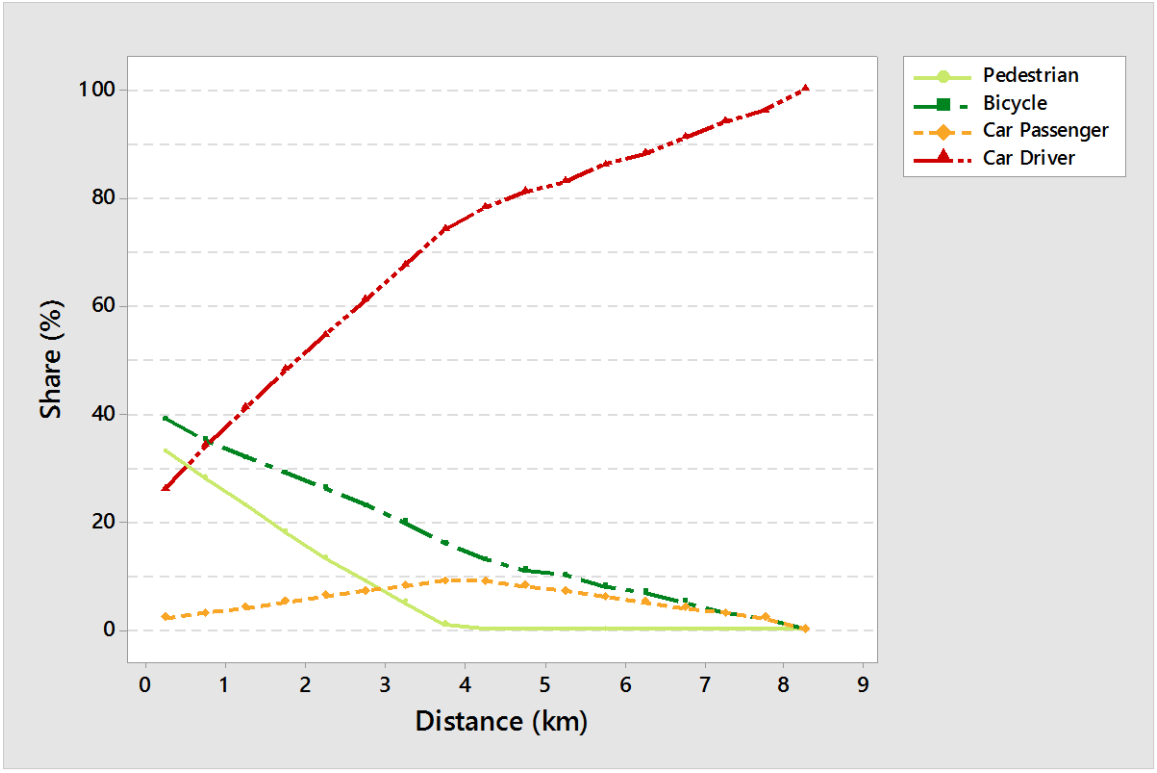

Figure 6.6: Mode shares for HBSa

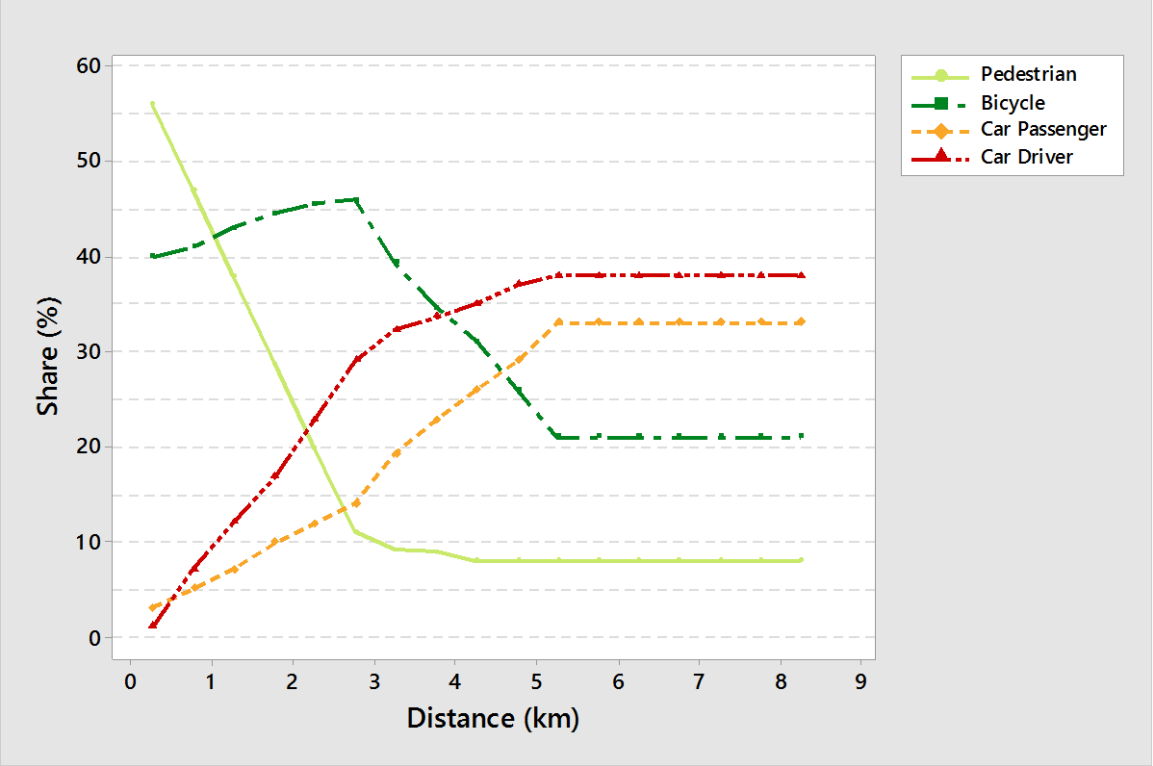

Figure 6.7: Mode shares for HBSb

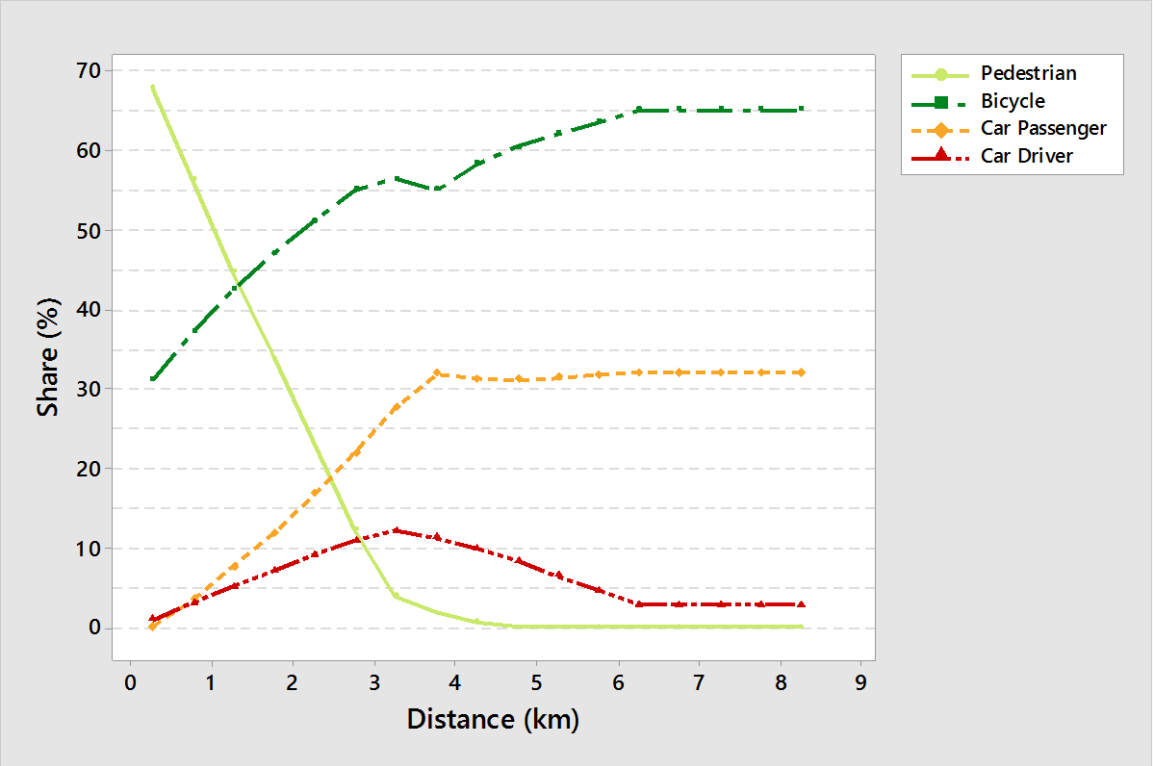

Figure 6.8: Mode shares for HBE

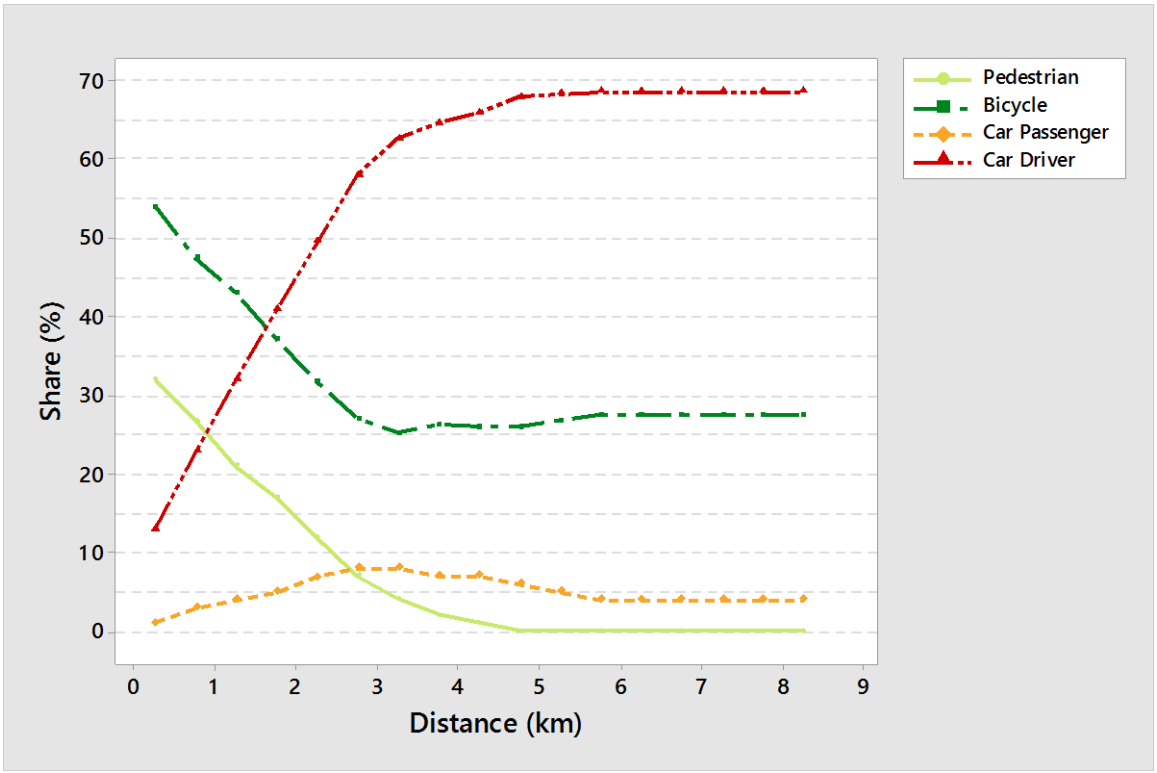

Figure 6.9: Mode shares for HBRa

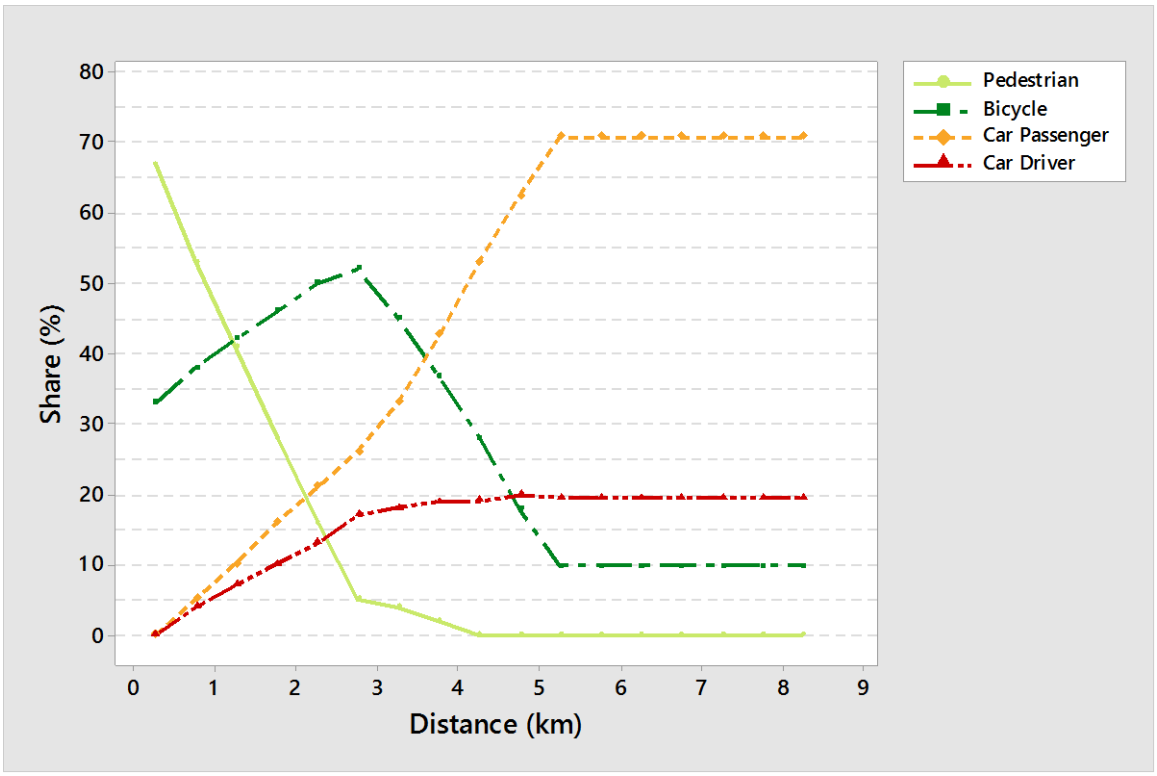

Figure 6.10: Mode shares for HBRb

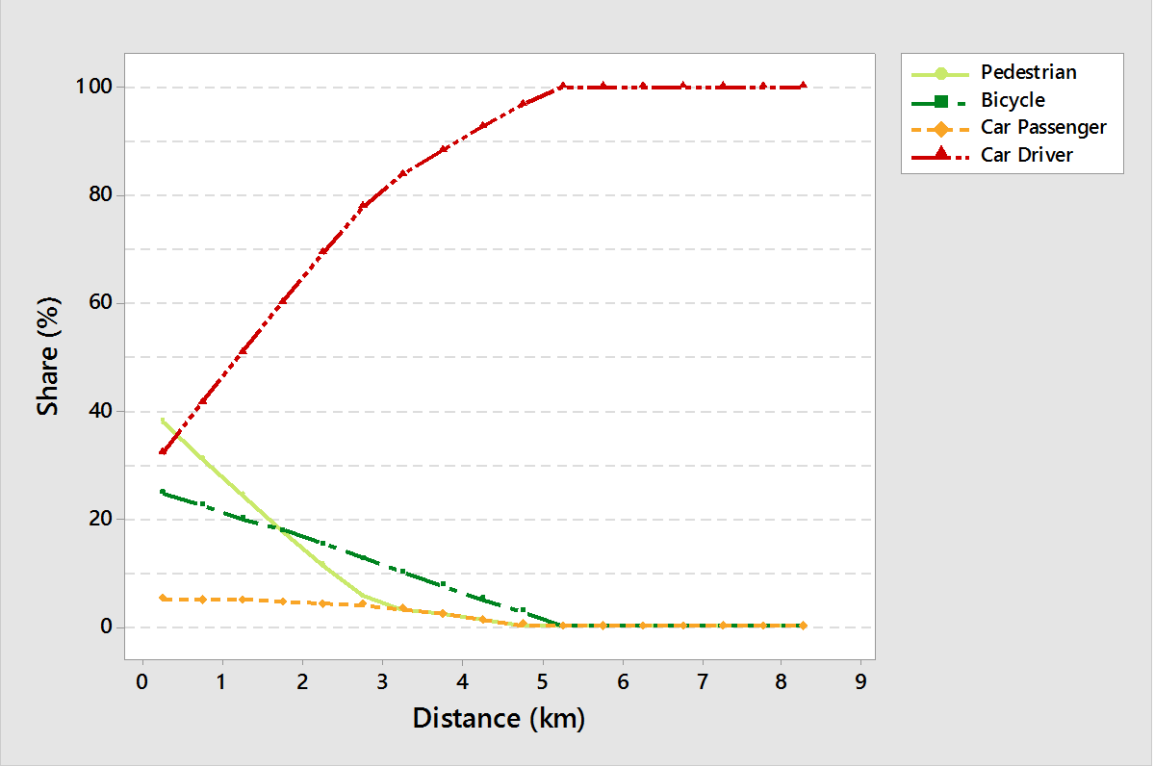

Figure 6.11: Mode shares for HBOa

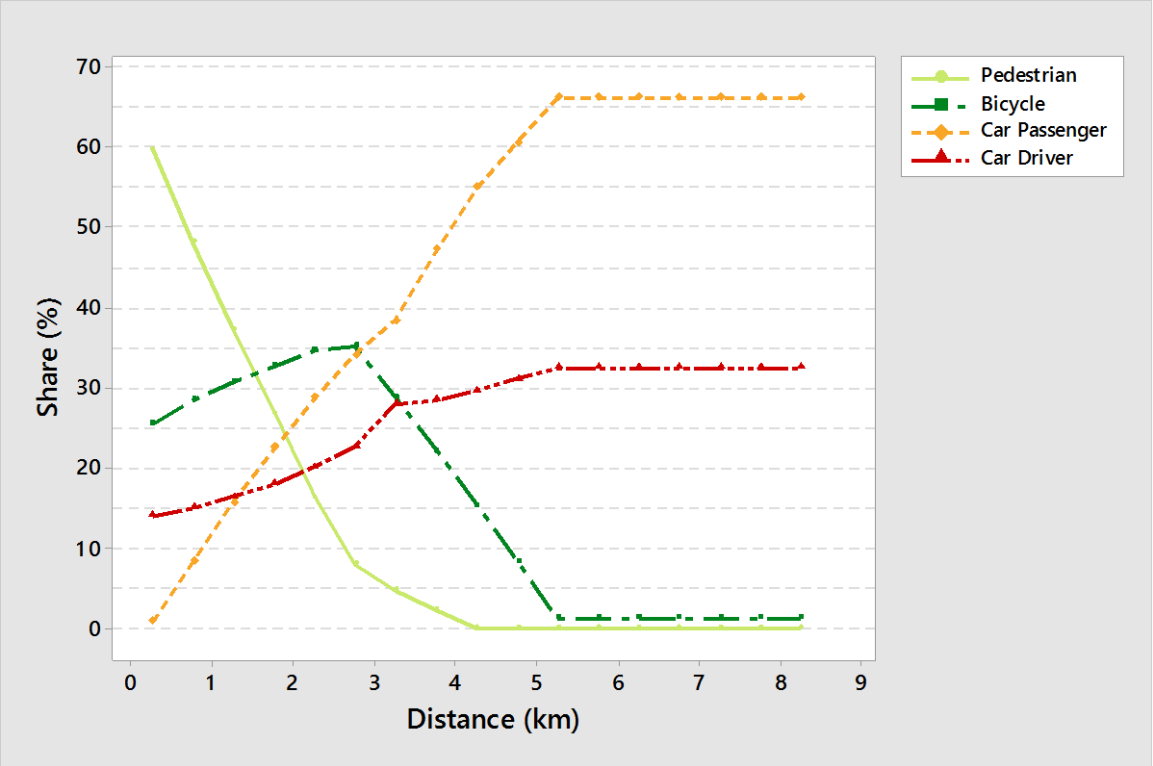

Figure 6.12: Mode shares for HBOb

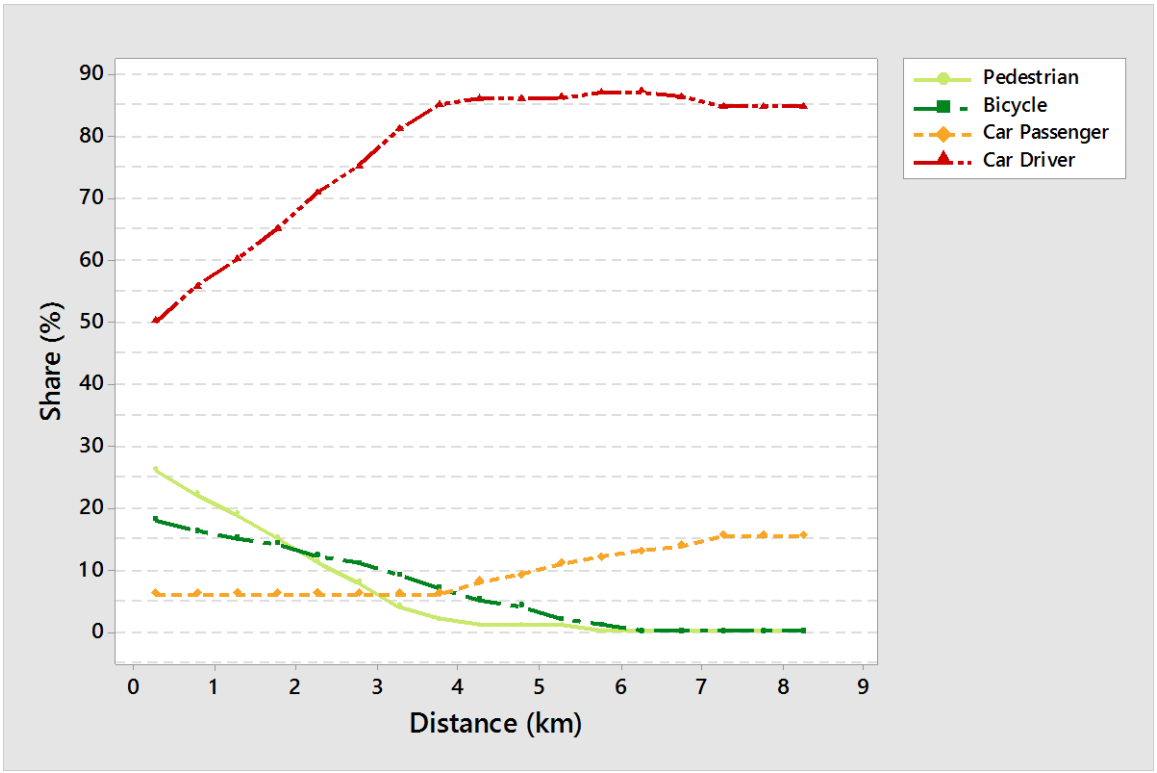

Figure 6.13: Mode shares for NHBa

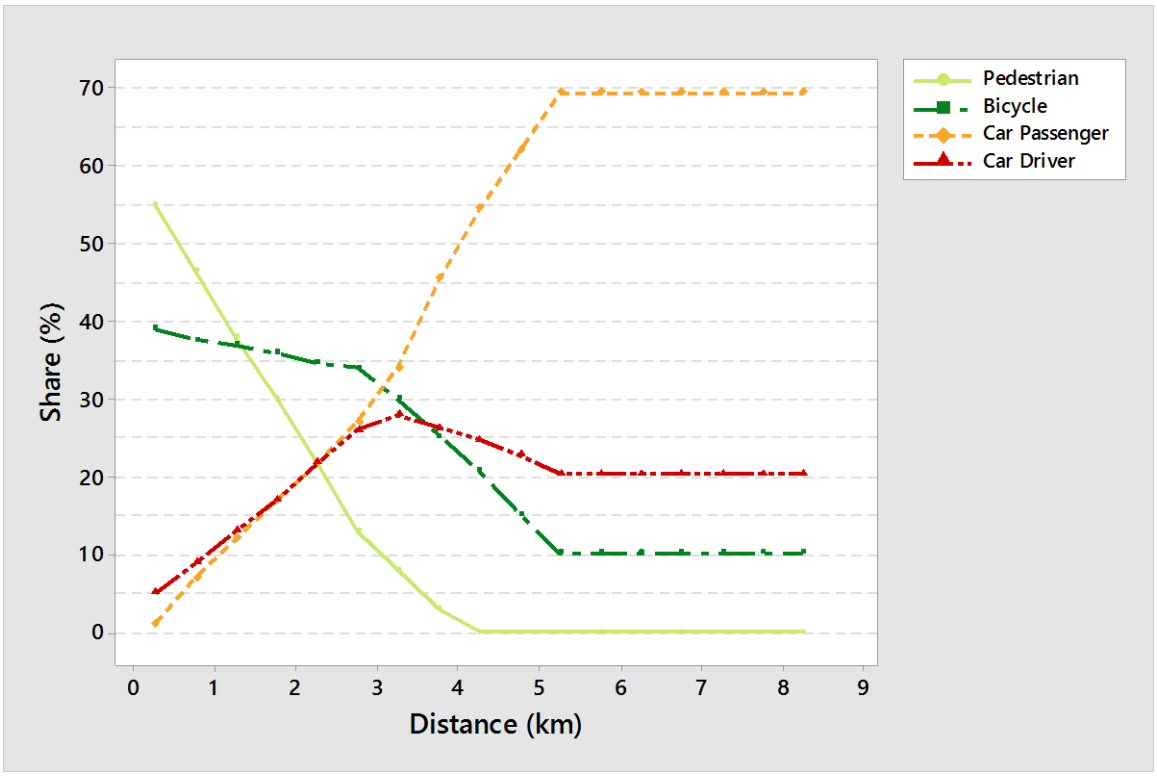

Figure 6.14: Mode shares for NHBb

The mode shares by distance were used to split the trip tables for the respective demand groups. The split trip tables were summed up by travel mode across the different demand groups, and the total pedestrian, bicycle, and car driver trips were assigned onto the pedestrian, bicycle and car network respectively using an all-or-nothing assignment. Since external trips were not considered in the study, the true effects of congestion could not be assessed and for that matter, the all-or-nothing assignment was sufficient to identify the effect of spatial aggregation on assignment result.

6.4 Comparison to the Classical Travel Demand Model

6.4.1 The Classical Travel Demand Model

In selecting a classical travel demand model against which comparisons would be made, the study considered the five model scenarios developed with the original TAZ system that are described in Section 4.4.1. Since the nearest neighbor method is a popular method used for the calculation of intrazonal impedances, the nearest-neighbor scenario was selected. Thus, the classical travel demand model was a model developed with the original TAZ system using the nearest neighbor technique for the calculation of intrazonal impedances.

Effectively, the only difference between the refined and classical travel demand models lay in the type of zone system used. The nearest neighbor technique was used to calculate intrazonal impedance in both models. Like the mode choice step in the refined model, mode shares by distance were used to split trip tables for the respective demand groups in the classical model. Similarly, the split trip tables were summed up by travel mode across the different demand groups, and the total pedestrian, bicycle, and car driver trips were assigned onto the pedestrian, bicycle and car network respectively using an all-or-nothing assignment.

6.4.2 Comparison of Zone Characteristics

To enable a visual inspection and comparison of the characteristics of the refined zone system and the original TAZ system, Figures 6.15 and 6.16 show the refined

zones and the original TAZ respectively. The refined zone system contains 587 zones whereas the original TAZ system has 102 zones.

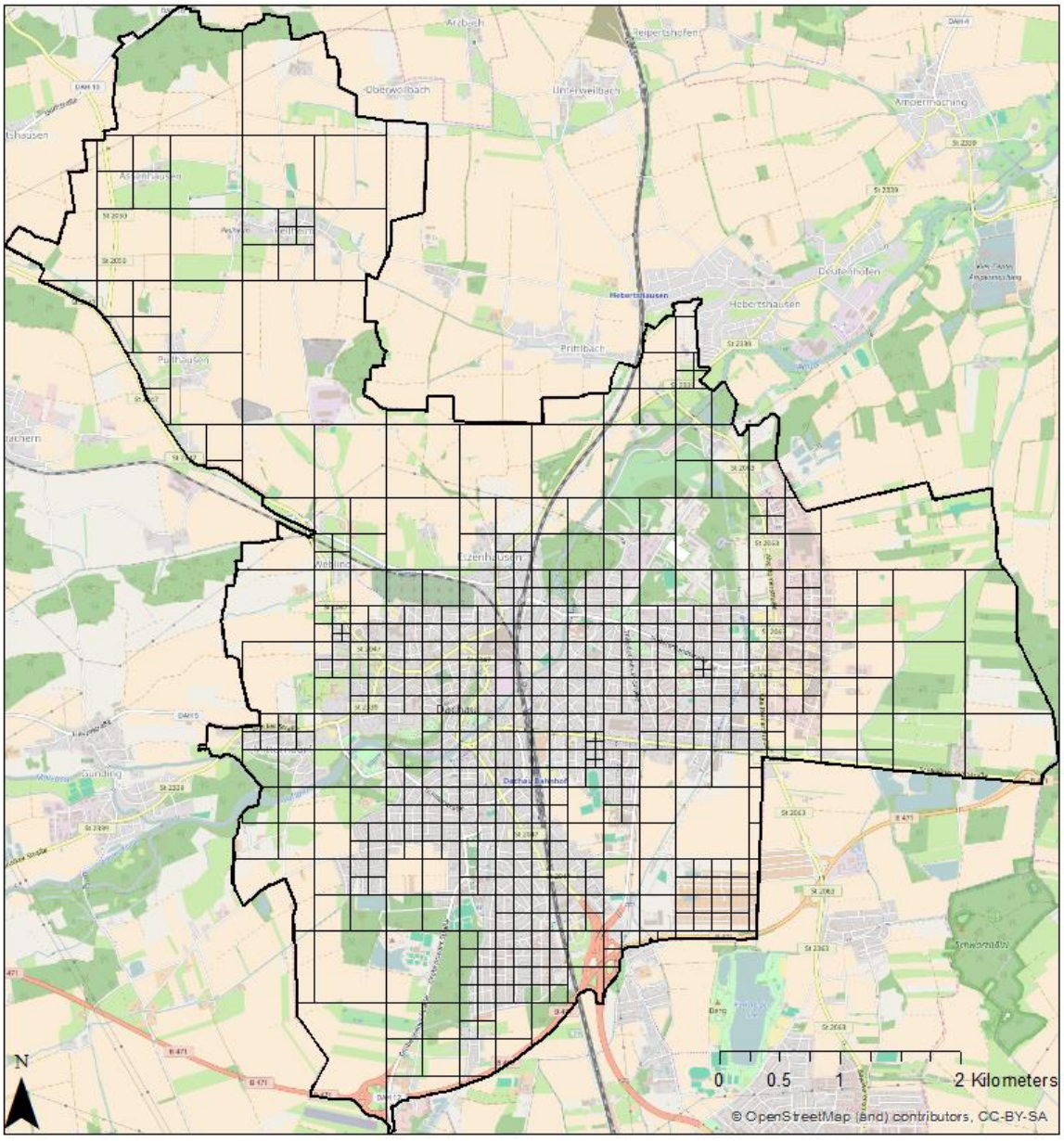

Figure 6.15: Refined zones in Dachau (Background image: OpenStreetMap contributors, 2016)

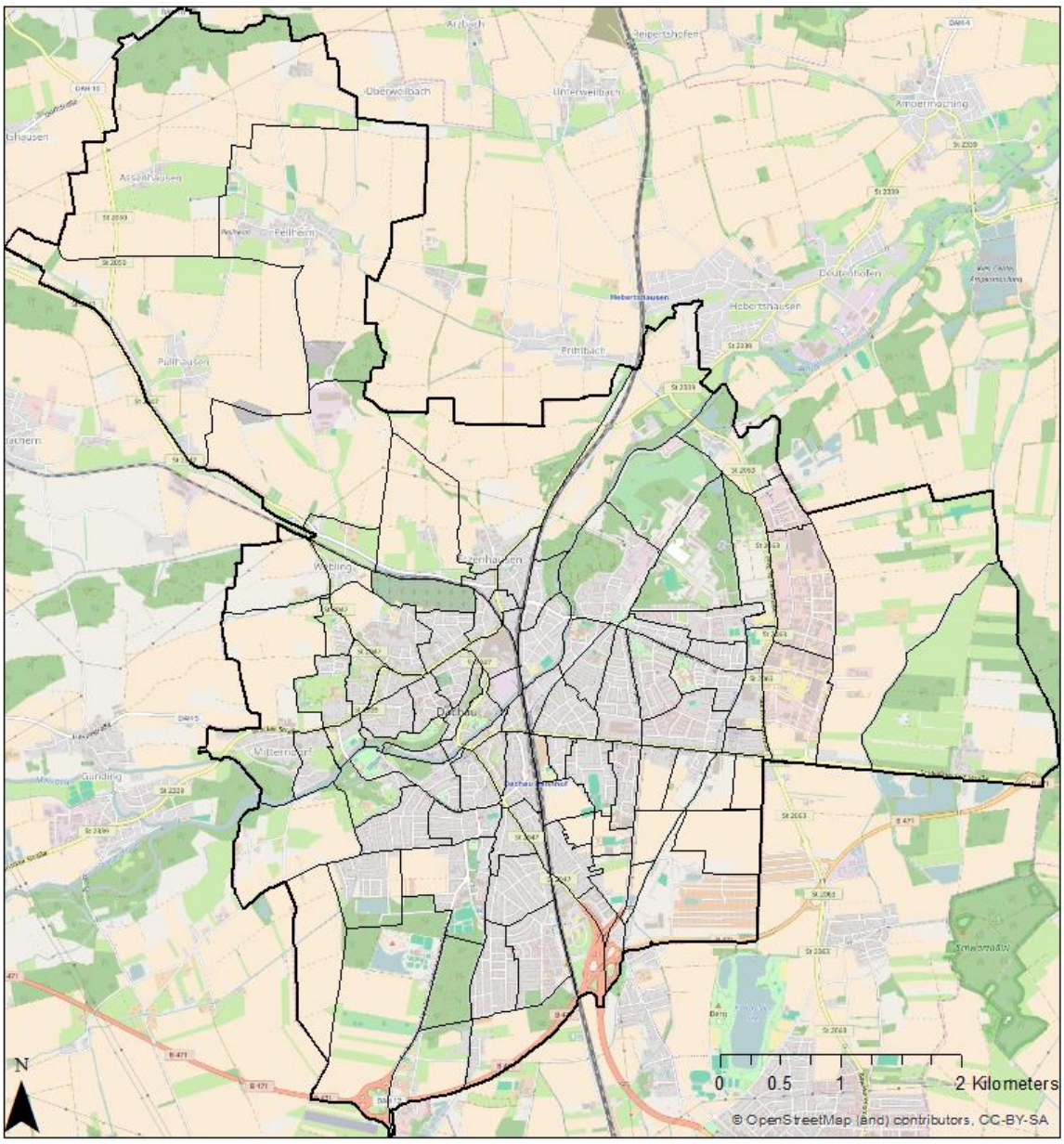

Figure 6.16: Original TAZ in Dachau (Background image: OpenStreetMap contributors, 2016)

As can be seen from Figures 6.15 and 6.16, whereas both systems offer zones that are exclusive, complete, and unique, the refined zone system is more detailed and as such offers a higher geographical precision than the original TAZ.

Regarding the respect of political, administrative, and statistical boundaries, the original TAZ have been designed along such lines whereas the rasterization process does not consider such boundaries in the definition of zones. Similarly, the manual definition of the original TAZ ensures that physical separators can be respected

whereas the rasterization process does not respect physical separators. Nevertheless, the disaggregation of data from the TAZ level to the refined zone level ensured the availability of data for the refined zone system. Although the assumptions made in disaggregation introduce errors, the errors involved are limited since the disaggregation is controlled by TAZ.

On the avoidance of zones as boundaries, whereas a conscious effort has been made to use main roads as boundaries for the original TAZ, the rasterization process inadvertently avoids the use of main roads as boundaries.

6.4.3 Comparison of Trip Generation Results

This section compares the two zone systems with respect to equity in terms of trip generation. Figures 6.17 and 6.18 show the variability in trip productions and attractions respectively by demand group for each zone system. Variability in trip productions depicts how the number of trips produced by the different zones of a particular zone system differ from one another whereas variability in trip attraction shows how the number of trips attracted to the different zones of a particular zone system differ from one another.

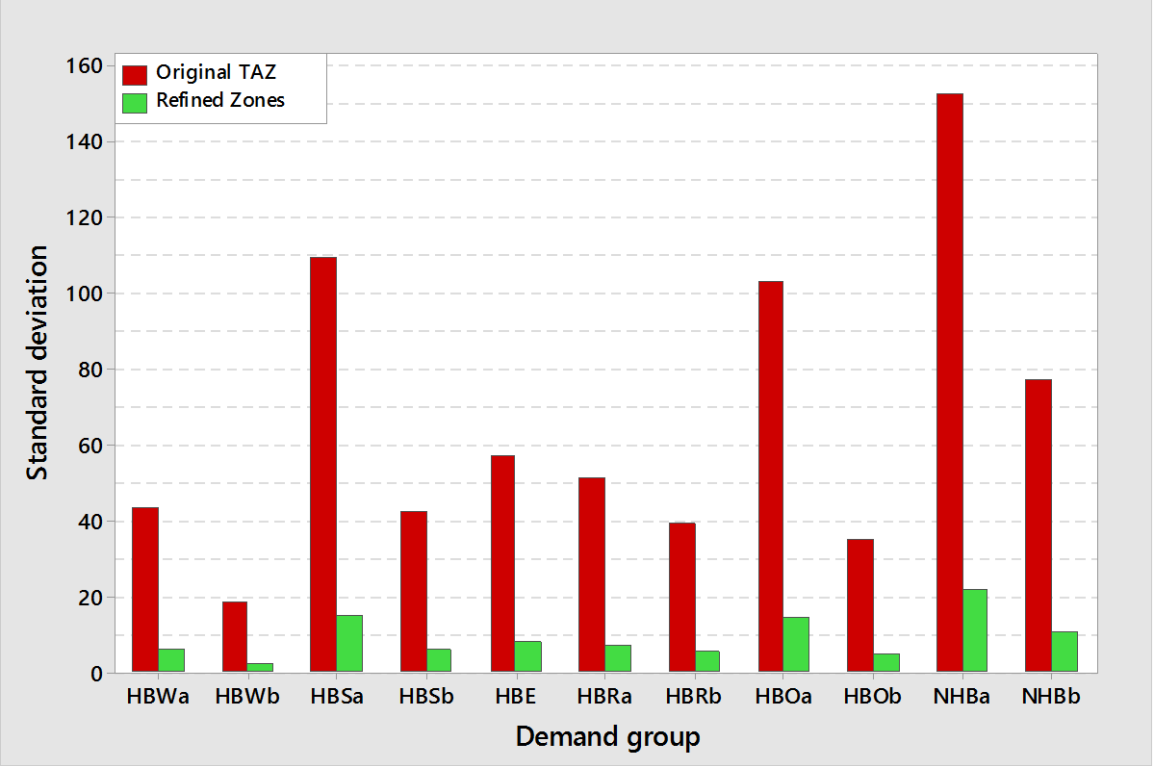

Figure 6.17: Variability in trip productions

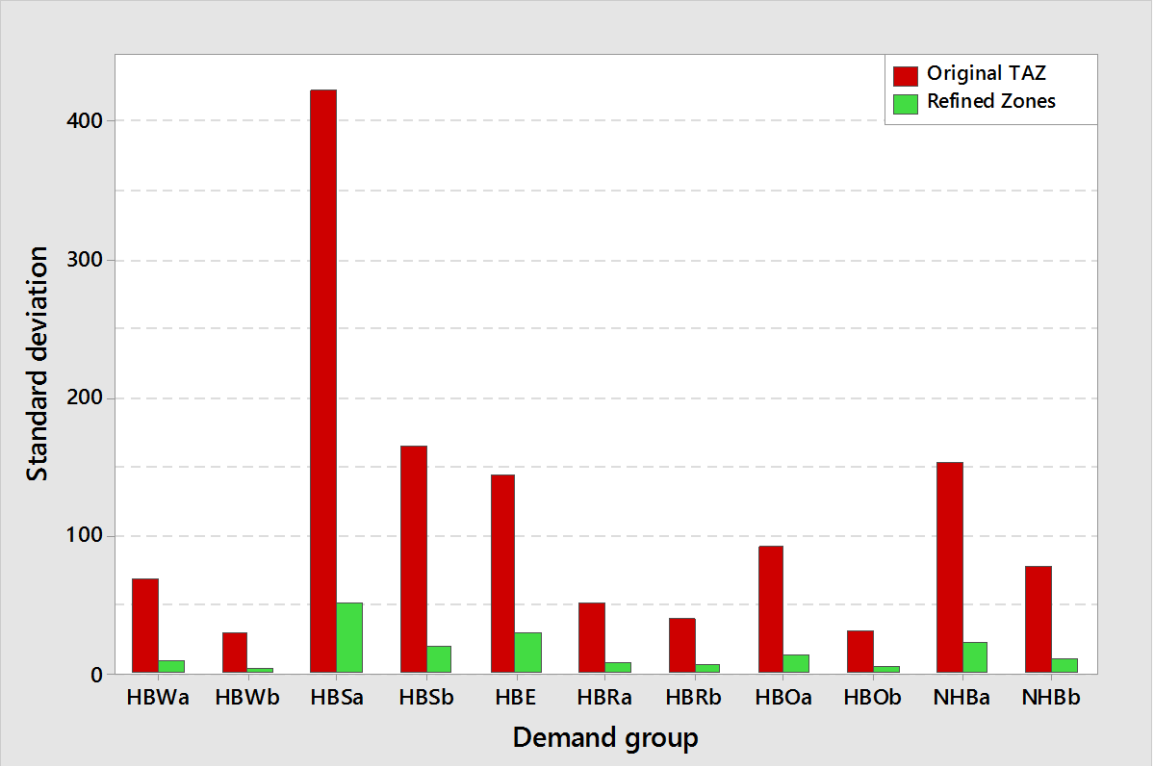

Figure 6.18: Variability in trip attractions

As can be seen from Figure 6.17, for each demand group, there is less variability in the number of trips produced by the refined zones than in the number of trips produced by the original TAZ. Similarly, Figure 6.18 shows that, for each demand group, there is less variability in the trip attraction values among the refined zones than in the trip attraction values among the original TAZ.

To ensure diverse trip assignments, it is recommended that the design of TAZ considers equity in trip generation so that every network segment has a chance to get loaded. In that regard, the refined zone system offers a better design than the original TAZ system.

The limited variability in trip productions and attractions of the refined zone system justifies the use of network density as proxy for levels of trip generation. Essentially, network length per raster cell can be deemed a good measure for defining threshold values to subdivide raster cells in the gradual rasterization process.

6.4.4 Comparison of Trip Distribution Results

Concerning the minimization of intrazonal trips, Figure 6.19 compares the intrazonal trip shares resulting from each zone system for the different demand groups.

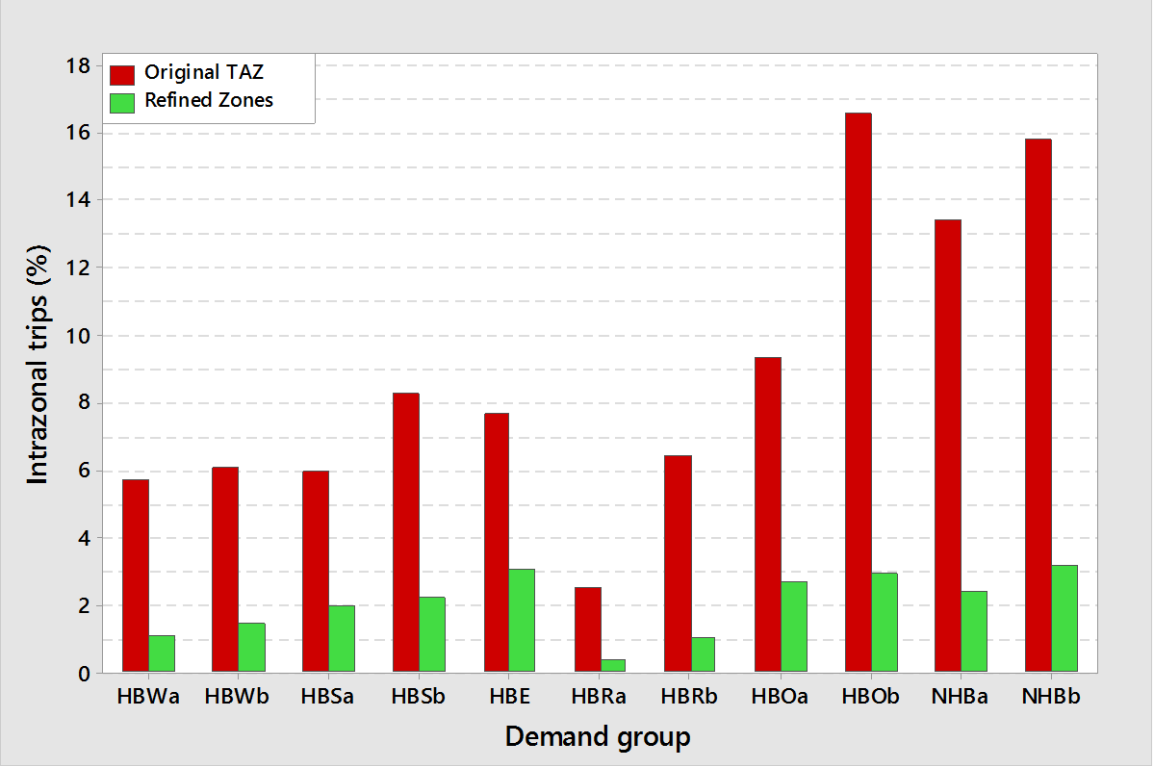

Figure 6.19: Intrazonal trips as a share of total trips

Figure 6.19 shows that the refined zone system greatly reduces the intrazonal trip share for all demand groups with the reduction in the case of HBO trips exceeding 13%. For all but the HBE and NHBb demand groups, the refined zone system produces intrazonal trip shares not exceeding 3%, and even for these two groups, the intrazonal trip shares are just a little over 3%. The intrazonal trips shares produced by the refined zone system for the HBE and NHBb demand groups are 3.1% and 3.2% respectively.

The use of the refined zone system therefore reduces the need to model intrazonal trips since a 3% loss of information is not big enough to significantly affect model results.

6.4.5 Comparison of Mode Choice Results

In order to assess the effect of the refined zone system on mode choice, Figure 6.20 shows the changes to mode shares resulting from the use of the refined zone system.

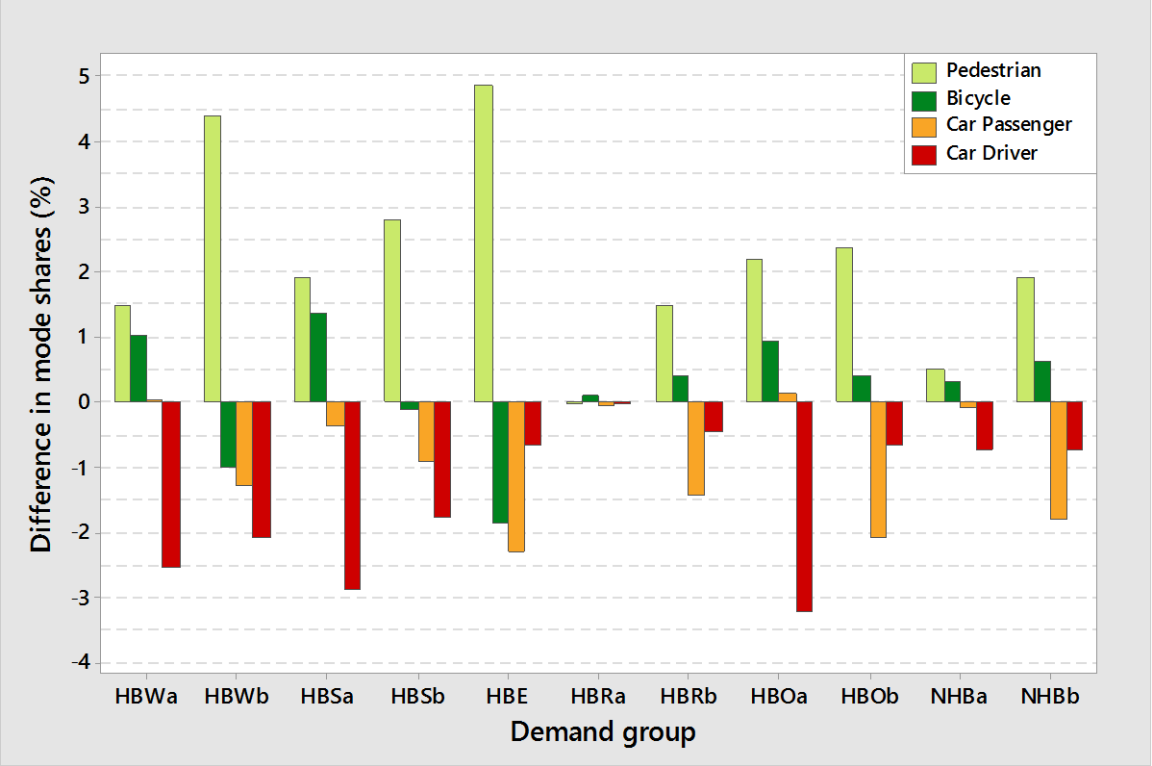

Figure 6.20: Difference in mode shares between refined and original TAZ systems

From Figure 6.20, it can be observed that, for all but the HBRa demand group which exhibits the least difference between the mode shares, the use of the refined zone system results in increases in the share of pedestrian trips while the share of car trips reduces. The insignificant difference between the mode shares of the HBRa demand group for both zone systems is as a result of the very low intrazonal trip shares involved in the HBRa group as can be seen in Figure 6.19

The share of bicycle trips also increases for eight out the 11 demand groups while the share of car passengers drops for nine out the 11 demand groups. Generally, the share of non-motorized trips increases when the refined zone system is used while the share of motorized trips reduces. The results indicate that the presence of intrazonal trips leads to the underestimation of non-motorized travel, and therefore mitigating the intrazonal problem invariably improves the modeling of non-motorized trips.

6.4.6 Comparison of Assignment Results

A percent root mean square error computed for the different modal networks with respect to differences in assigned network volumes between the original TAZ system and the refined zone system indicates a difference of 119%, 93%, and 96% for pedestrian, bicycle and car networks respectively.

The values indicate that the assignment results are significantly different and this can be attributed to the differences in the variability of trip productions and attractions observed in Figures 6.17 and 6.18. The chances that a network link will get loaded is more likely in the refined zone system than the original TAZ system since the refined zone systems satisfies the trip generation equity criteria better than the original TAZ system.

6.5 Chapter Summary and Conclusion

This chapter described the application of the research outcomes in the travel demand model of Dachau and compared model results to results form a classical travel demand model of Dachau developed with the original TAZ system.

In creating a refined zone system for Dachau, the gradual rasterization process was adopted with a threshold of 1,000 m network length per raster cell. Travel demand model was developed for the refined zone system, and for mode choice, mode-share-by-distance curves were used to split trip tables for the refined model as well as the classical model. Split trip tables were summed up by travel mode across different demand groups and assigned onto their respective networks using an all-or-nothing assignment.

The results show that the refined zone system offers a better zone design than the original TAZ with the lone shortcoming being its disregard of statistical boundaries and physical separators. Although the rasterization process does not take these boundaries and separators into account, post rasterization adjustments can be made to ensure satisfaction of the boundary criteria. Subsequently, data at the statistical boundary level can be disaggregated to the refined zone level.

In addition to the equity of trip generation criterion that the refined zone system satisfies better than the original TAZ system, the use of the refined zone system results in the minimization of intrazonal trips. With respect to the improvements to macroscopic modeling of non-motorized trips that the study sought to achieve, the mode choice results indicate that the use of the refined zone system improves non-motorized trip estimates.

The limited variability in trip productions and attractions of the refined zone system also indicates that the use of network density as proxy for levels of trip generation is a good assumption. Essentially, network length per raster cell can be deemed a good measure for defining threshold values to subdivide raster cells in the gradual rasterization process.

7 Conclusions and Outlook

7.1 Summary of Findings

The aim of the research was to enhance the capability of macroscopic travel demand models in modeling non-motorized travel demand by finding a suitable method for calculating intrazonal impedances, and identifying an appropriate level of spatial resolution for TAZ. The study was motivated by the recognition of the role of non-motorized travel in sustainable mobility, the usefulness of models in forecasting travel demand, and the limited representation of non-motorized trips in macroscopic travel demand models. To find a suitable method for calculating intrazonal impedances, and to identify an appropriate level of resolution for modeling non-motorized trips, the research worked with the hypotheses that: (1) the average impedance between network node pairs within a zone is a better measure of the zone's intrazonal impedance than values calculated with existing methods; (2) better estimates of intrazonal impedances guarantee better estimates of intrazonal trips; and (3) if zone resolution is made finer, while network detail among other things is held constant, a point will be reached beyond which further increases in zone resolution will lead to decreases in overall model benefits.

In finding a suitable method for calculating intrazonal impedances, the research considered existing methods as well as a method developed by the author that calculates intrazonal impedance as the average impedance between network node pairs within a zone. Having compared values of intrazonal impedances calculated by the different methods, the study found out the proposed method provided better estimates of intrazonal impedances than the existing methods. The finding supports the first hypothesis which posits that the average impedance between network node pairs within a zone is a better measure of the zone's intrazonal impedance than values calculated with existing methods. Whereas the proposed method provided the best estimates of intrazonal impedances, it did not provide the best estimates of intrazonal trips. For some demand groups, the proposed method provided the worst estimates. The second hypothesis is thus contradicted by this finding.

To identify an appropriate level of spatial resolution for macroscopic modeling of non-motorized trips, the research applied the gradual rasterization process. Using different thresholds, 24 different raster cell systems were generated for a test area. Having compared the number of raster cells and the deviations in network volumes from each generated raster cell system, the study defined a cost function whose minimum was considered an appropriate level of spatial resolution. The study identified 1,000 m network length per raster cell as appropriate for the test area. Before this level, model results could be improved at low cost by increasing the level of spatial resolution. However, any increase in spatial resolution beyond this level led to increases in overall costs. The results show that there is a limit beyond which the benefits derived by further increases in spatial resolution is not worth the costs associated with the extremely high increase in the resultant number of zones. The third hypothesis is thus supported by this finding.

The application of the research outcomes in the travel demand model of Dachau showed that the identified appropriate level of spatial resolution offered a better zone design than the original TAZ. Specifically, modeling at the appropriate level of spatial resolution ensured equity in trip generation, minimized the number of intrazonal trips, and improved non-motorized trip estimates. The findings show that mitigating the intrazonal problem improves the modeling of non-motorized trips.

7.2 Significance of Research

Although the study sought to enhance the modeling of non-motorized trips in macroscopic models, the contributions of the research findings extend beyond the macroscopic modeling of non-motorized trips. The research outcome has implications for the broader field of travel demand modeling and sustainable mobility.

First of all, the findings dismiss the long held view that improving intrazonal impedance estimates will improve intrazonal trip estimates. Non-motorized trips can therefore not be adequately handled in macroscopic models by improvements to the calculation of intrazonal impedances. This recognition should enable researchers to shift away from the quest for better intrazonal impedance calculation. Efforts aimed

at improving the calculation of intrazonal impedances should be geared towards reducing the need to deal with intrazonal trips.

Secondly, the findings give credence to the use of the nearest neighbor technique in calculating intrazonal impedances. The need for values of intrazonal impedance should be treated as the need for a value big enough to capture intrazonal trips but small enough to avoid the misallocation of interzonal trips within the same zone. Considering the logic and ease of measurement as well as its performance with regards to the calculation of intrazonal trips, the nearest neighbor technique is sufficient for approximating intrazonal impedances.

Furthermore, the research introduces a TAZ definition approach that considers the interdependence of zone and network detail, and can be used to define appropriate levels of spatial resolution for any area. Whereas the study assigned equal weights to the input variables of the objective function, the variables can be assigned different weights in other applications to reflect the relative importance of each variable. Similarly, the range of threshold values considered can be different in other applications. This should enable transport planning agencies to easily redefine their zoning systems to achieve appropriate levels of spatial resolution.

The research mitigates the intrazonal problem of macroscopic models to enhance their capability in modeling non-motorized travel. This should facilitate the integration of bicycle and pedestrian travel, which forms a high share of trips in urban areas, in the models of transport planning agencies in Dachau and other areas with the desire to do so. Subsequently, planning agencies would be able to evaluate the usage and benefits arising from improvements to non-motorized transport, model out priorities for improvement to non-motorized facilities, and assess the impacts of actions taken to encourage non-motorized travel. This should ensure the successful development and implementation of sustainable mobility concepts.

7.3 Limitations of the Study

The main limitation of the current study relates to the level of resolution of the available data. The study required data at a more detailed level. However, the data

were available at the TAZ level and therefore needed to be disaggregated. Although the disaggregation assumed an even distribution of data among building blocks within a TAZ, trip generation levels of building blocks differ in reality. However, since the disaggregation was controlled by TAZ, the errors involved are expected to be limited.

Another limitation relates to the number of trip records. There were not enough trip records per demand group to enable maximum likelihood estimation for mode choice model. Nevertheless, mode shares were calculated with a share-distance curve developed with the survey data. The exclusion of access and egress trips also meant an under-representation of non-motorized trips.

Furthermore, there were no non-motorized count data against which assignment results could be validated. The research had to rely on assignments results from a disaggregated zone system as reference for the comparison of assignment results.

7.4 Further Research Needs

New knowledge can be gained from studies that expand upon the existing research scope and explore additional findings that were not directly related to the main objectives.

First, given the many instances of data disaggregation in this research, it is evident that a re-definition of zone systems will require disaggregation of structural data from the geographic units for which data are usually available. The study assumed an even distribution of TAZ data over building block areas. However, building blocks covering the same area may differ in function and height, thereby generating different levels of trip. Errors are inherent in data disaggregation, and the bigger the difference in resolution between the re-defined zones and the data units, the larger the errors involved. Future research should explore approaches to limiting the errors involved in data disaggregation.

Second, the research used network density as proxy for trip generation levels. Whereas the lack of network in an area indicates a lack of trip generator, network

links that are a few meters long can have different number of trip origins and destinations depending on the urban form and density. Therefore, areas with higher network densities will not always have more trip origins and destinations. Althogh the findings indicated that the use of network density as proxy for levels of trip generation was a good assumption, it would be a valuable exercise to research further into the relationship between network density and trip generation levels. While the current study used network length per zone to represent network density, future research work can look into other network attributes.

Third, future research efforts should seek to define an optimal level of spatial resolution for TAZ. Whereas this work used assignment results and the number of generated raster cells to determine an appropriate level of spatial resolution, other variables can be considered in the definition of an optimal level of spatial resolution. The ease with which zone systems can be generated with the network-based gradual rasterization process should facilitate the generation of multiple zone systems to enable comparisons across different levels of spatial resolution.

Finally, it would be a valuable exercise to compare model results between a highly disaggregate model and a macroscopic model with a refined zone system to ascertain the sufficiency or otherwise of macroscopic models when zones are refined.

References

Batty, M. (1976). *Urban Modelling: Algorithms, Calibrations, Predictions*. Cambridge University Press.

Bayerisches Landesamt für Statistik. (2016). GENESIS-Online Bayern. Retrieved October 1, 2016, from https://www.statistikdaten.bayern.de/genesis/online/data?Menu=Willkommen

Bhat, C. R., Guo, J. Y., and Sardesai, R. (2005). Non-Motorized Travel in the San Francisco Bay Area. University of Texas, Austin.

Bhatta, B. P., and Larsen, O. I. (2011). Are intrazonal trips ignorable? *Transport Policy*, *18*(1), 13–22.

Boarnet, M. G. (2012). Frontiers in Land Use and Travel Research. In *The Oxford Handbook of Urban Planning*. Oxford University Press.

Borgatti, S. P. (2005). Centrality and network flow. *Social Networks*, *27*(1), 55–71.

Cambridge Sytematics Inc. (2010). *Travel Model Validation and Reasonableness Checking Manual Second Edition*.

Center for Urban Transportation Studies. (1999). *Guidebook on Statewide Travel Forecasting*. Milwaukee.

Cervero, R., and Duncan, M. (2003). Walking, bicycling, and urban landscapes: evidence from the San Francisco Bay Area. *American Journal of Public Health*, *93*(9), 1478–1483.

Cervero, R., and Kockelman, K. (1997). Travel demand and the 3Ds: Density, diversity, and design. *Transportation Research Part D: Transport and Environment*, *2*(3), 199–219.

Cervero, R., Sarmiento, O. L., Jacoby, E., Gomez, L. F., and Neiman, A. (2009). Influences of built environments on walking and cycling: lessons from Bogotá. *International Journal of Sustainable Transportation*, *3*(4), 203–226.

Clifton, K. J., Singleton, P. A., Muhs, C. D., Schneider, R. J., and Lagerwey, P. (2013). *Improving the Representation of the Pedestrian Environment in Travel Demand Models, Phase I*.

Daganzo, C. F. (1980). An equilibrium algorithm for the spatial aggregation problem of traffic assignment. *Transportation Research Part B: Methodological*, *14*(3), 221–228.

Ding, C. (1998). The GIS-based human-interactive TAZ design algorithm: examining

the impacts of data aggregation on transportation-planning analyisis. *Environment and Planning B: Planning and Design*, *25*(4), 601–616.

Dowling, R. G. (2005). *Predicting air quality effects of traffic-flow improvements: final report and user's gude* (Vol. 535). Transportation Research Board.

Eash, R. (1999). Destination and mode choice models for nonmotorized travel. *Transportation Research Record: Journal of the Transportation Research Board*, (1674), 1–8.

Forschungsgesellschaft für Straßen- und Verkehrswesen (FGSV). (2014). *Hinweise zur Nahmobilität: Strategien zur Stärkung des nichtmotorisierten Verkehrs auf Quartiers- und Ortsteilebene*. Köln: FGSV Verlag GmbH.

Freeman, L. (1977). A set of measures of centrality based on betweenness. *Sociometry*, 35–41.

Freeman, L. (1978). Centrality in social networks conceptual clarification. *Social Networks*, *1*(3), 215–239.

Friedrich, M., and Galster, M. (2009). Methods for generating connectors in transport planning models. *Transportation Research Record: Journal of the Transportation Research Board*, (2132), 133–142.

Gevas Humberg & Partner GmbH. (2010). *Ergebnisse zur Haushalts- und Kordonbefragung zur Mobilität im Jahre 2009*.

Gölz, H. (2007). *Aufbau eines Radverkehrsmodells für die Radverkehrsplanung in Stuttgart*. Thesis submitted at the Department of Transportation Planning and Traffic Engineering, University of Stuttgart, https://www.baufachinformation.de/Aufbau-eines-Radverkehrsmodells-f%C3%BCr-die-Radverkehrsplanung-in-Stuttgart/dis/2007079022043.

Greenwald, M. J. (2006). The relationship between land use and intrazonal trip making behaviors: Evidence and implications. *Transportation Research Part D: Transport and Environment*, *11*(6), 432–446.

Guo, J. Y., Bhat, C. R., and Copperman, R. B. (2007). Effect of the built environment on motorized and nonmotorized trip making: substitutive, complementary, or synergistic? *Transportation Research Record: Journal of the Transportation Research Board*.

Hagar66. (2010). File:Dachau in DAH.svg. Public domain. Retrieved October 11, 2016, from https://commons.wikimedia.org/wiki/File:Dachau_in_DAH.svg

Khatib, Z., Chang, K., and Ou, Y. (2001). Impacts of analysis zone structures on

modeled statewide traffic. *Journal of Transportation Engineering*, *127*(1), 31–38.

Kordi, M., Kaiser, C., and Fotheringham, A. S. (2012). A possible solution for the centroid-to-centroid and intra-zonal trip length problems. In *International Conference on Geographic Information Science, Avignon*.

Kuzmyak, J. R., Walters, J., Bradley, M., and Kockelman, K. M. (2014). *Estimating bicycling and walking for planning and project development: A guidebook* (No. Project 08-78).

Larson, R. C., and Odoni, A. R. (1981). *Urban operations research*.

Litman, T., Blair, R., Demopoulos, B., Eddy, N., Fritzel, A., Laidlaw, D., … Forster, K. (2015). *Pedestrian and bicycle planning*. Victoria Transport Policy Institute, Victoria, British Columbia.

Liu, F., Evans, J. E. (Jay), and Rossi, T. (2012). Recent practices in regional modeling of nonmotorized travel. *Transportation Research Record: Journal of the Transportation Research Board*, (2303), 1–8.

Martin, W. A., and McGuckin, N. A. (1998). *Travel estimation techniques for urban planning*. Washington D.C.: National Academy Press.

Martínez, L. M., Viegas, J. M., and Silva, E. A. (2009). A traffic analysis zone definition: a new methodology and algorithm. *Transportation*, *36*(5), 581–599.

Moeckel, R., and Donnelly, R. (2015). Gradual rasterization: redefining spatial resolution in transport modelling. *Environment and Planning B: Planning and Design*, *42*(5), 888–903.

Newman, M. (2004). Analysis of weighted networks. *Physical Review E*, *70*(5).

Okrah, M. B. (2012). *Development of a method for estimating intrazonal travel times in transport models*. Thesis submitted to the Master's Program Infrastructure Planning, University of Stuttgart.

Openshaw, S. (1977). Optimal zoning systems for spatial interaction models. *Environment and Planning A*, *9*(2), 169–184.

OpenStreetMap contributors. (2014). Planet dump (planet_11.354_48.236_b8341355.osm.xz from August 25, 2014). Retrieved from http://www.openstreetmap.org/

OpenStreetMap contributors. (2016). Planet dump (ArcGIS Basemap from October 1, 2016). Retrieved from http://planet.openstreetmap.org/

Opsahl, T., Agneessens, F., and Skvoretz, J. (2010). Node centrality in weighted networks: Generalizing degree and shortest paths. *Social Networks*, *32*(3), 245–

251.

Ortúzar, J. de D., and Willumsen, L. G. (2011). *Modelling Transport* (4th ed.). Chichester: John Wiley & Sons.

Porter, C., Suhrbier, J., and Schwartz, W. L. (1999). Forecasting bicycle and pedestrian travel: state of the practice and research needs. *Transportation Research Record: Journal of the Transportation Research Board*, (1674), 94–101.

Rodríguez, D. a., and Joo, J. (2004). The relationship between non-motorized mode choice and the local physical environment. *Transportation Research Part D: Transport and Environment*, *9*(2), 151–173.

Sallis, J. F., Frank, L. D., Saelens, B. E., and Kraft, M. K. (2004). Active transportation and physical activity: opportunities for collaboration on transportation and public health research. *Transportation Research Part A: Policy and Practice*, *38*(4), 249–268.

Schiller, P. L., Bruun, E. C., and Kenworthy, J. R. (2010). *An Introduction to sustainable transportation: Policy, planning and implementation*. Earthscan.

Schwartz, W. L., Porter, C. D., Payne, G. C., Suhrbier, J. H., Moe, P. C., and Wilkinson III, W. L. (1999). *Guidebook on Methods to Estimate Non-Motorized Travel: Overview of Methods* (No. FHWA-RD-98-165).

Sener, I. N., Eluru, N., and Bhat, C. R. (2009). An analysis of bicycle route choice preferences in Texas, US. *Transportation*, *36*(5), 511–539.

Seneviratne, P. N., and Morrall, J. F. (1985). Analysis of factors affecting the choice of route of pedestrians. *Transportation Planning and Technology*, *10*(2), 147–159.

Singleton, P. A., and Clifton, K. J. (2013). Pedestrians in regional travel demand forecasting models: State-of-the-practice. In *92nd Annual Meeting of the Transportation Research Board, Washington, DC*.

Stadt Dachau. (2011). *Bericht Verkehrsmodell Dachau 2009 - 2025*.

Stadt Dachau. (2012). *Leitbild und Leitsätze*. Gut Häusern.

Stinson, M. A., and Bhat, C. R. (2003). Commuter Bicyclist Route Choice: Analysis Using a Stated Preference Survey. *Transportation Research Record*, (1828).

United States Bureau of Public Roads. (1965). *Calibrating & testing a gravity model for any size urban area.* Washington: U.S. Dept. of Commerce Bureau of Public Roads Office of Planning; for sale by the Supt. of Docs. U.S. Govt. Print Off.

Van Audenhove, F.-J., Dauby, L., Korniichuk, O., and Pourbaix, J. (2014). *The Future of Urban Mobility 2.0: Imperatives to shape extended mobility ecosystems of tomorrow*.

Venigalla, M. M., Chatterjee, A., and Bronzini, M. S. (1999). A specialized equilibrium assignment algorithm for air quality modeling. *Transportation Research Part D: Transport and Environment*, *4*(1), 29–44.

Viegas, J. M., Martínez, L. M., and Silva, E. A. (2009). Effects of the modifiable areal unit problem on the delineation of traffic analysis zones. *Environment and Planning B: Planning and Design*, *36*(4), 625–643.

Wegener, M. (2011). From macro to micro - how much micro is too much? *Transport Reviews*, *31*(2), 161–177.

Weinstein Agrawal, A., Schlossberg, M., and Irvin, K. (2008). How far, by which route and why? A spatial analysis of pedestrian preference. *Journal of Urban Design*, *13*(1), 81–98.

Wulfhorst, G. (2013). Travel demand modeling 1. Lecture on Transport Planning Models at the Technical University of Munich on 23.10.2013.

Appendices

Appendix 1 Python Script for Calculating Intrazonal Times

```
##################################################################
#
# @title: Calculating Intrazonal Times
# @author: Matthew Bediako Okrah
# @date: Thur April 14, 2016
#
##################################################################

#Load Library
import numpy
import VisumPy.helpers
from VisumPy.matrices import*
from numpy import inf

#Create Attribute ZoneNumber for Nodes in Visum
#Use filter to get rid of irrelevant nodes in Visum
#Set polygon allocation to link zone numbers to relevant nodes in Visum

#Create User Defined Attributes for Zones to Store Intrazonal Costs
Visum.Net.Zones.AddUserDefinedAttribute("CBase","CBase","CBase",2,2)
Visum.Net.Zones.AddUserDefinedAttribute("CDegree","CDegree","CDegree",2,2)
Visum.Net.Zones.AddUserDefinedAttribute("CCloseness","CCloseness","CCloseness",2,2)
Visum.Net.Zones.AddUserDefinedAttribute("CAreaBased","CAreaBased","CAreaBased",2,2)
Visum.Net.Zones.AddUserDefinedAttribute("CNearest","CNearest","CNearest",2,2)

Visum.Net.Zones.AddUserDefinedAttribute("BBase","BBase","BBase",2,2)
Visum.Net.Zones.AddUserDefinedAttribute("BDegree","BDegree","BDegree",2,2)
Visum.Net.Zones.AddUserDefinedAttribute("BCloseness","BCloseness","BCloseness",2,2)
Visum.Net.Zones.AddUserDefinedAttribute("BAreaBased","BAreaBased","BAreaBased",2,2)
Visum.Net.Zones.AddUserDefinedAttribute("BNearest","BNearest","BNearest",2,2)

Visum.Net.Zones.AddUserDefinedAttribute("PBase","PBase","PBase",2,2)
Visum.Net.Zones.AddUserDefinedAttribute("PDegree","PDegree","PDegree",2,2)
Visum.Net.Zones.AddUserDefinedAttribute("PCloseness","PCloseness","PCloseness",2,2)
Visum.Net.Zones.AddUserDefinedAttribute("PAreaBased","PAreaBased","PAreaBased",2,2)
Visum.Net.Zones.AddUserDefinedAttribute("PNearest","PNearest","PNearest",2,2)


#Loop through zones
AllZones=Visum.Net.Zones.GetAll
for aZone in AllZones:
   CurrentZone = aZone.AttValue("NO")

   #Define area-based variables
   Area = aZone.AttValue("AreaKm2")
   Distance = math.sqrt(Area/(2*math.pi))

   CarIntraTime = 60*Distance/30.0
   BikeIntraTime = 60*Distance/15.5
```

```
PedIntraTime = 60*Distance/5.0

#Select subzonable nodes in current zone
NodeFilter=Visum.Filters.NodeFilter()
NodeFilter.Init()
NodeFilter.UseFilter=True
NodeFilter.AddCondition("OP_NONE" ,False, "AddVal1", "EqualVal", CurrentZone)

#Use Isochrones to get skim values in a matrix
CIsocValMatrix=[]
BIsocValMatrix=[]
PIsocValMatrix=[]

Subzones=Visum.Net.Nodes.GetAllActive
z=len(Subzones)

#Avoid calculations for zones with less than 2 subzones
if z < 2:

   CBaseIntrazonalCost = 99999
   CDegreeIntrazonalCost = 99999
   CClosenessIntrazonalCost = 99999

   BBaseIntrazonalCost = 99999
   BDegreeIntrazonalCost = 99999
   BClosenessIntrazonalCost = 99999

   PBaseIntrazonalCost = 99999
   PDegreeIntrazonalCost = 99999
   PClosenessIntrazonalCost = 99999

else:
   for aSubzone in Subzones:
      IsocNodes = Visum.CreateNetElements()
      IsocNodes.Add(aSubzone)

      #car time
      Visum.Analysis.Isochrones.Clear()
      Visum.Analysis.Isochrones.ExecutePrT(IsocNodes,"CAR",0)
      CIsocVal=numpy.array(Visum.Net.Nodes.GetMultiAttValues("IsocTimePrT", True))[:,1]
      CIsocVal[CIsocVal>720]=0
      for i in range(len(CIsocVal)):
         CIsocValMatrix.append(CIsocVal[i])

      #bike time
      Visum.Analysis.Isochrones.Clear()
      Visum.Analysis.Isochrones.ExecutePrT(IsocNodes,"BIKE",2)
      BIsocVal=numpy.array(Visum.Net.Nodes.GetMultiAttValues("IsocTimePrT", True))[:,1]
      BIsocVal[BIsocVal>2460]=0
      for i in range(len(BIsocVal)):
         BIsocValMatrix.append(BIsocVal[i])
```

```
        #ped time
        Visum.Analysis.Isochrones.Clear()
        Visum.Analysis.Isochrones.ExecutePrT(IsocNodes,"PED",0)
        PIsocVal=numpy.array(Visum.Net.Nodes.GetMultiAttValues("IsocTimePrT", True))[:,1]
        PIsocVal[PIsocVal>9180]=0
        for i in range(len(PIsocVal)):
            PIsocValMatrix.append(PIsocVal[i])


    #Get Skim Matrix
    CPreSkimMatrix=numpy.array(CIsocValMatrix).reshape(z,z)
    CSkimMatrix = CPreSkimMatrix/60

    BPreSkimMatrix=numpy.array(BIsocValMatrix).reshape(z,z)
    BSkimMatrix = BPreSkimMatrix/60

    PPreSkimMatrix=numpy.array(PIsocValMatrix).reshape(z,z)
    PSkimMatrix = PPreSkimMatrix/60

    #Calculate Base Weight Matrix
    CBaseMatrix = CSkimMatrix/CSkimMatrix
    CBaseMatrix[numpy.isnan(CBaseMatrix)]=0

    BBaseMatrix = BSkimMatrix/BSkimMatrix
    BBaseMatrix[numpy.isnan(BBaseMatrix)]=0

    PBaseMatrix = PSkimMatrix/PSkimMatrix
    PBaseMatrix[numpy.isnan(PBaseMatrix)]=0


    #Calculate Denominator for Degree and Closeness Weights
    Denominator = z-1

    #Calculate Intrazonal Skim using Base Weights
    CBaseWeightedMatrix = CBaseMatrix*CSkimMatrix
    CBaseIntrazonalCost = (numpy.sum(CBaseWeightedMatrix))/(numpy.sum(CBaseMatrix))

    BBaseWeightedMatrix = BBaseMatrix*BSkimMatrix
    BBaseIntrazonalCost = (numpy.sum(BBaseWeightedMatrix))/(numpy.sum(BBaseMatrix))

    PBaseWeightedMatrix = PBaseMatrix*PSkimMatrix
    PBaseIntrazonalCost = (numpy.sum(PBaseWeightedMatrix))/(numpy.sum(PBaseMatrix))

    #Calculate Intrazonal Skim using Degree Weights
    DegreeOrigin = \
(numpy.array(numpy.array(Visum.Net.Nodes.GetMultiAttValues("Sum:OutLinks\Length", \
True))[:,1]).reshape(z,1))/Denominator
    DegreeDestination = \
(numpy.array(numpy.array(Visum.Net.Nodes.GetMultiAttValues("Sum:InLinks\Length",  \
True))[:,1]).reshape(1,z))/Denominator
```

```
      CDegreeMatrix = DegreeOrigin*CBaseMatrix*DegreeDestination
      CDegreeWeightedMatrix = CDegreeMatrix*CSkimMatrix
      CDegreeIntrazonalCost =  \
(numpy.sum(CDegreeWeightedMatrix))/(numpy.sum(CDegreeMatrix))

      BDegreeMatrix = DegreeOrigin*BBaseMatrix*DegreeDestination
      BDegreeWeightedMatrix = BDegreeMatrix*BSkimMatrix
      BDegreeIntrazonalCost = \
(numpy.sum(BDegreeWeightedMatrix))/(numpy.sum(BDegreeMatrix))

      PDegreeMatrix = DegreeOrigin*PBaseMatrix*DegreeDestination
      PDegreeWeightedMatrix = PDegreeMatrix*PSkimMatrix
      PDegreeIntrazonalCost = \
(numpy.sum(PDegreeWeightedMatrix))/(numpy.sum(PDegreeMatrix))

      #Calculate Intrazonal Skim using Closeness Weights
      numpy.seterr(divide='ignore')
      CInvertedSkimMatrix = 1/CSkimMatrix
      CInvertedSkimMatrix[CInvertedSkimMatrix==inf]=0
      CClosenessOrigin = (CInvertedSkimMatrix.sum(axis=1).reshape(z,1))/Denominator
      CClosenessDestination =(CInvertedSkimMatrix.sum(axis=0).reshape(1,z))/Denominator
      CClosenessMatrix = CClosenessOrigin*CBaseMatrix*CClosenessDestination
      CClosenessWeightedMatrix = CClosenessMatrix*CSkimMatrix
      CClosenessIntrazonalCost = \
(numpy.sum(CClosenessWeightedMatrix))/(numpy.sum(CClosenessMatrix))

      numpy.seterr(divide='ignore')
      BInvertedSkimMatrix = 1/BSkimMatrix
      BInvertedSkimMatrix[BInvertedSkimMatrix==inf]=0
      BClosenessOrigin = (BInvertedSkimMatrix.sum(axis=1).reshape(z,1))/Denominator
      BClosenessDestination =(BInvertedSkimMatrix.sum(axis=0).reshape(1,z))/Denominator
      BClosenessMatrix = BClosenessOrigin*BBaseMatrix*BClosenessDestination
      BClosenessWeightedMatrix = BClosenessMatrix*BSkimMatrix
      BClosenessIntrazonalCost = \
(numpy.sum(BClosenessWeightedMatrix))/(numpy.sum(BClosenessMatrix))

      numpy.seterr(divide='ignore')
      PInvertedSkimMatrix = 1/PSkimMatrix
      PInvertedSkimMatrix[PInvertedSkimMatrix==inf]=0
      PClosenessOrigin = (PInvertedSkimMatrix.sum(axis=1).reshape(z,1))/Denominator
      PClosenessDestination =(PInvertedSkimMatrix.sum(axis=0).reshape(1,z))/Denominator
      PClosenessMatrix = PClosenessOrigin*PBaseMatrix*PClosenessDestination
      PClosenessWeightedMatrix = PClosenessMatrix*PSkimMatrix
      PClosenessIntrazonalCost = \
(numpy.sum(PClosenessWeightedMatrix))/(numpy.sum(PClosenessMatrix))

   #Assigning Intrazonal Skim to Zone Attributes
   aZone.SetAttValue("CBase",CBaseIntrazonalCost)
   aZone.SetAttValue("CDegree",CDegreeIntrazonalCost)
   aZone.SetAttValue("CCloseness",CClosenessIntrazonalCost)
   aZone.SetAttValue("CAreaBased",CarIntraTime)
```

```
aZone.SetAttValue("BBase",BBaseIntrazonalCost)
aZone.SetAttValue("BDegree",BDegreeIntrazonalCost)
aZone.SetAttValue("BCloseness",BClosenessIntrazonalCost)
aZone.SetAttValue("BAreaBased",BikeIntraTime)

aZone.SetAttValue("PBase",PBaseIntrazonalCost)
aZone.SetAttValue("PDegree",PDegreeIntrazonalCost)
aZone.SetAttValue("PCloseness",PClosenessIntrazonalCost)
aZone.SetAttValue("PAreaBased",PedIntraTime)

#Clear Filters
Visum.Filters.InitAll()
Visum.Analysis.Isochrones.Clear()
```

Appendix 2 Python Script for Gradual Rasterization

```
# -*- coding: utf-8 -*-
"""
Created on Thu Sep 24 10:44:39 2015

@author: Matthew Okrah
"""

import arcpy, os
arcpy.env.overwriteOutput = True

# Set start workspace
startgdb = "C:/Users/ga37jav/Desktop/Start Dissertation/Gradual Rasterization/GIS"
arcpy.env.workspace = startgdb

# Declaring Variable Variables
initialpoly = "Single75.shp"
joinFeatures = "Link75.shp"
threshold = 1000

# Declaring Fixed Variables
finalgdb = str(arcpy.CreateFolder_management(startgdb, 'finalfolder.gdb').getOutput(0))
remnant = os.path.join(finalgdb, 'rem')
count = 0

# Copying the initial polygon
startpoly = os.path.join(startgdb, 'startpolygon.shp')
arcpy.CopyFeatures_management(initialpoly, startpoly)

# Spatial Join
targetFeatures = startpoly
outfc = os.path.join(startgdb, 'quadtreeinput.shp')

fieldmappings = arcpy.FieldMappings()
fieldmappings.addTable(targetFeatures)
fieldmappings.addTable(joinFeatures)
LengthFieldIndex = fieldmappings.findFieldMapIndex('Length')
fieldmap = fieldmappings.getFieldMap(LengthFieldIndex)
field = fieldmap.outputField
field.name = 'SumNet'
field.aliasName = 'SumNet'
fieldmap.outputField = field
fieldmap.mergeRule = 'sum'
fieldmappings.replaceFieldMap(LengthFieldIndex, fieldmap)

arcpy.env.outputCoordinateSystem = arcpy.Describe(joinFeatures).spatialReference
arcpy.SpatialJoin_analysis(targetFeatures, joinFeatures, outfc, '#', '#', fieldmappings, 'CONTAINS')
```

```
# Find maximum length of network per zone
MaxLength = max(row[0] for row in arcpy.da.SearchCursor(outfc,['SumNet']))

# Threshold test
while MaxLength > threshold:
   count = count + 1

   gdb = str(arcpy.CreateFolder_management(startgdb, 'special').getOutput(0))

   try:
      arcpy.MakeFeatureLayer_management(outfc, 'tosame_lyr', '"SumNet" <= %d' % threshold)
      sameout = os.path.join(finalgdb, 'same_{0}'.format(count))
      arcpy.CopyFeatures_management("tosame_lyr", sameout)
      arcpy.Delete_management("tosame_lyr")
   except:
      print arcpy.GetMessages()

   # Create Layer of objects not exceeding threshold and copy to finalgdb
   arcpy.MakeFeatureLayer_management(outfc, 'checksize_lyr', '"SumNet" > %d' % threshold) #,
'SumNet <= threshold')
   startfish = os.path.join(startgdb, 'startfishing.shp')
   arcpy.CopyFeatures_management("checksize_lyr", startfish)
   arcpy.Delete_management("checksize_lyr")

   # split cells in batches of 100
   netsize = int(arcpy.GetCount_management(startfish).getOutput(0))
   t1 = 0

   while netsize > 100:
      t1 = t1 + 1

      gdb1 = str(arcpy.CreateFolder_management(startgdb, 'special1.').getOutput(0))

      f1 = os.path.join(gdb, 'fishes1_{0}'.format(t1))

      # cells to be split in this run
      arcpy.MakeFeatureLayer_management(startfish, 'tofish_lyr', '"FID" < 100')
      prefish = os.path.join(startgdb, 'prefishing.shp')
      arcpy.CopyFeatures_management("tofish_lyr", prefish)
      arcpy.Delete_management("tofish_lyr")

      # cells to be split in a later run
      arcpy.MakeFeatureLayer_management(startfish, 'backto_lyr', '"FID" >= 100')
      restartfish = os.path.join(startgdb, 'restartfishing.shp')
      arcpy.CopyFeatures_management("backto_lyr", restartfish)
      arcpy.Delete_management("backto_lyr")
      arcpy.CopyFeatures_management(restartfish, startfish)
      arcpy.Delete_management(restartfish)
```

```
      # split cells to be split in this run
      with arcpy.da.SearchCursor(prefish, ['SHAPE@', 'OID@']) as rows:
         for row in rows:
            ext = row[0].extent
            st = '%f %f' % (ext.XMin, ext.YMin)
            orien = '%f %f' % (ext.XMin, ext.YMax)
            opp = '%f %f' % (ext.XMax, ext.YMax)
            out = os.path.join(gdb1, 'fish1_{0}'.format(row[1]))

            arcpy.CreateFishnet_management(out, st, orien, '0', '0', '2', '2', opp, labels='NO_LABELS', \
geometry_type='POLYGON')

      arcpy.Delete_management(prefish)
      arcpy.env.workspace = gdb1
      fishnets = arcpy.ListFeatureClasses()
      arcpy.Merge_management(fishnets[:], f1)
      arcpy.Delete_management(gdb1)

      arcpy.env.workspace = startgdb
      netsize = int(arcpy.GetCount_management(startfish).getOutput(0))
      print(netsize)

   # split the last batch of cells
   with arcpy.da.SearchCursor(startfish, ['SHAPE@', 'OID@']) as rows:
      for row in rows:
         ext = row[0].extent
         st = '%f %f' % (ext.XMin, ext.YMin)
         orien = '%f %f' % (ext.XMin, ext.YMax)
         opp = '%f %f' % (ext.XMax, ext.YMax)
         out = os.path.join(gdb, 'fish1_{0}'.format(row[1]))

         arcpy.CreateFishnet_management(out, st, orien, '0', '0', '2', '2', opp, labels='NO_LABELS', \
geometry_type='POLYGON')

   arcpy.Delete_management(startfish)

   # ensure that cells of size 75 m × 75 m are not split further
   checklimit = os.path.join(startgdb, 'checkinglimit.shp')

   arcpy.env.workspace = gdb
   allfishnets = arcpy.ListFeatureClasses()
   arcpy.Merge_management(allfishnets[:], checklimit)

   arcpy.Delete_management(gdb)

   arcpy.env.workspace = startgdb

   arcpy.AddField_management(checklimit, "checkarea", "DOUBLE")
```

```
    arcpy.CalculateField_management(checklimit, "checkarea", \
"float(!SHAPE.area@SQUAREMETERS!)", "PYTHON_9.3")

    try:
        arcpy.MakeFeatureLayer_management(checklimit, 'tolimit_lyr', 'checkarea < 5626')
        limitout = os.path.join(finalgdb, 'limit_{0}'.format(count))
        arcpy.CopyFeatures_management("tolimit_lyr", limitout)
        arcpy.Delete_management("tolimit_lyr")
    except:
        print arcpy.GetMessages()

    try:
        arcpy.MakeFeatureLayer_management(checklimit, 'checksize_lyr', 'checkarea > 5626')
        arcpy.CopyFeatures_management("checksize_lyr", targetFeatures)
        arcpy.Delete_management("checksize_lyr")
        arcpy.Delete_management(checklimit)
        arcpy.env.outputCoordinateSystem = arcpy.Describe(joinFeatures).spatialReference
        arcpy.SpatialJoin_analysis(targetFeatures, joinFeatures, outfc, '#', '#', fieldmappings)

        MaxLength = max(row[0] for row in arcpy.da.SearchCursor(outfc,['SumNet']))
        print(MaxLength)

    except:
        print arcpy.GetMessages()
        break

# Copy the remaining polygon into the final folder and delete from start folder
try:
    arcpy.CopyFeatures_management(outfc, remnant)
    arcpy.Delete_management(outfc)
except:
    print arcpy.GetMessages()

# Group all elements in the final folder into one feature class and delete individual elements
arcpy.env.workspace = finalgdb
finalnets = arcpy.ListFeatureClasses()

arcpy.Merge_management(finalnets[:], targetFeatures)
arcpy.Delete_management(finalgdb)

# Run spatial join to get the final zone system with network length
arcpy.env.workspace = startgdb
finaloutfc = os.path.join(startgdb, 'finalpolygon.shp')
arcpy.env.outputCoordinateSystem = arcpy.Describe(joinFeatures).spatialReference
arcpy.SpatialJoin_analysis(targetFeatures, joinFeatures, finaloutfc, '#', '#', fieldmappings)

arcpy.Delete_management(startpoly)
```

ISBN 978-3-9814676-7-3

ISSN 2192-9459

Univ.-Prof. Dr.-Ing. Gebhard Wulfhorst

Chair of Urban Structure and Transport Planning

Focus Area Mobility and Transportation Systems

Technical University of Munich

Arcisstraße 21 · 80333 München · Germany

www.sv.bgu.tum.de